Using paleolimnology to assess influence of Peace River regulation on lakes along two transects in the northern portion of the Peace-Athabasca Delta

by

Anita Ghosh

A thesis

presented to the University of Waterloo

in fulfilment of the

thesis requirement for the degree of

Master of Science

in

Biology

Waterloo, Ontario, Canada, 2022

Author's Declaration

I hereby declare that I am the sole author of this thesis. This is a true copy of the thesis, including any required final revisions, as accepted by my examiners.

I understand that my thesis may be made electronically available to the public.

Abstract

The Peace-Athabasca Delta (PAD), northern Alberta, Canada, is an ecologically and culturally important floodplain where debate has persisted for more than 60 years about causes of water-level drawdown of its abundant, shallow perched lakes. Hydroelectric regulation of Peace River flow by the W.A.C. Bennett Dam, located ~1100 km upstream of the delta at the river's headwaters, is widely considered to be the main cause of perched lake drying via reduction in occurrence of ice-jam flood events. However, prior paleolimnological studies have identified that flood frequency and lake levels began to decline in the late 1800s and early 1900s, many decades before construction of the dam, in response to climate change. Here, we further assess for evidence of shifting lake hydrology associated with the timing of river regulation using analyses of sediment cores from twelve lakes in the northern portion of the PAD. Lakes were arranged along two transects adjacent to Moose Island and Rocky Point, respectively, that span a 27-km stretch of the Peace River and vary up to 9.7 km from the river. Sediment cores from each lake were analyzed for variation in sediment composition by loss-on-sequential-heating, and organic carbon and nitrogen elemental and isotope composition to reconstruct past hydrological change. Cores from seven of the lakes possessed sediment records that could be dated using activity profiles of ^{210}Pb and ^{137}Cs. Mineral matter content, C/N ratios, and δ^{15}N decline in upper strata of all the sediment cores, trends that can be interpreted as consistent with observations and other evidence of reduction in flood frequency at the Peace sector of the PAD. Use of breakpoint analysis identified that 17 of 21 records (3 sedimentary variables x 7 lakes with dated cores) infer a decline of river influence one to five decades after 1968, whereas only 3 records infer a decline of river influence coincident with 1968. These findings do not provide strong support for widely held contention that perched lake drying at the PAD began in 1968 due to effects of the W.A.C. Bennett Dam on the ice-jam

flood regime. Instead, climatic shifts to lower snowpack and warmer temperatures since at least the mid-1970s appear to be a main driver. However, it is not possible to discount the possibility that climatic trends may have caused the river flow regime to pass a threshold and delay effects of the W.A.C. Bennett Dam. Regardless of the cause, perched lake drawdown in the PAD has negative consequences for ecosystem function and Indigenous land users, and requires adaptative and/or mitigative strategies.

Acknowledgement of land

I respectfully acknowledge that the research communicated in this Thesis centers on Treaty 8 lands in northern Alberta in a region known as the Peace-Athabasca Delta to investigate environmental concerns. The Peace-Athabasca Delta is the Traditional Territory of the Athabascan Chipewyan First Nation, Mikisew Cree First Nation, and Fort Chipewyan Métis Association (Local 125 of the Métis Nation of Alberta).

The University of Waterloo, Ontario, where my lab work is performed, is located on Treaty 4 land and is the Traditional Territory of the Attawandaron, Anishnaabeg and Haudenosaunee peoples. The University of Waterloo is on the Haldimand Tract which is land granted to the Six Nations and extends to six miles on both sides of the Grand River.

Acknowledgments

To my supervisors, Dr. Roland Hall and Dr. Brent Wolfe, thank you for all the opportunities you provided me with and your encouragement to learn and lead. Roland, thank you for all the support and understanding you provided me throughout my academic journey. Brent, thank you for all the conversations and guidance as I navigated writing this thesis.

To Dr. John Johnston, thank you for your wonderful insight on my project, and the motivation to always be curious in all aspects of my work.

To Dr. Heidi Swanson, thank you for teaching me with kindness, and providing me with support when I needed it most. You have inspired and encouraged me to always be myself. Every conversation with you was both insightful and entertaining.

To Dr. Lauren MacDonald, thank you for your amazing guidance and friendship. You were always there with a pep talk, great ideas, or just an ear to listen whenever I needed it. Your help both in the lab and throughout the writing process is something I will always be grateful for. I would not have made it to the finish line without you and all the kindness you had to offer.

To Barbara and Robert Grandjambe, thank you for your warmth, bringing me into your home, and sharing all about your life. You have taught me so much, and I will forever cherish the time you spent with me.

To all of those in the Hall/Wolfe lab, thank you for providing me with assistance and input. Dr. Johan Wiklund, thank you for your support in both dating my cores and sharing your bottomless curiosity for science. Dr. Jennifer Adams, thank you for your support in writing and patience when explaining concepts. James Telford, thank you for being a wonderful, playful person that taught me not only all about sediment core collection, but also how to take the time to enjoy life even when things were tough. Nelson Zabel, thank you for all your encouragement and always making time for wonderful conversations. Amanda Soliguin, thank you for all your support in the lab, and for always putting a smile on my face. Thank you to the undergraduate and co-op students, Joanne Armstrong and Amy Lacey, for all your hard work on the laboratory analyses for this project.

To my friends, Hannah Thibault, Corin Seelemann, Michaella Miller, Brenda Yu, and Kris Chan, thank you for being my found family. You all mean more to me than words can express, but I will make an attempt. Hannah, thank you for holding my hand throughout graduate school as we tried to navigate all its difficulties and joys together. Corin, thank you for never hesitating to offer your shoulder for my endless screaming and hair pulling throughout both my undergraduate and graduate degrees. Michaella, I would like to thank you for your confidence in me when I had none, you are an inspiration. Brenda, thank you for your friendship and support, I am so grateful to have gone through my undergraduate degree with you by my side. Kris, you are not only one of my best friends, but also my counterpart, and your support for nearly two decades is the only reason I have made it as far as I have. I love you all.

To Mom and Dad, thank you for your support, and I love you both.

Finally, to my partner Dani Homme, thank you so much for everything you have done for me these past five years. You stood by me through every difficult moment, and no matter how lost I felt, you were there to help me navigate it. Thank you for your constant love, support, and encouragement, helping me grow into the person I am today. I love you so very much.

Dedication

For my beautiful family, Charlie, Ginny, Bagel, Luna, and Dani.

Table of Contents

List of Figures

List of Tables

Chapter 1 - Introduction

The threat of degradation of freshwater ecosystems by multiple human-induced stressors (e.g., industrial activities, urban development, agriculture) is compounded by anthropogenic climatic warming (Schindler & Smol, 2006; Ormerod et al., 2010; Smol, 2010). Concerns about the future of freshwater supply are particularly acute in northwestern Canada where climate warming has been pronounced in recent decades, resulting in a decrease of snow and ice cover and change in precipitation patterns (Schindler & Donahue, 2006; IPCC, 2013). Our ability to discern the roles of various stressors on the deterioration of freshwater ecosystems is hampered by insufficient long-term monitoring in many regions (Smol, 2010).

1.1 Lake-level drawdown concerns in the Peace-Athabasca Delta

At the Peace-Athabasca Delta (PAD, northern Alberta), the world's largest inland boreal freshwater delta (~6000 km^2), climate warming, river regulation, and industrial activities have raised concerns regarding sustainability of the water supply. Eighty percent of the PAD is located within Wood Buffalo National Park (WBNP; Timoney, 2002; Figure 1.1). The PAD is fed by three major rivers: the Peace, Athabasca, and Birch. The Peace River bypasses the PAD most of the time, except during episodic ice-jam floods, which have the potential to inundate elevated (i.e., perched) lakes in the northern Peace sector (Prowse & Lalonde, 1996; Prowse & Conly, 1998; Figure 1.1). In contrast, the Athabasca River provides a source of floodwater to lakes in the southern Athabasca sector during both the ice-jam and open-water seasons (Remmer et al., 2020; Neary et al., 2021). The PAD provides important habitat and resources for waterfowl and peregrine falcons, and supports species at risk (e.g., the whooping crane) and the largest free-roaming herd of bison (Timoney, 2006, 2013). The Athabascan Chipewyan First Nation, Mikisew Cree First Nation, and Métis Nation of Alberta mainly live within the village of Fort Chipewyan, located near

the shore of Lake Athabasca adjacent to the PAD, and access the delta's natural resources (Timoney, 2006; Remmer et al., 2018; 2020; Vannini & Vannini, 2019). Due to its ecological and cultural importance, the PAD was designated a Ramsar Wetland of International Importance in 1982 and contributed to the designation of WBNP as a UNESCO World Heritage Site in 1983 (Timoney, 2002). Despite these designations and protections, concern has grown and intensified among the local Indigenous communities and other stakeholders (e.g., Parks Canada) due to observed water-level drawdown of the shallow perched basins in the PAD during the past several decades (Flett et al., 1996; MCFN, 2014; Straka et al., 2018; WBNP, 2019).

Annual evaporation often exceeds precipitation at the PAD, which leads to drawdown of perched basin water levels in the absence of sufficient input of river floodwaters (Timoney, 2002, 2013; Remmer et al., 2018, 2020). Consequently, river flooding is important for maintenance of hydrological and ecological conditions of the perched basins (Timoney, 2002, 2013; Wiklund et al., 2012). Concern over water-level drawdown of perched basins in the PAD has existed since construction in 1968 and subsequent operation of the W.A.C. Bennett Dam at the headwaters of Peace River, ~1100 km upstream of the PAD, due to widespread consideration that the dam has reduced frequency of ice-jam floods on the Lower Peace River at the PAD (Timoney, 2013; Beltaos, 2020). This concern, among others, motivated the Mikisew Cree First Nation to file a petition to UNESCO to enlist WBNP as 'World Heritage in Danger' because recent drying of the perched basins has consequences for land-user access and ecosystem health (MCFN, 2014). The petition led to a Reactive Monitoring Mission and a report from the International Union for Conservation of Nature and the World Heritage Center, which concluded that regulation of the Peace River has coincided with the drying of the PAD (IUNC/WHC, 2017). Subsequently, an

Action Plan has been developed on the basis that the impacts of the dam need to be mitigated (WBNP, 2019).

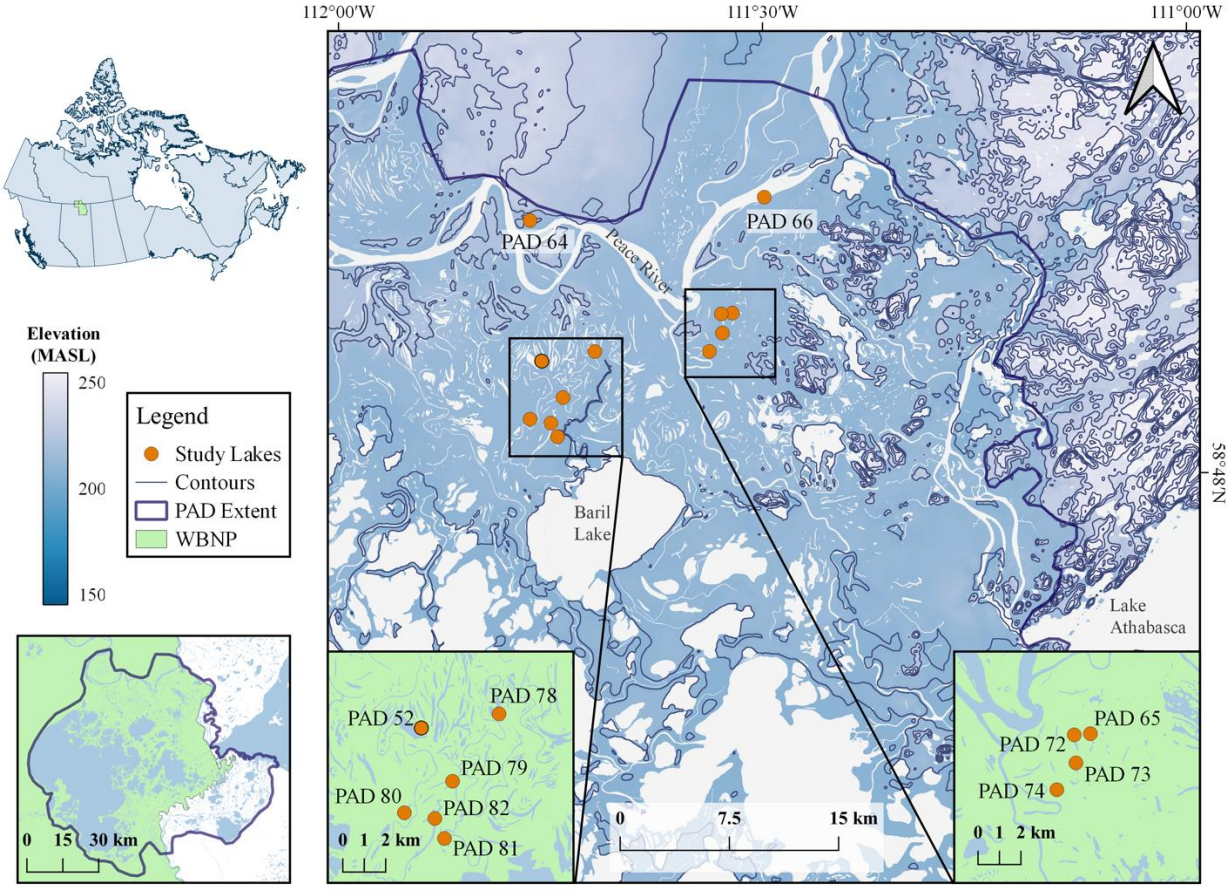

Figure 1.1. Map displaying the locations of the Peace-Athabasca Delta (PAD), the Wood Buffalo National Park boundary (left panels) and the study lakes (right panel). The ten study lakes plus PAD 52 and PAD 65 that are the focus of this thesis research are marked by orange circles. Lakes PAD 52, PAD 64, PAD 78, PAD 79, PAD 80, PAD 81, and PAD 82 form a transect in the Moose Island Region. PAD 65, PAD 66, PAD 72, PAD 73, and PAD 74 form a transect in the Rocky Point Region. The extent of the PAD is outlined in purple. Elevation data extracted from Maps Canada – Geospatial Data Extraction (https://maps.canada.ca/czs/index-en.html). Map was created in QGIS version 3.10 (A Coruna).

Ice-jam flood (IJF) events on the Peace River at the PAD occur in late-winter/early-spring of years when river flow, augmented by the input from melt of snowpack, causes mechanical break-up of river ice. Ice-jams form at narrow points and bends in the river, and they cause river water to rise to levels that often overflow the riverbank and spill across the PAD, inundating the

perched basins (PADPG, 1973; PADTS, 1996; Prowse & Conly 2002). For IJF events to occur, river ice must be sufficiently strong that ice break-up is mechanical, or dynamic, rather than thermal when the ice melts in place (Prowse et al., 2002; Beltaos et al., 2006; Lamontagne et al., 2021). Climate warming can decrease the likelihood of ice-jam flooding on the Peace River by reducing river ice thickness, reducing volume of snowpack runoff, and altering the timing and duration of snowmelt runoff (Prowse & Conly, 1998; Beltaos et al., 2006; Lamontagne et al., 2021). IJFs at the PAD typically occur during a 3-week period from the last week of April through the first two weeks of May (Beltaos & Peters, 2020). During this period, however, Peace River discharge has not been substantially altered by river regulation (Beltaos & Peters, 2020; Figure 1.2). This raises the prospect that regulation of Peace River flow may not be the main factor responsible for a reduction in the frequency or magnitude of IJFs at the PAD (Lamontagne et al., 2021). On the other hand, Peace River discharge has been markedly reduced during the summer months because the W.A.C. Bennett Dam captures snowmelt runoff from high elevation portions of the watershed that contributed substantial flow before regulation (Figure 1.2). This raises the possibility that if there is an effect of the dam on perched basin water balance it may result from reduction in river flow during the open-water season, and not at the time of IJFs. However, prior studies have failed to identify that high discharge events during the open-water season can provide floodwaters to perched basins (Prowse & Lalonde, 1996).

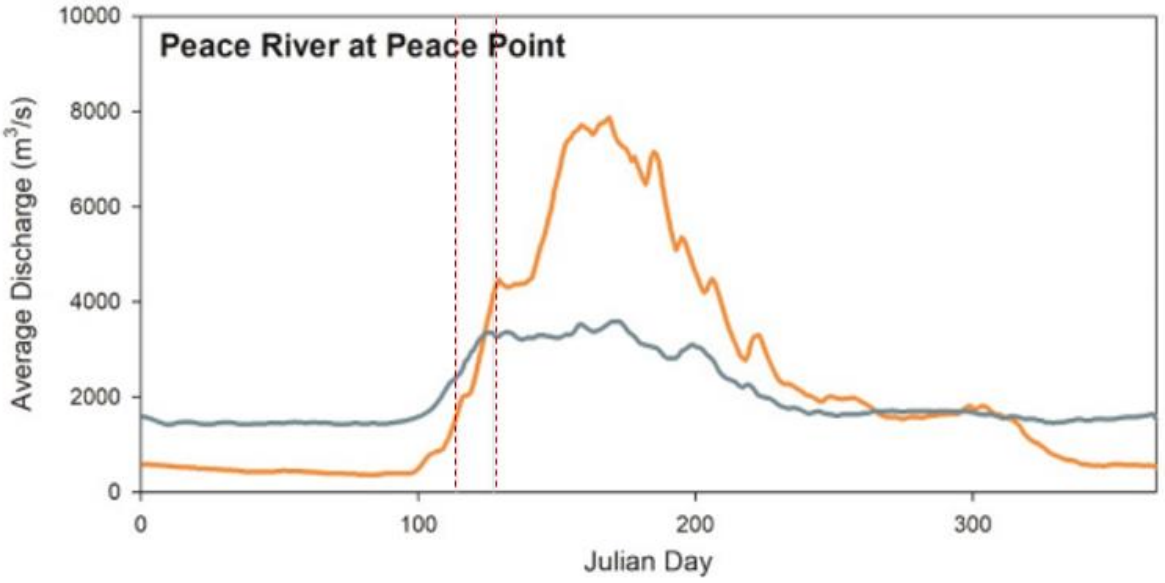

Figure 1.2. Average daily discharge for the Peace River at Peace Point, modified from Peters and Prowse (2001). The orange line represents the pre-regulation period (1960-1967), and the grey line represents the post-regulation period (1968-2019). The three-week period during which ice-jam floods have previously occurred is indicated by two vertical red dashed lines which span Julian Days 114-127 (the last week of April and the first two weeks of May). Data sourced from wateroffice.ec.gc.ca. Figure modified from Faber (2020, p. 7*)*.

1.2 Prior Studies in the Peace-Athabasca Delta

Previous studies in the PAD have attempted to use the history and Traditional Knowledge record of IJF events to estimate the frequency at which they occurred in the PAD prior to regulation of Peace River flow by the W.A.C. Bennett Dam, and to project the expected IJF frequency at the PAD without regulation (e.g., Timoney et al., 1997; Beltaos, 2014, 2018; Beltaos & Peters, 2020). Other methods have utilized modelling to simulate the expected natural discharge and IJF frequency of the Peace River at the PAD using hydrometric records that span approximately nine years prior (1960-1967) to the construction of the Bennett Dam (e.g., Peters & Prowse, 2001; Beltaos & Peters, 2020). However, effectiveness of these approaches is hampered by the short, fragmented hydrometric records at the time of IJFs and a limited number of gauging stations at and near to the PAD. The studies that have utilized hydrometric and historical records, or that have created models of Peace River levels using these datasets, have typically concluded that the PAD

has experienced less frequent ice-jam floods since the onset of river regulation in 1968 (but see Timoney, 2021). However, none of these studies directly assessed the flood regimes and water-balance variations of the perched lakes in the PAD. There has been a short-term study to simulate the persistence of water in the perched basins, but it was unable to inform on the full range of the hydrological variation of these basins over multi-decadal timescales (Peters et al., 2006).

Due to difficulties in capturing natural hydrological variation with short instrumental records and models, paleolimnological approaches have been employed to determine longer temporal and broader spatial scales of variation in flood frequency and perched lake water balance, and causes of declining freshwater abundance in the PAD. Prior paleolimnological studies have examined lakes across much of the PAD and have demonstrated long-term drying trends since the late 1800s and early 1900s, well before the W.A.C. Bennett Dam was constructed (e.g., Wolfe et al., 2006; 2008a; 2011; 2012), and that changes in flood regimes in the southern Athabasca sector were caused by a natural geomorphic event that altered Athabasca River distributary flow (e.g., Wolfe et al., 2008b; Kay et al., 2019) and by fluctuations in Lake Athabasca water levels that altered river levels and the area of inundation (Johnston et al., 2010; Sinnatamby et al., 2010; Wolfe et al., 2011). Of the paleolimnological studies reviewed by Wolfe et al. (2012), none showed evidence of directional drying coincident with the construction of the W.A.C. Bennett Dam. Instead, water-level drawdown began in the early to mid-1900s, before onset of Peace River hydrometric records, which matched well to changes depicted in historical maps (Sinnatamby et al., 2010; Wolfe et al., 2012). Overall, these studies have concluded that while many lakes have indeed experienced water-level drawdown, the cause of this drawdown is predominantly climate change, not river regulation (Wolfe et al., 2012, 2020).

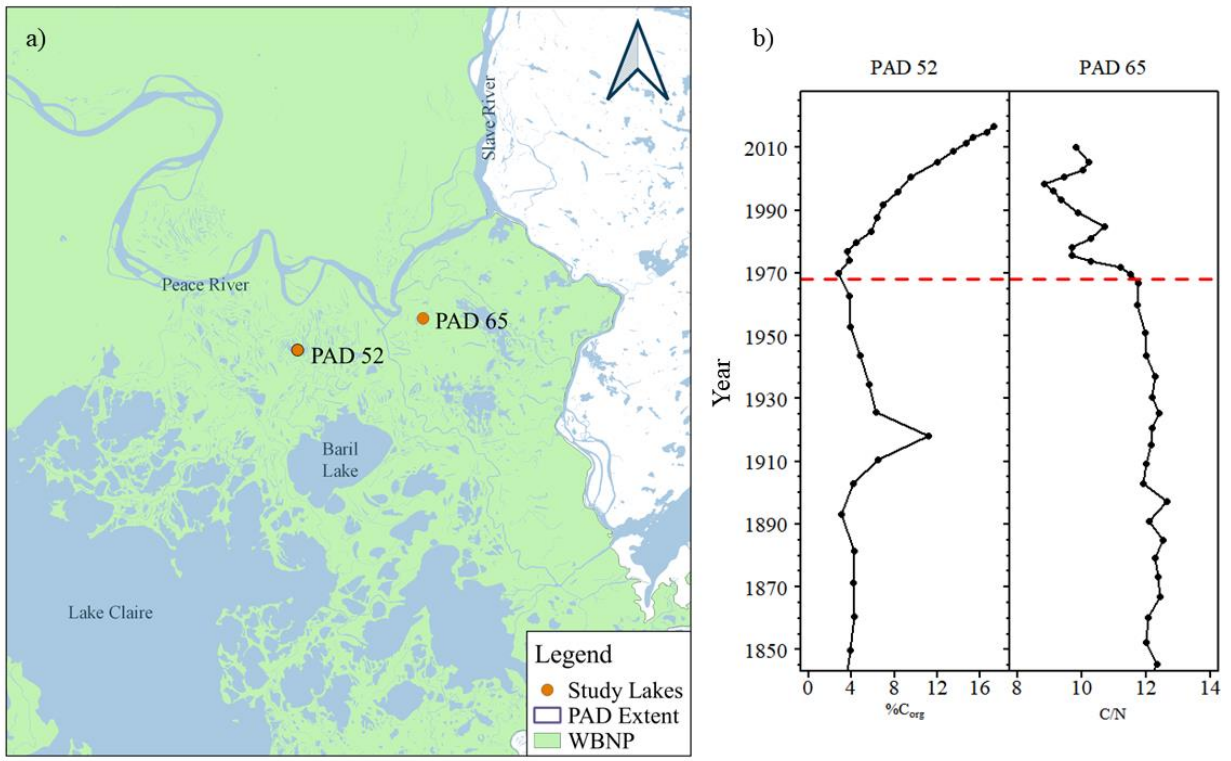

Figure 1.3. Panel a) displays a map of the northern Peace Sector of the PAD. Two previously studied lakes, PAD 52 and PAD 65, are marked by orange circles. Panel b) displays the stratigraphic variation of organic carbon content (% of dry mass) and organic carbon to nitrogen (C/N) ratios in sediment cores obtained from PAD 52 and PAD 65, respectively (data from Faber, 2020). The horizontal dashed red line denotes 1968, the year that regulation of Peace River flow began.

While prior paleolimnological records show climate to be the main driver of reduced flood frequency and drawdown of perched basins in the PAD, two recently obtained sediment records at lakes located in a relatively low-lying area near the Peace River (PAD 52 and PAD 65) may show some evidence that is consistent with reduced influence of river floodwaters since construction of the W.A.C. Bennett Dam (Faber, 2020). Sediment cores from these two lakes show an increase in organic carbon content after ~1970 at PAD 52 and a shift to a lower elemental carbon to nitrogen ratio after ~1970 at PAD 65, suggesting an increase in aquatic productivity and/or a decline in supply of mineral sediment as a result of decreasing floodwater influence coincident with the onset of river regulation (Faber, 2020; Figure 1.3). These lake sediment records suggest that there may be a zone of lake drying in low lying areas adjacent to the Peace River that may

have been caused, at least partially, by regulation of Peace River flow, and which deserves further investigation.

1.3 Study objectives

To further test the temporal and spatial representativeness of the PAD 52 and PAD 65 paleohydrological records and to continue to address the potential causes of declining flood frequency, sediment cores were analyzed from ten additional lakes within the northern portion of the PAD that are situated along two transects from locations where IJFs often form on the Peace River (Moose Island, Rocky Point; Prowse & Conly, 1998; Belatos et al., 2006; Beltaos, 2018). The Moose Island transect is in the northwestern portion of the Peace sector and includes seven lakes at varying distances from the Peace River (including PAD 52 analyzed originally by J. Faber, 2020). The Rocky Point transect is situated farther downstream in the northeastern region of the Peace sector and includes five lakes at varying distances from the Peace River (including PAD 65 analyzed originally by J. Faber, 2020; Figure 1.1; Table 2.1). The objectives of this study are to 1) reconstruct past changes in the influence of river floodwaters from analysis of sediment cores at the flood-prone lakes located along the Moose Island and Rocky Point transects, and 2) determine the timing of changes in flood influence and assess if they coincide with the onset of Peace River flow regulation by the W.A.C. Bennett Dam, which began in 1968.

Chapter 2 - Methods

2.1 Study Sites

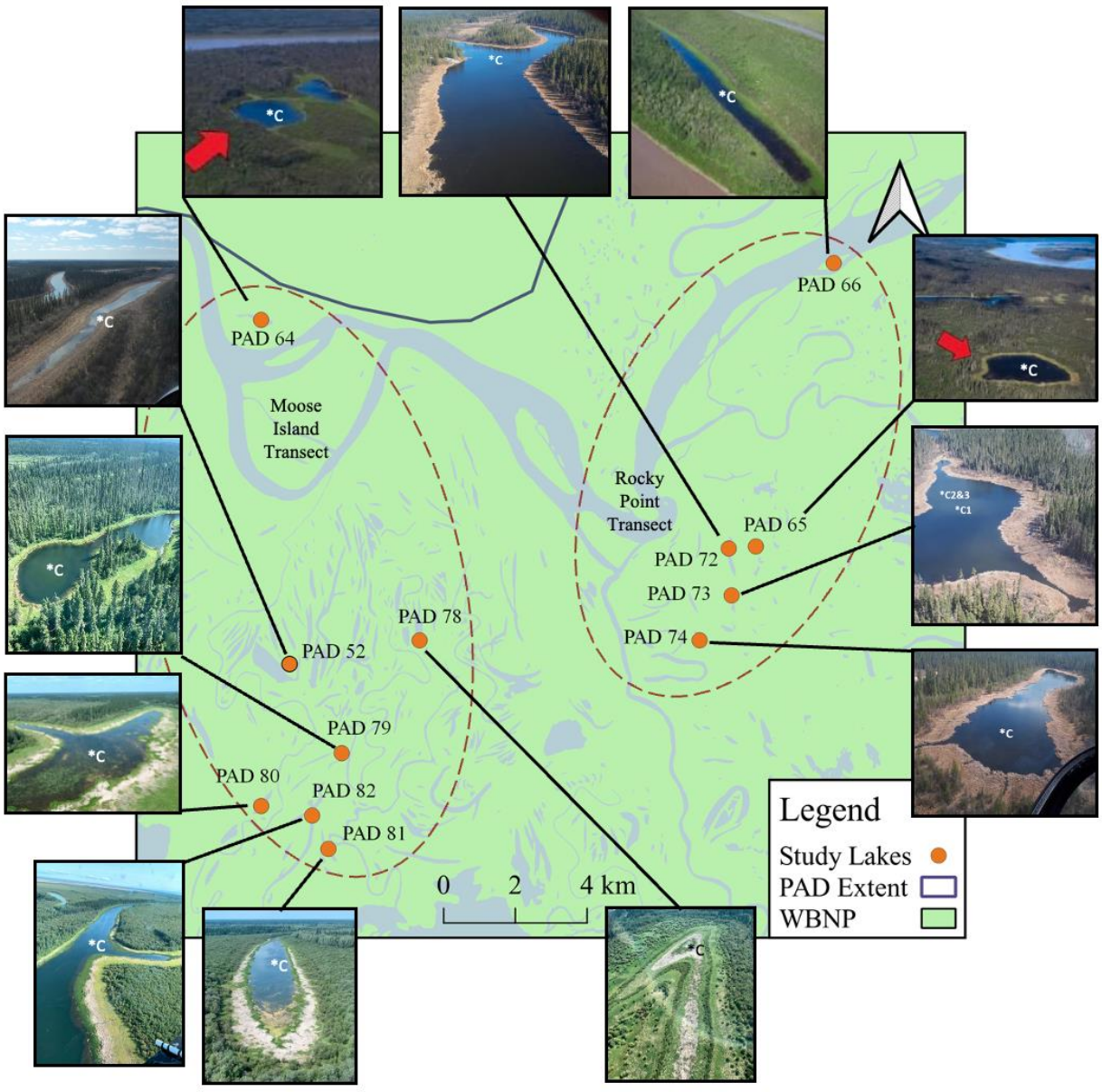

Figure 2.1. Locations and photos of the twelve study lakes in the northern portion of the Peace Delta. The general area of both transects are outlined in red dashed ellipses. Photos were taken at the time of core collection and '*C' indicates the approximate coring location. Photos for PAD 52, PAD 64, PAD 65, and PAD 66 are from Faber (2020).

For this study, the 12 lakes span an approximately 27 km stretch along the Peace River. Lakes were selected because they displayed observable signs of lake-level drawdown (e.g.,

receding shorelines and/or rings of higher former shorelines; Figure 2.1) and contained sufficient water to potentially preserve an undisturbed sediment record. Almost all the study lakes are surrounded by mature coniferous trees and willows (Figure 2.1). Based on their location and elevation, all study lakes are expected to receive floodwaters during major ice-jam flood events and possibly from episodes of high Peace River discharge during the open-water season. The Moose Island transect consists of seven lakes (including PAD 52) ranging from 1.0 to 9.7 km from the river (Figure 1.1, 2.1; Table 2.1). Lakes in the Moose Island transect varied in elevation from 210 to 217 masl (Figure 1.1; Table 2.1). The Rocky Point transect has five lakes (including PAD 65) ranging from 0 to 3.0 km from the Peace River (Figure 1.1, 2.1; Table 2.1). Lakes in the Rocky Point transect varied in elevation from 213 to 215 masl (Figure 1.1; Table 2.1). Lakes PAD 66, PAD 72, PAD 73, PAD 74, PAD 79, PAD 81, and PAD 82 appear to occupy former river channels. PAD 66 is on an island within Peace River, and readily receives floods. Field observations did not identify active inlets or outlets at any of the lakes and therefore all lakes are considered perched basins (Figure 2.1)

Table 2.1. Core depth, number, designation, date collected, coordinates of coring location, depth of water at the coring location, elevation, and distance from Peace River (PR) of all twelve lakes spanning the two transects (Moose Island and Rocky Point). Data for PAD 52, PAD 64, PAD 65, PAD 66 were obtained from Faber (2020). Distance from Peace River was approximated by measuring from the coring location to the closest point along the Peace River. Elevation and distance from Peace River were obtained from Google Earth Pro (Version 7.3.4.8573).

Lake	Working core	Secondary	Archive	Date	Coordinates		Distance from PR	Water Depth	Elevation
	(cm, core no.)	(cm, core no.)	(cm, core no.)		Latitude	Longitude	(km)	(m)	(masl)
Moose Island transect (Northwestern)									
PAD 64	59 (C-2)	59 (C-1)	N/A	29/06/2016	58°57'11.80"N	111°46'23.10"W	1.0	2.8	217
PAD 52	36 (C-1)	36 (C-2)	N/A	15/09/2017	58°52'29.10"N	111°45'00.10"W	3.8	0.5	212
PAD 78	39.5 (C-2)	36.0 (C-1)	30.0 (C-3)	11/07/2019	58°52'28.18"N	111°41'55.26"W	4.9	0.1	213
PAD 79	71.5 (C-2)	65.0 (C-3)	85.0 (C-1)	13/07/2019	58°50'45.07"N	111°44'07.60"W	7.0	9.1	213
PAD 80	40.0 (C-3)	31.5 (C-2)	21.5 (C-1)	11/07/2019	58°49'57.26"N	111°46'29.10"W	8.4	0.3	213
PAD 82	58.0 (C-1)	59.0 (C-2)	56.5 (C-3)	13/07/2019	58°49'50.03"N	111°44'57.11"W	8.6	5.0	213
PAD 81	31.5 (C-2)	27.0 (C-1)	22.5 (C-3)	11/07/2019	58°49'15.05"N	111°44'24.95"W	9.7	1.0	210
Rocky Point transect (Northeastern)									
PAD 66	39 (C-2)	36 (C-1)	N/A	30/06/2016	58°58'10.40"N	111°29'35.70"W	0.0	0.5	215
PAD 72	31.5 (C-3)	35.0 (C-2)	32.5 (C-1)	15/05/2018	58°53'46.23"N	111°32'52.89"W	1.6	1.0	213
PAD 65	54 (C-1)	57 (C-2)	N/A	29/06/2016	58°53'49.00"N	111°32'08.90"W	2.3	0.8	213
PAD 73	46.5 (C-2)	35.0 (C-3)	24.5 (C-1)	16/05/2018	58°53'08.36"N	111°32'50.13"W	2.4	0.8	213
PAD 74	45.0 (C-3)	44.5 (C-3)	43.0 (C-1)	16/05/2018	58°52'25.64"N	111°33'42.51"W	3.0	1.0	213

2.2 Sediment core collection

Sediment cores were collected from near the center or at the deepest part of each of the twelve study lakes during the open water season of their respective years (from 2016-2019; Table 2.1). In 2016 and 2017, a hammer-driven Glew gravity corer (Glew et al., 2001) was operated from an inflatable kayak to collect two cores from lakes PAD 52, PAD 64, PAD 65, and PAD 66. In 2018 and 2019, three sediment cores were collected from lakes PAD 72, PAD 73, PAD 74, PAD 78, PAD 79, PAD 80, PAD 81, and PAD 82 using a modified Glew hammer-driven gravity corer (Telford et al., 2021) operated from the pontoon of a helicopter. Of the cores collected, one was designated the working core with a second designated the secondary core to be used when there was insufficient mass for all analyses. The third core collected in 2018 and 2019 provides an archive core (Table 2.1). The working core was selected based on observations of core length, an undistributed sediment-water interface, and when present, evidence the sediment core possessed laminations. Sediment cores collected in 2016 and 2017 were sectioned into 1-cm intervals, and cores collected in 2018 and 2019 were sectioned into 0.5-cm intervals. The sediment cores collected in 2016 and 2017 were initially intended for examining metal concentrations from the Peace River and did not require a finer timescale for the study, so 1-cm intervals were used. Thinner intervals were used for the sediment cores collected in 2018 and 2019 to capture higher temporal resolution. All cores were sectioned at the field base in Fort Chipewyan within 24 hours of collection. The samples were then transported to the University of Waterloo and stored at 4°C in the dark.

2.3 Sediment core analyses

2.3.1 Loss-on-sequential heating

Loss-on-sequential-heating (LOSH) analysis was used to measure stratigraphic variation in the content of water, organic matter, carbonate, and mineral matter. Previous research in the PAD has demonstrated that during intervals of increased river floodwater influence, sediment cores have high mineral matter content due to the input of inorganic river sediment (Wolfe et al., 2006; Kay et al., 2019). Also, the floodwater input increases turbidity within the basin which can suppress aquatic plant production and lower the organic matter content of the sediment (Wiklund et al., 2010, 2012; McGowan et al., 2011). Thus, stratigraphic variation in mineral matter and organic matter content is used to infer past changes in strength of flood influence. From each 1-cm or 0.5-cm interval, a subsample of wet sediment (0.5 ± 0.05 g) was analyzed by weight loss on sequential heating for content of moisture at 90°C (for 24 hours), organic matter at 550°C (for 2 hours) and carbonate at 950°C (for 2 hours). Between each heating step, samples were cooled in a desiccator and weighed. The amount of carbonate-free mineral matter was measured by the amount of mass remaining after the 950°C heating. The inorganic matter content was determined as the sum of carbonate-free mineral matter content plus carbonate content within each sample (Heiri et al., 2001).

2.3.2 Geochronology

Activities of ^{210}Pb, ^{226}Ra (through their daughter isotopes ^{214}Pb and ^{214}Bi, respectively), and ^{137}Cs were measured by gamma spectrometry on mostly every second 0.5-cm or 1.0-cm interval to a sufficient depth to establish sediment core chronologies, where possible. For each sample, the sediment was freeze dried and ~3-6 g was packed into pre-weighed polycarbonate

tubes to a height of 35 mm. A silicon septum and 1 ml of 2-ton clear epoxy were then placed on top of the samples to create an airtight environment. The samples were left for at least three weeks to allow the decay products (^{214}Pb and ^{214}Bi) to reach equilibrium with ^{226}Ra. Activities of the radioisotopes were measured by analysing samples for 23-95 hours using Ortec co-axial HPGe Digital gamma ray spectrometers interfaced with Maestro 32 software.

For sediment cores where a chronology could be established, the Constant Rate of Supply (CRS) model was used to establish age-depth relations based on ^{210}Pb activity profiles and to estimate dry mass sedimentation rate. The chronology was linearly extrapolated below the stratigraphic horizon of unsupported ^{210}Pb activity, where it matches supported ^{210}Pb activity, using average dry mass sedimentation rates (Appleby and Oldfield, 1978; Appleby, 2001). Additionally, a ^{137}Cs activity peak, where evident, was used as an independent time marker and verification of 1963, a distinctive maximum peak of fallout from above ground nuclear testing (Appleby and Oldfield, 1978; Appleby, 2001). For PAD 79 and PAD 82, an independent reference date of 1963 was used before applying the CRS model, to improve accuracy in the ^{210}Pb profile (Appleby, 2001). The reference date (1963) was used to set a reference level for the excess ^{210}Pb inventory, from which the ^{210}Pb inventory above the reference level is captured by ^{210}Pb activity between 1963 and the time of core collection (2019 for PAD 79 and PAD 82). The ^{210}Pb inventory above the reference level was then used to estimate the ^{210}Pb inventory below the reference level (Eq. 35; Appleby, 2001), and then the total ^{210}Pb inventory was calculated using the ^{210}Pb inventory above and below the reference level (Eq. 36; Appleby, 2001). These calculations were used to constrain the total excess ^{210}Pb inventory and the CRS model was used to establish age-depth relations. The chronologies for PAD 79 and PAD 82 were then linearly extrapolated below the lowest stratigraphic horizon of the ^{210}Pb inventory using the average dry mass sedimentation rate

above the reference date (1963). For PAD 64, PAD 66, PAD 78, PAD 80 and PAD 81, where a geochronology could not be established, no further analyses beyond estimation of sediment composition by LOSH were conducted, with the exception of PAD 81 where further analyses were performed before knowing that a geochronology could not be established.

2.3.3 Organic carbon and nitrogen elemental and isotope composition

Past changes in aquatic productivity and nutrient supply can be tracked using stratigraphic measurements of organic carbon (C) and nitrogen (N) elemental and isotope composition in sediment cores (Meyers & Teranes, 2001; Leng et al., 2006; Wolfe et al., 2006). Tracking changes in productivity can provide an understanding of shifts in river influence through time (e.g., with reduced river influence an increase in lake productivity is expected; Leng et al., 2006; Wolfe et al., 2006). C/N ratios can be used to delineate the origin of organic matter, with C/N ratios above 15 generally indicative of allochthonous organic matter (e.g., terrestrial plant matter) supplied from sources outside the lakes (Meyers & Teranes, 2001; Leng et al., 2006). In contrast, C/N ratios below 15 are indicative of autochthonous organic matter from growth of algae and phytoplankton within the lakes (Meyers & Teranes, 2001; Leng et al., 2006). Isotopic ratios of carbon can be used to track changes in aquatic productivity because algae will preferentially take up the lighter carbon isotope (^{12}C) causing ^{13}C-enrichment of the remaining dissolved inorganic carbon (DIC). As productivity increases the remaining DIC becomes ^{13}C-enriched, and the changes are captured in organic matter preserved in the sediment record (Meyers & Teranes, 2001; Leng et al., 2006). Similarly, nitrogen isotope composition can be used to track nitrogen dynamics as there is also a preferential uptake of the lighter nitrogen isotope (^{14}N) by phytoplankton causing an enrichment

of ^{15}N in the remaining dissolved inorganic nitrogen (DIN) which can be preserved in lake sediment (Leng et al., 2006).

For each sediment core with an established geochronology (and PAD 81), a subsample of wet sediment from each 1-cm or 0.5-cm interval was treated with ~45 ml of 10% HCL (by volume) at 60°C for 2 hours to remove carbonate minerals and shells (Wolfe et al., 2001). The supernatant of the samples was then aspirated after the sediment settled and samples were then replenished with deionized water. The samples were then aspirated, after each period of settling, and rinsed with deionized water until the pH of the sample matched that of the deionized water. Samples were then freeze dried and passed through a sieve (250 µm) to remove coarse particles which may originate from terrestrial materials. The content of organic carbon, nitrogen (from which C/N weight ratios were derived) and organic carbon and nitrogen isotope composition were measured in an elemental analyser interfaced with a continuous flow isotope-ratio mass spectrometer (CF-IRMS) at the University of Waterloo – Environmental Isotope Laboratory (UW-EIL). Data provided includes organic %C and %N from which the C/N ratios were calculated. Additionally, $\delta^{13}C$ and $\delta^{15}N$ are provided and reported as δ-notation = $[(R_{sample} / R_{standard}) - 1]x10^3$ where R = $^{13}C/^{12}C$ or $^{15}N/^{14}N$ with respect to international standards and respective analytical uncertainties for $\delta^{13}C$ (‰ VPDB ±0.2‰) and $\delta^{15}N$ (‰ AIR ±0.3‰).

2.4 Numerical and Statistical Analyses

Preliminary exploration of stratigraphic variation in all sediment core measurements revealed that mineral matter content, C/N ratios and $\delta^{15}N$ produced interpretable profiles capable of addressing the study's objectives. Breakpoint analysis was used to assess for evidence of directional change coincident with 1968, the onset of operation of the W.A.C. Bennett Dam. Only sediment cores with an established geochronology were used for breakpoint analysis (i.e., cores from lakes PAD 52, PAD 65, PAD 72, PAD 73, PAD 74, PAD 79, and PAD 82). Breakpoint analysis involved developing a broken-line or piecewise linear regression model between a dependent variable (mineral matter content, C/N or $\delta^{15}N$) and the independent variable (estimated year of deposition based on ^{210}Pb and/or ^{137}Cs dating). Using the piecewise linear regression model for a given sedimentary variable, two linear regressions were estimated and assessed for evidence of a change in slope through the 'difference-in-slope' parameter in the model, which denotes a breakpoint when a significant difference in slope is found (Muggeo, 2008). The number of breakpoints is set by the user, and, in this case, one breakpoint was used for each dependent variable for a sediment core record (i.e., the record is modeled as a piecewise linear model with two segments; Muggeo, 2008). An analysis of variance (ANOVA) test was used to determine if a linear regression model significantly differs from a two-segment piecewise linear regression model, with an alpha of 0.05. Lastly, once it was shown that the models were significantly different, a 95% confidence interval was established for the breakpoint to estimate the uncertainty in breakpoint determination (Table C1- C3). The breakpoint analysis was performed using R-Studio with the 'Segmented' package (Muggeo, 2008).

Chapter 3 - Results

3.1 Geochronology

Sediment cores from seven of the twelve lakes could be dated using ^{210}Pb methods (PAD 52, PAD 65, PAD 72, PAD 73, PAD 74, PAD 79, and PAD 82; Figure 3.1). Cores from three of the lakes (PAD 52, PAD 65, PAD 74) have stratigraphic profiles of declining ^{210}Pb activity with depth until background values are reached. Cores from the four other lakes (PAD 72, PAD 73, PAD 79, and PAD 82) have a subsurface peak in ^{210}Pb activity before declining with depth until background activity is reached (Figure 3.1). In most of these cores, ^{210}Pb activity declines markedly, likely due to dilution of radioisotope activity by influx of sediment supplied from flood events. Exceptions to these two patterns include PAD 79 and PAD 82, where PAD 79 displays more variable supported ^{210}Pb activity and PAD 82 shows variability of unsupported ^{210}Pb downcore (Figure 3.1a). Sediment cores from PAD 64, PAD 78, PAD 80, and PAD 81 were unable to be dated due to insufficient unsupported ^{210}Pb activity compared to the supported ^{210}Pb activity, and low ^{137}Cs activity that did not exceed minimum detection limits. This suggests that rapid sedimentation diluted activities of ^{210}Pb and ^{137}Cs in the cores from these lakes or that the sediment profiles had undergone mixing (Appleby, 2001). Dating was not attempted for the core from PAD 66 because the organic matter content was very low and similar to that of other lakes where dating was attempted and was unsuccessful. For this thesis, sediment records with established chronologies will be plotted by time and sediment records without will be plotted by depth.

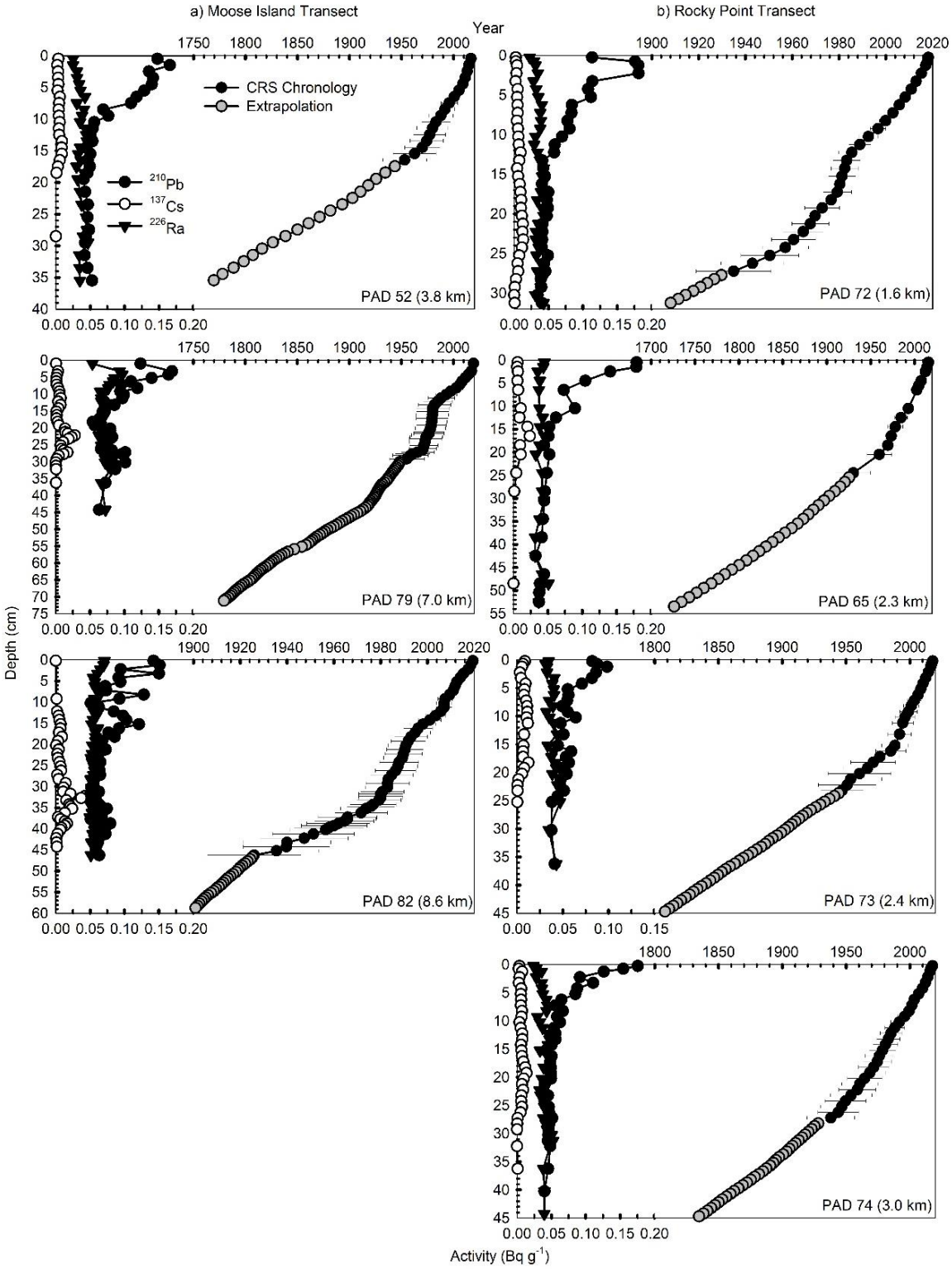

Figure 3.1. The left panel displays radiometric dating results at three of the lakes in the Moose Island transect, arranged by distance from Peace River (PAD 52, PAD 79, PAD 82). The right panel displays radiometric dating results at the four of the lakes in the Rocky Point transect, arranged by distance from Peace River (PAD 72, PAD 65, PAD 73, PAD 74). Included are the activities of ^{210}Pb, ^{226}Ra (estimated through daughter isotopes ^{214}Pb and ^{214}Bi) and ^{137}Cs, and age-depth relations based on the CRS model. Results for PAD 52 and PAD 65 are from Faber (2020).

Sediment records from the Moose Island transect reached background ^{210}Pb activity at 16.5 cm for PAD 52, 29.75 cm for PAD 79, and 46.25 cm for PAD 82 (mid-point interval depths), suggesting variable sedimentation rates among the lakes (Figure 3.1a). ^{137}Cs profiles were used to support CRS dates when ^{137}Cs peaks aligned closely to 1963, corresponding to the maximum ^{137}Cs fallout from aboveground nuclear testing, for the sediment record from PAD 52 (Appleby, 2001). For the records from PAD 79 and PAD 82, the CRS model was applied after an independent reference date was used to constrain the total ^{210}Pb inventory (Appleby, 2001). CRS age determinations, extrapolated using average dry mass sedimentation rates, indicated that basal dates of the sediment cores from lakes along the Moose Island transect are ~1770 CE at PAD 52, ~1780 CE at PAD 79, and ~1901 CE at PAD 82.

Sediment records from the Rocky Point transect reached background ^{210}Pb activity at relatively consistent depths in the cores (23.5 cm for PAD 73, 24.5 cm for PAD 65, 27.25 cm for PAD 72, and 27.75 cm for PAD 74; mid-point interval depths). The consistently shallower depth at which background ^{210}Pb activity was reached at these lakes indicates sedimentation rates are slower and less variable in lakes of the Rocky Point transect than in lakes of the Moose Island transect. At PAD 72 and PAD 74, the ^{137}Cs profiles displayed a peak that was assumed to represent 1963, which was used to support CRS dates (Figure 3.1b). Distinct ^{137}Cs peaks were not found in the sediment cores from PAD 65 or PAD 73, due possibly to post-depositional mobility of ^{137}Cs or to rapid influx of sediment during a coincident flood event since dating could be established from the ^{210}Pb activity profiles. CRS age determinations indicated that basal dates of the cores are ~1726 CE at PAD 65, ~1795 CE at PAD 73, ~1835 CE at PAD 74, and ~1908 CE at PAD 72.

3.2 Stratigraphic Variation in Mineral Matter Content

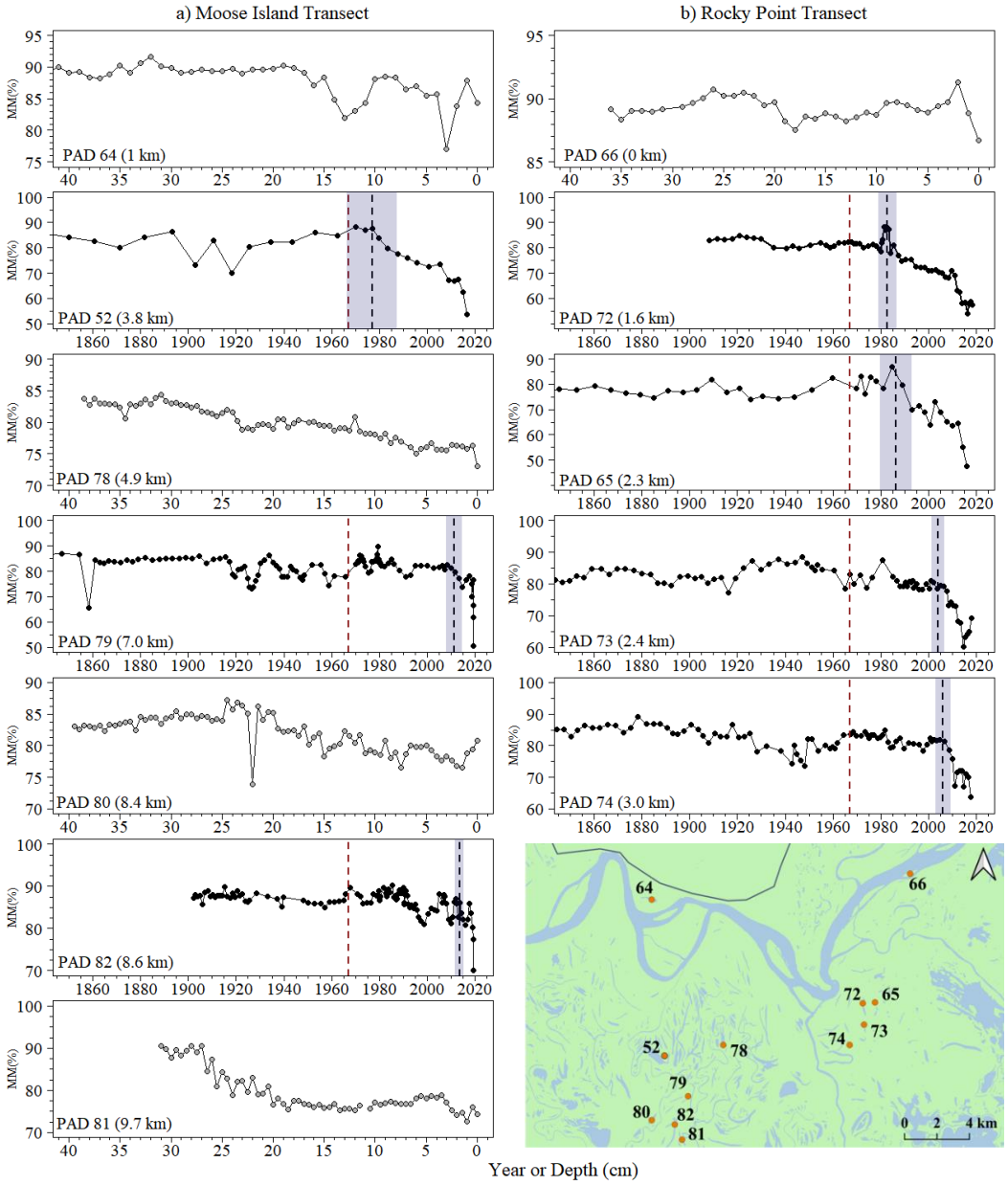

Figure 3.2. Graphs showing stratigraphic variation in mineral matter content (%MM) by estimated age (Year CE) or by depth at the study lakes. Panel a) includes the seven lakes along the Moose Island transect, arranged by distance from the Peace River (PAD 64, PAD 52, PAD 78, PAD 79, PAD 80, PAD 82, PAD 81). Panel b) includes the five lakes along the Rocky Point transect in order of distance from the Peace River (PAD 66, PAD 72, PAD 65, PAD 73, PAD 74). Note varying y-axis scales. Profiles with gray symbols could not be dated by measuring ^{210}Pb and ^{137}Cs activity, whereas those with black symbols have an established geochronology from measuring ^{210}Pb activity. Profiles with an established geochronology display stratigraphic profiles from ~1850 to 2020. Results of breakpoint analysis are indicated with a vertical black dashed line and the 95% confidence interval for the breakpoint is shaded in gray. The vertical red dashed lines identify 1968, the year when regulation of Peace River flow by the W.A.C. Bennett Dam began. A map in the bottom right corner depicts the location of each lake, created in QGIS version 3.10 (A Coruna). Results from PAD 52, PAD 64, PAD 65, and PAD 66 are from Faber (2020).

Sediment cores from all twelve lakes along the Moose Island and Rocky Point transects possess very high mineral matter content, which is indicative of strong river influence (since at least ~1850 for sediment cores that could be dated; Figure 3.2). For lakes in the Moose Island transect, mineral matter content ranged from ~50.4 – 91.6% throughout the cores (Figure 3.2a). Mineral matter content for these lakes was fairly consistent for most of the record until declines occur in the upper strata. Breakpoint analysis places these declines, which infer a decline in river influence, at ~1977 for PAD 52 [95% CI 1967, 1988], ~2011 for PAD 79 [95% CI 2008, 2015] and ~2014 for PAD 82 [95% CI 2012, 2015] (Figure 3.2a; Table C1). All breakpoints are statistically significant (ANOVA, $P<0.001$; Table C1). The 95% confidence intervals (CI) for the age of the breakpoint at PAD 79 and PAD 82 occur after 1968. The lower bound of the 95% CI at PAD 52 dates to ~1967, which is coincident with the onset of river regulation, and the upper bound is 20 years later (~ 1988; Figure 3.2a; Table C1). The confidence intervals are narrow at PAD 79 and PAD 82 (±~3.4 and ±~1.9 years from the breakpoint, respectively), but much wider at PAD 52 (±~10.5 years from the breakpoint; Figure 3.2a, Table C1). Lakes in the Moose Island transect without established chronologies (PAD 64, PAD 78, PAD 80 and PAD 81) also displayed consistently high mineral matter content in deeper strata (typically below 25 cm depth; below 15 cm at PAD 64) and mineral matter content generally declined in the upper strata, but the age of the shift to declining values is unknown. Mineral matter content was consistently high in the core from PAD 64 (typically 85-92%, with only 4 samples below 85%), the lake in the transect that is closest to the Peace River, suggesting persistent strong influence of floodwater throughout the record (Figure 3.2a). For the three lakes with dated cores in the Moose Island transect, the breakpoints denoting a decline in river water influence occur later the farther the lake is located from the Peace River (Figure 3.2a).

For lakes in the Rocky Point transect, mineral matter content ranged from ~47.4 – 91.3% throughout the cores (Figure 3.2b). Mineral matter content was also fairly consistent for most of the records until declines occur in the upper strata, suggesting decreased river influence in more recent years. Breakpoint analysis places these declines, which infer a reduction in river influence, at ~1983 for PAD 72 [95% CI 1979, 1987], ~1986 for PAD 65 [95% CI 1980, 1993], ~2004 for PAD 73 [95% CI 2001, 2007], and ~2006 for PAD 74 [95% CI 2003, 2009] (Figure 3.2b; Table C1). Mineral matter content breakpoints for the Rocky Point transect records are statistically significant (ANOVA, $P<0.001$; Appendix Table C1). The lower bound of all the 95% CIs for the breakpoints date to after 1968 (Figure 3.2b; Table C1). The breakpoints at PAD 72, PAD 73 and PAD 74 had narrow 95% CIs (±~3.9, ±~2.6, and ±~3.1 years, respectively), whereas the 95% CI for PAD 65 was slightly wider 95% CI (±~6.5 years; Figure 3.2b, Table C1). PAD 66, a lake located on an island within Peace River and immediately adjacent to the river, displayed higher mineral matter content and lower variation than all the other lakes in this transect (~86.7 – 91.3%; Figure 3.2b). The high mineral matter content at PAD 66 suggests persistent strong river influence throughout the record, similar to findings at PAD 64 in the Moose Island transect, but the age of the shift to declining values is unknown. Consistent with findings at the Moose Island transect, the breakpoints denoting a decline in river influence occur later the farther the lake is from the Peace River along the Rocky Point transect (Figure 3.2b).

3.3 Organic Carbon to Nitrogen Ratio (C/N)

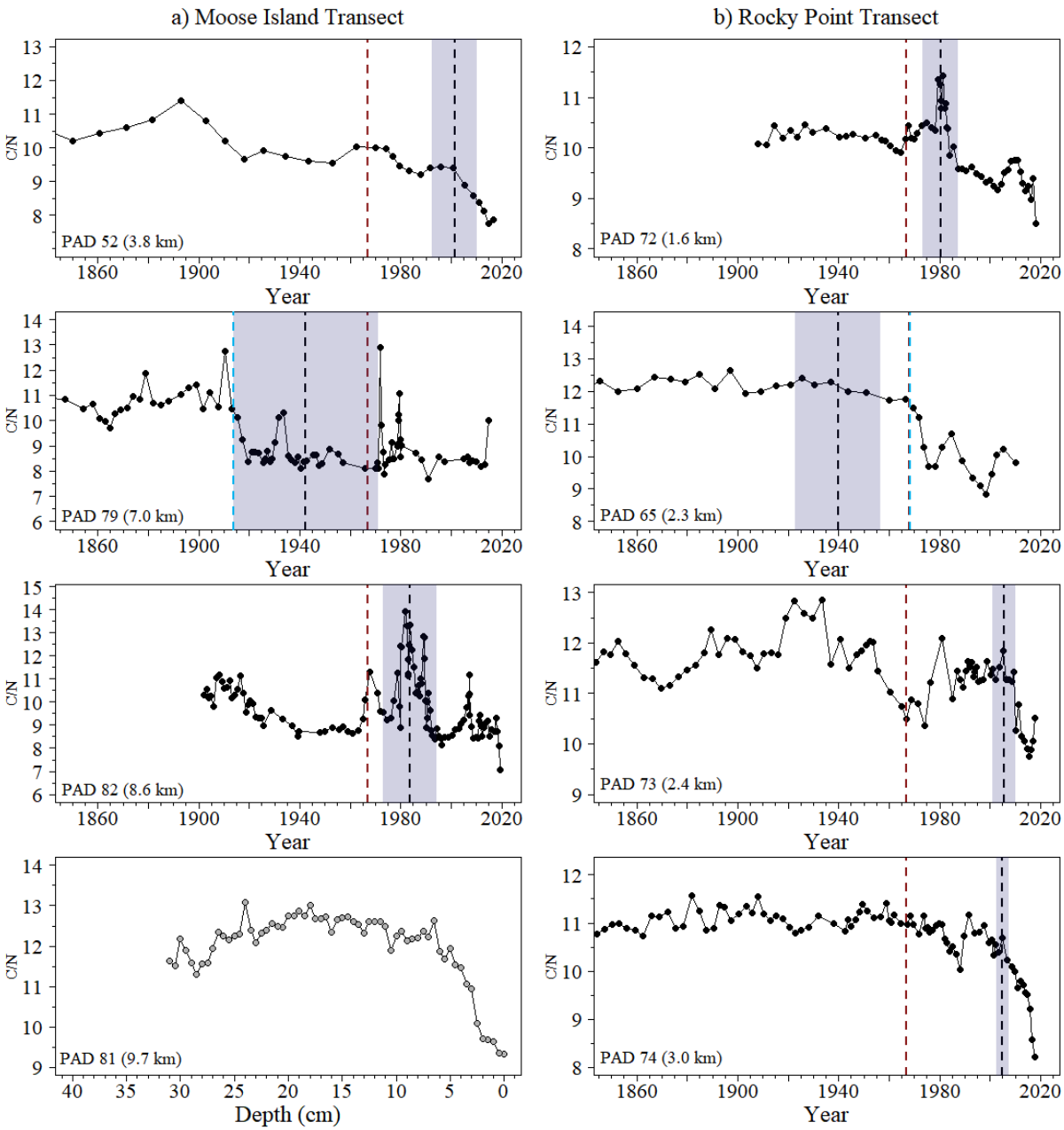

Figure 3.3. Graphs showing stratigraphic variation in organic carbon to nitrogen (C/N) ratios, by depth or time, at the study lakes. Panel a) includes four lakes at the Moose Island transect, arranged by distance from the Peace River (PAD 52, PAD 79, PAD 82, PAD 81). Panel b) includes four lakes along the Rocky Point transect, arranged by distance from the Peace River (PAD 72, PAD 65, PAD 73, PAD 74). Note varying y-axis scales. Profiles with gray symbols could not be dated by measuring ^{210}Pb and ^{137}Cs activity, whereas those with black symbols have an established geochronology from measuring ^{210}Pb activity. Profiles with an established geochronology display stratigraphic profiles from ~1850 to 2020. Breakpoint analysis results are indicated with vertical black dashed lines and the 95% confidence intervals for the breakpoint are shaded in gray. The vertical red dashed lines identify 1968, the year when regulation of Peace River flow by the W.A.C. Bennett Dam began. The blue dashed lines identify an estimate for the points of change at PAD 79 and PAD 65, based on a visual assessment, where it was evident that a breakpoint did not accurately capture the most marked point of change. Results from PAD 52 and PAD 65 are from Faber (2020).

Organic carbon to nitrogen (C/N) ratios are variable in the sediment records from the eight lakes spanning both the Moose Island and Rocky Point transects, and declined in the upper strata at all lakes, except PAD 79 (Figure 3.3a). For lakes in the Moose Island transect, C/N ratios ranged from ~7.1 – 13.0 throughout the cores (Figure 3.3a). For the two lakes with records extending back to the mid-1800s (PAD 52, PAD 79), C/N ratios were highest prior to the early 1900s. Breakpoint analysis for C/N ratios places the main change in trend at ~1943 for PAD 79 [95% CI 1914, 1971], ~1984 for PAD 82 [95% CI 1973, 1994], and ~2001 for PAD 52 [95% CI 1993, 2010] (Figure 3.4a; Table C2). All the breakpoints are statistically significant (ANOVA, $P<0.001$; Table C2). At PAD 79, breakpoint analysis placed the change in slope of linear segments within the middle of an interval of fairly consistent values and did not identify the more marked decline evident at ~1914 as the breakpoint, and which is followed by relatively consistent values thereafter (Figure 3.3a). Also, the 95% CI for the breakpoint at PAD 79 spans a broad interval (~1914-1971). The breakpoints and associated 95% CIs at PAD 52 and PAD 82 occur after 1968 and the 95% CIs span ±~9 and ±~10.6 years about the breakpoint, respectively (Figure 3.3a; Table C2). At PAD 82, C/N ratios rose markedly shortly after ~1968, which infer an increase in influence of floodwaters, and they decline after the breakpoint identified at ~1984. The sediment core from PAD 81 does not have an established chronology, but the record does show a marked shift to lower C/N ratios in sediments above ~5-cm depth (Figure 3.3a). For the three sites with dateable sediment cores along the Moose Island transect, the timing of the breakpoints based on stratigraphic variation in C/N ratios does not differ systematically with distance from Peace River (Figure 3.3a).

For lakes in the Rocky Point transect, C/N ratios ranged from 8.5 – 13.2, and values declined in the upper strata of all cores analyzed (Figure 3.3b). Breakpoint analysis for the C/N

ratios identified changes at ~1940 for PAD 65 [95% CI 1923, 1957], ~1980 for 72 [95% CI 1973, 1988], ~2005 for PAD 74 [95% CI 2003, 2008], and ~2006 for PAD 73 [95% CI 2001, 2010] (Figure 3.3b; Table C2). All breakpoints are statistically significant (ANOVA, $P<0.001$; Table C2). The breakpoint at PAD 72, ~1980 [95% CI 1973, 1988], captures a spike in C/N before a subsequent decrease and a trend of declining values shortly after (Figure 3.3b). Like at PAD 79, breakpoint analysis at PAD 65 identified the change in slope between linear segments to lie within a protracted interval of fairly constant C/N ratios rather than at the subsequent marked shift to declining values that dates to ~1968 (Figure 3.3b). The 95% CI associated with the breakpoint at PAD 65 is considerably broader (±~16.8 years) than those at the other three lakes in the Rocky Point transect (±~2.5-7.1 years). At the other three lakes (PAD 72, PAD 73, PAD 74), the breakpoints and their associated 95% CIs occur after 1968 (Figure 3.3b; Table C2). At all four lakes along the Rocky Point transect, C/N ratios were not discernibly higher between the mid-1800s and early 1900s compared to sediment deposited since the early 1900s, as occurred for lakes along the Moose Island transect.

Overall, stratigraphic variations in C/N ratios across both transects indicate that most lakes have experienced a shift to decreasing values within the past several decades, starting as early as ~1914 (PAD 79) and as late as ~2006 (PAD 73; Figure 3.3b; Table C2). Directional changes to lower C/N ratios, which infer a decline in influence of Peace River floodwaters, coincided with ~1968 at only one of the seven lakes for which sediment cores could be dated (PAD 65), which is from one of the lakes previously analyzed by Faber (2020). Sediment cores collected from all lakes that form part of the current study reveal changes that occurred more than a decade after 1968 (~1980 to ~2006), except for PAD 79 where the record shows no discernible decline since ~1940.

Cores from three of the lakes reveal a rise in C/N ratios coincident with or shortly after ~1968 (PAD 72, PAD 79, PAD 82), which infers an increase in influence of Peace River floodwaters.

3.4 Nitrogen Isotope Composition ($\delta^{15}N$)

Stratigraphic records from eight lakes spanning both the Moose Island and Rocky Point transects possess relatively consistent $\delta^{15}N$ values until they decline in the upper strata (Figure 3.4). For lakes in the Moose Island transect, $\delta^{15}N$ ranged from -1.26 to 3.14 ‰ throughout the cores (Figure 3.4a). Breakpoint analysis placed the onset of the declining trends at ~1972 for PAD 79 [95% CI 1962, 1982], ~1985 for PAD 52 [95% CI 1976, 1994], and ~1996 for PAD 82 [95% CI 1992, 2000] (Figure 3.4a; Table C3). All breakpoints are statistically significant (ANOVA, $P<0.001$; Table C3). For all records from the Moose Island transect, the breakpoints occur after the onset of river regulation in 1968 (Figure 3.4a; Table C3). The lower bound of the 95% CIs post-date the onset of Peace River regulations at PAD 52 and PAD 82, but not at PAD 79 (Figure 3.4a; Appendix Table C3). The 95% CI is the narrowest at PAD 82 (±~3.8 years), while 95% CIs are wider at PAD 52 (± ~9.2 years) and PAD 79 (± ~10.3) (Figure 3.4a; Table C3). In the core from PAD 81, which does not have an established chronology, $\delta^{15}N$ decreases gradually through the upper ~20 cm (Figure 3.4a). For the $\delta^{15}N$ profiles of the Moose Island transect, the age of the breakpoints does not display a clear relationship with distance from Peace River (Figure 3.4a).

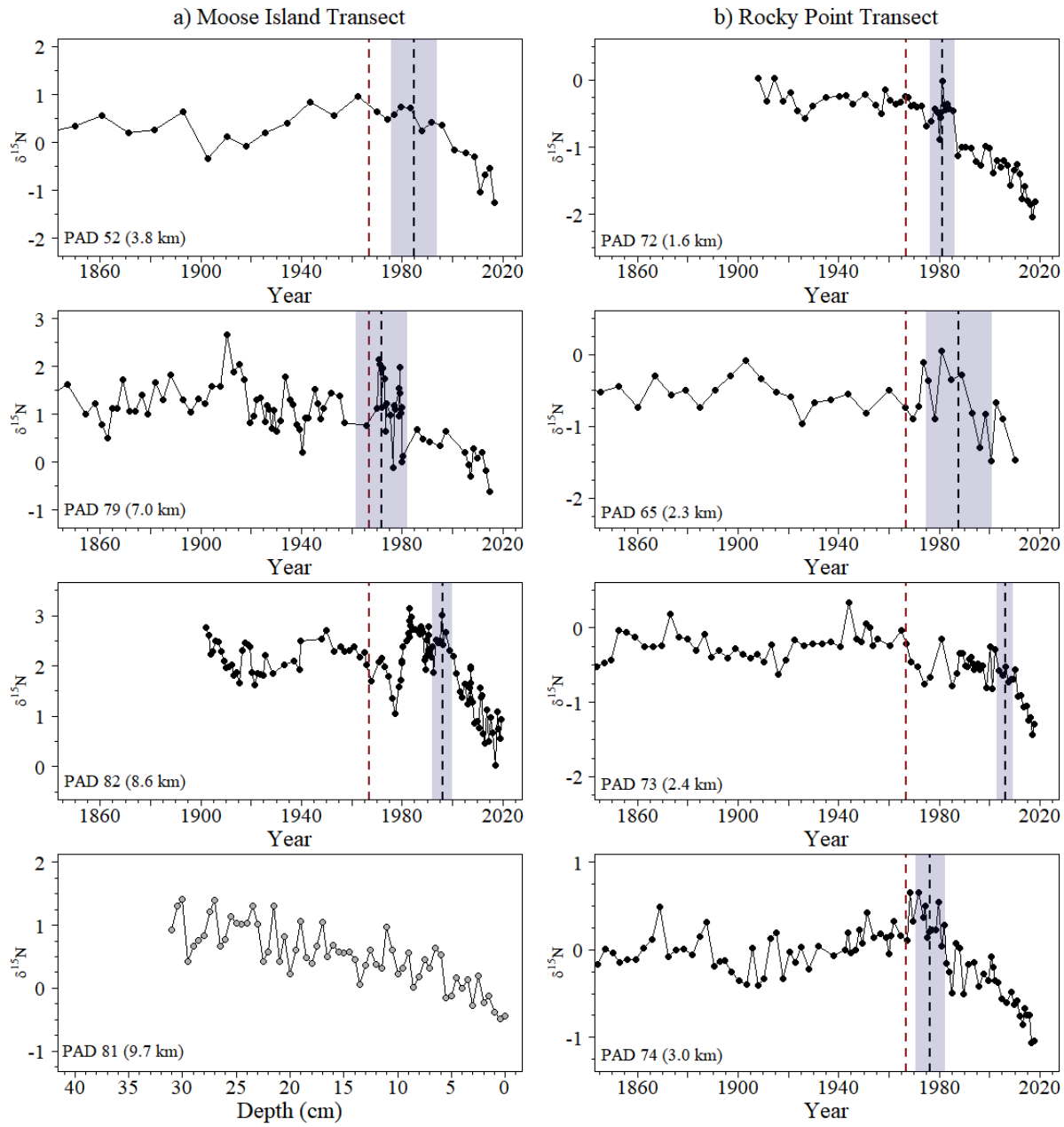

Figure 3.4. Graphs showing stratigraphic variation in $\delta^{15}N$ by depth or time at the study lakes. Panel a) includes four lakes at the Moose Island transect, arranged by distance from the Peace River (PAD 52, PAD 79, PAD 82, PAD 81). Panel b) includes four lakes along the Rocky Point transect, arranged by distance from the Peace River (PAD 72, PAD 65, PAD 73, PAD 74). Note varying y-axis scales. Profiles with gray symbols could not be dated by measuring ^{210}Pb and ^{137}Cs activity, whereas those with black symbols have an established geochronology from measuring ^{210}Pb activity. Profiles with an established geochronology display stratigraphic profiles from ~1850 to 2020. Breakpoint analysis results are indicated with vertical black dashed lines and the 95% confidence intervals for the breakpoint are shaded in gray. The vertical red dashed lines identify 1968, the year when regulation of Peace River flow by the W.A.C. Bennett Dam began. Results from PAD 52 and PAD 65 are from Faber (2020).

For lakes in the Rocky Point transect, stratigraphic values of $\delta^{15}N$ ranged from -2.03 to 0.66 ‰ (Figure 3.4b). Breakpoint analysis placed the onset of the declining trends at ~1977 for PAD 74 [95% CI 1971, 1983], ~1981 for PAD 72 [95% CI 1977, 1986], ~1988 for PAD 65 [95% CI 1975, 2001], and ~2006 for PAD 73 [95% CI 2003, 2009] (Figure 3.4b; Table C3). All breakpoints are statistically significant (ANOVA, $P<0.05$; Table C3). At all four lakes, the lower bound of the 95% CIs about the breakpoints post-date the 1968 onset of Peace River flow regulation (Figure 3.4b; Table C3). Records from PAD 72 (±~4.8 years), PAD 73 (±~3.1 years) and PAD 74 (±~6.0 years) have narrower 95% CI's than the record from PAD 65 (±~13.0 years; Figure 3.4b; Table C3). For the three lakes closest to the river, the timing of the $\delta^{15}N$ breakpoints is sequentially later with distance from the Peace River, but the farthest lake (PAD 74) has a breakpoint that is equivalent to that of the closest lake (Figure 3.4b). Overall, the $\delta^{15}N$ records from both transects indicate that lakes have experienced a shift to decreasing $\delta^{15}N$ within the past several decades, starting as early as ~1972 (PAD 79) and as late as ~2006 (PAD 73; Figure 3.4b; Table C3).

Chapter 4 – Discussion

The relative roles of river regulation and climate change on frequency of ice-jam floods on the Lower Peace River at the Peace-Athabasca Delta (PAD) and associated lake drawdown have been debated for more than 60 years (Timoney, 2013). Several studies that have utilized hydrometric records for Lower Peace River and the modelling of those data, as well as historical and Traditional Knowledge records of flood frequency, have concluded that the declines began in 1968, immediately with the onset of river regulation (e.g., Peters & Prowse, 2001; Beltaos, 2014, 2018; Beltaos & Peters, 2020). In contrast, paleolimnological studies conducted on oxbow lakes and perched basins across the PAD, which include several decades to centuries of information about hydrological conditions prior to regulation of Peace River flow, have demonstrated that climate change and natural geomorphic events, not river regulation, are the main drivers of change to flood regimes and lake drawdown at the PAD (e.g., Wolfe et al., 2006; 2008a; 2008b; 2011; 2012; Kay et al., 2019). Other than two oxbow lake records originally reported in Wolfe et al. (2006), the northern portion of the Peace Sector of the PAD had remained relatively under-investigated until Faber (2020) identified stratigraphic changes in sediment cores from lakes PAD 52 and PAD 65, located near to the Peace River, that appeared to coincide with the onset of river regulation in 1968. To further investigate for evidence of directional hydrologic changes at lakes proximal to the Peace River, this thesis provides broad and targeted spatial coverage of paleolimnological analyses from additional lakes within the Peace Sector that vary in distance (up to 9.7 km) from the Peace River along two transects and include PAD 52 (Moose Island transect) and PAD 65 (Rocky Point transect). Here, sediment records of twelve flood-prone lakes, seven of them with established chronologies, are used to reconstruct past variation in influence of river floodwaters.

The three variables analyzed in the sediment records from all lakes in this study (mineral matter content, C/N ratio and $\delta^{15}N$) do not capture a signal of decline in influence of river floodwaters in the late 1880s to early 1900s, as has been identified in analyses of sediment records from other lakes across the Peace Sector of the PAD (e.g., Wolfe et al., 2005; 2006; 2008a; 2012). The sole exception to this is a decline in C/N ratios beginning at ~1914 at PAD 79. Relatively high mineral matter content throughout the sediment records of all the study lakes suggests they have received frequent inputs of minerogenic sediments via river floodwaters and may be sufficiently flood-prone that the measured variables did not shift their values in response to the decline of flood influence in the late 1800s and early 1900s inferred at other locations. Organic matter content typically increases in sediments of lakes in the PAD when influence of floodwater wanes due to less dilution by influx of minerogenic suspended sediment and associated increase in primary production with increased water clarity (Wiklund et al., 2012; Kay et al., 2019), but an increase may not be recorded in some lakes if a rise in the rate of decomposition offsets the processes that increase organic matter content. Notably, application of a mixing model to metal concentrations in the sediment cores from many of these lakes (including PAD 52, PAD 65, PAD 72, PAD 79, PAD 82) infers marked decline of sediment input from the Peace River between ~1890 and 1930, consistent with a decline in influence of floodwaters occurring decades before regulation of Peace River flow (Kay et al., 2021; Kay, 2022). Thus, the variables utilized in this thesis may not be the most sensitive to shifting hydrological conditions at these highly flood-prone lakes. Nonetheless, stratigraphic variations in mineral matter content, C/N ratios and $\delta^{15}N$ at the study lakes also identify declines in influence of floodwaters during more recent decades (~1967-2016), and below these data are discussed with respect to the potential cause(s) of this decline.

4.1 Assessment of directional change towards reduced influence of Peace River floodwaters and potential cause(s)

Breakpoint analysis was used to determine when directional change occurred in stratigraphic records of mineral matter content, C/N ratios and $\delta^{15}N$ at the study lakes, and to evaluate if they coincide with onset of regulation of Peace River flow in 1968 by the W.A.C. Bennett Dam. There are uncertainties and errors inherent in the age-depth relations established for the sediment cores, as well as in the location of breakpoints in stratigraphic records of sedimentary variables, which need to be taken into consideration when assessing for the occurrence and timing of directional change. Uncertainty in sediment core chronologies increases with depth and age of the intervals analyzed (Appleby, 2001). For the seven study lakes with dated sediment records, uncertainty in age estimates based on CRS modelling of ^{210}Pb activity profiles for the sediment intervals that include the year 1968 ranged from ±7.7 to ±18.4 years (uncertainty expressed as 2 sigma; Tables A1 to A7). A distinctive peak in ^{137}Cs activity, assumed to represent the maximum fallout of ^{137}Cs from above-ground nuclear bomb testing in 1963, occurred in records from three of the lakes and provided additional confidence in accuracy of the ^{210}Pb-based chronologies. The ^{137}Cs peaks at PAD 65 (16.5 cm mid-point depth) and PAD 82 (32.25 cm) corresponded to 1973.6 and 1975.4 based on the ^{210}Pb dating, and 1968 falls within the range of uncertainty of the ^{210}Pb ages (±9.5 and 15.5 years respectively, based on 2 sigma). The ^{137}Cs peak at PAD 79 (22.25 cm) corresponded to a slightly younger age (1980.1), and 1968 falls close to, but just outside, the lower range of uncertainty of the ^{210}Pb age estimate (±9.4 years; lower bound represents 1970.7). These results provide confidence in ability of the age-depth models to identify the 1968 onset of Peace River flow regulation in the stratigraphic records.

Breakpoint analysis is a statistically robust approach that has been used in prior studies to objectively determine points of change associated with anthropogenic stressors (e.g., Stevenson et al., 2016). Key assumptions of breakpoint analysis include that the piece-wise linear models generally follow a linear trend, that the residuals are normally distributed and that the samples are independently and randomly selected. The piece-wise linear models were found to generally follow a linear trend and analysis of residuals suggest they do not deviate markedly from a normal distribution (Appendix C). Samples within a core are, however, sequenced by time of deposition. For this study, the breakpoint analysis was used to assess for evidence of a single breakpoint because the focus was to determine the point of greatest change in the stratigraphic profiles of the measured variable at each lake and assess if it coincides with onset of Peace River flow regulation in 1968. However, analysis for a single breakpoint can be complicated if stratigraphic variation in a sedimentary variable possesses multiple points of change or step-shifts. Among the twenty-one breakpoint analyses formed (dated sediment records at seven lakes multiplied by three variables analyzed on each record), there were only two main instances where the breakpoint analysis failed to identify the point of most apparent change based on visual inspection. These instances occurred in the stratigraphic profiles of C/N ratios from PAD 65 and PAD 79 (Figure 3.3). At PAD 79, a step-shift is apparent at ~1914 when the C/N ratio declined markedly during an interval of ~5 years and remained relatively constant thereafter (except in a few sporadic samples with higher values). However, the breakpoint analysis identified the main change to have occurred at ~1943 when a directional change in the C/N ratio is not as evident. Breakpoint analysis determined the main change in C/N ratios at PAD 65 to occur at ~1940, which falls during an interval without apparent directional change spanning ~1850-1968 rather than the more obvious decline at ~1968 (Figure 3.3). Hereafter, we use the adjusted dates based on visual determination to report the timing of

greatest change in the C/N ratios at PAD 65 (~1968) and PAD 79 (~1914; see Figure 4.1). The other 19 breakpoint analyses performed on the three sedimentary variables across the sediment cores from seven lakes (including the 95% CIs) appeared to capture well the visually detectable main changes in their stratigraphic records (Figures 3.2-3.4).

To assess if the timing of inferred decline of river influence coincides with onset of Peace River flow regulation by the W.A.C. Bennett Dam in 1968, results for the breakpoint analyses of stratigraphic variation in mineral matter content, C/N ratios and $\delta^{15}N$ at the study lakes are compiled in Figure 4.1. When considering the range of uncertainty captured by the 95% CIs, only three of the twenty-one breakpoints (seven lake sediment records with established sediment core chronologies and three variables each) coincide with 1968. These include declines in mineral matter content at PAD 52, $\delta^{15}N$ at PAD 79, and C/N ratio at PAD 65 (Figure 4.1). At PAD 52, breakpoints for $\delta^{15}N$ and the C/N ratio occur one to three decades later than that for mineral matter content. At PAD 79, breakpoints for all three variables differ widely, which confounds ability to attribute the coincidental breakpoint for $\delta^{15}N$ to effects of the W.A.C. Bennett Dam. At PAD 65, breakpoints for the other two variables (mineral matter content, $\delta^{15}N$) are coincidental and infer a decline in influence of floodwaters began ~1980-1995 based on the 95% CIs, which is more than a decade after river regulation began. Of the remaining 18 breakpoint analyses, one predates the W.A.C. Bennett Dam by several decades (~1914 based on C/N ratios at PAD 79) and 17 occur several years to decades after regulation of Peace River flow began. Given long- and wide-held contention that flood frequency and perched lake water levels declined *beginning at 1968* (PADPG, 1973; Timoney et al., 1997; Peters & Prowse, 2001; Beltaos, 2014, 2018; Beltaos & Peters, 2020), results from this study do not provide strong evidence that flood-prone lakes adjacent to the Peace River within the PAD have been strongly affected by operation of the W.A.C.

Bennett Dam. Instead, inferred decline of flood influence based on these variables post-dates the dam by many years and decades, which could just as likely support a strong role of climate. Interestingly, many of the breakpoints in this thesis fall within the 1980s, a period with known lower flood frequency (an observation that is noted in historical records collected by Timoney et al., 1997; Figure 4.1c). Thus, many of the breakpoints likely identify the responses of the lakes to the more recent and intensive drier conditions in the 1980s (Figure 4.1). Another period of lower flood frequency in the 2000s has been noted and appears to also be captured by a second group of breakpoints in some lakes in this study (Timoney, 2021). These correspondences lend confidence that the breakpoints are accurately identifying points of change associated with climate-driven lake drying. Given that all but four of the breakpoints post-date the onset of Peace River flow regulation, a contributing role of the W.A.C. Bennett Dam cannot be fully discounted because it is possible that shifts in climatic conditions may have crossed thresholds where combined effects of climate and river regulation exert a delayed influence on hydrological processes and sediment deposition at the study lakes.

The timing of the breakpoints based on $\delta^{15}N$ appear to be more consistent among lakes in the Moose Island and Rocky Point transects than for the breakpoints based on mineral matter content and C/N ratios (Figure 4.1). This feature stimulated interest to explore possible factors influencing relatively consistent timing of decline in $\delta^{15}N$, as presented in the next section.

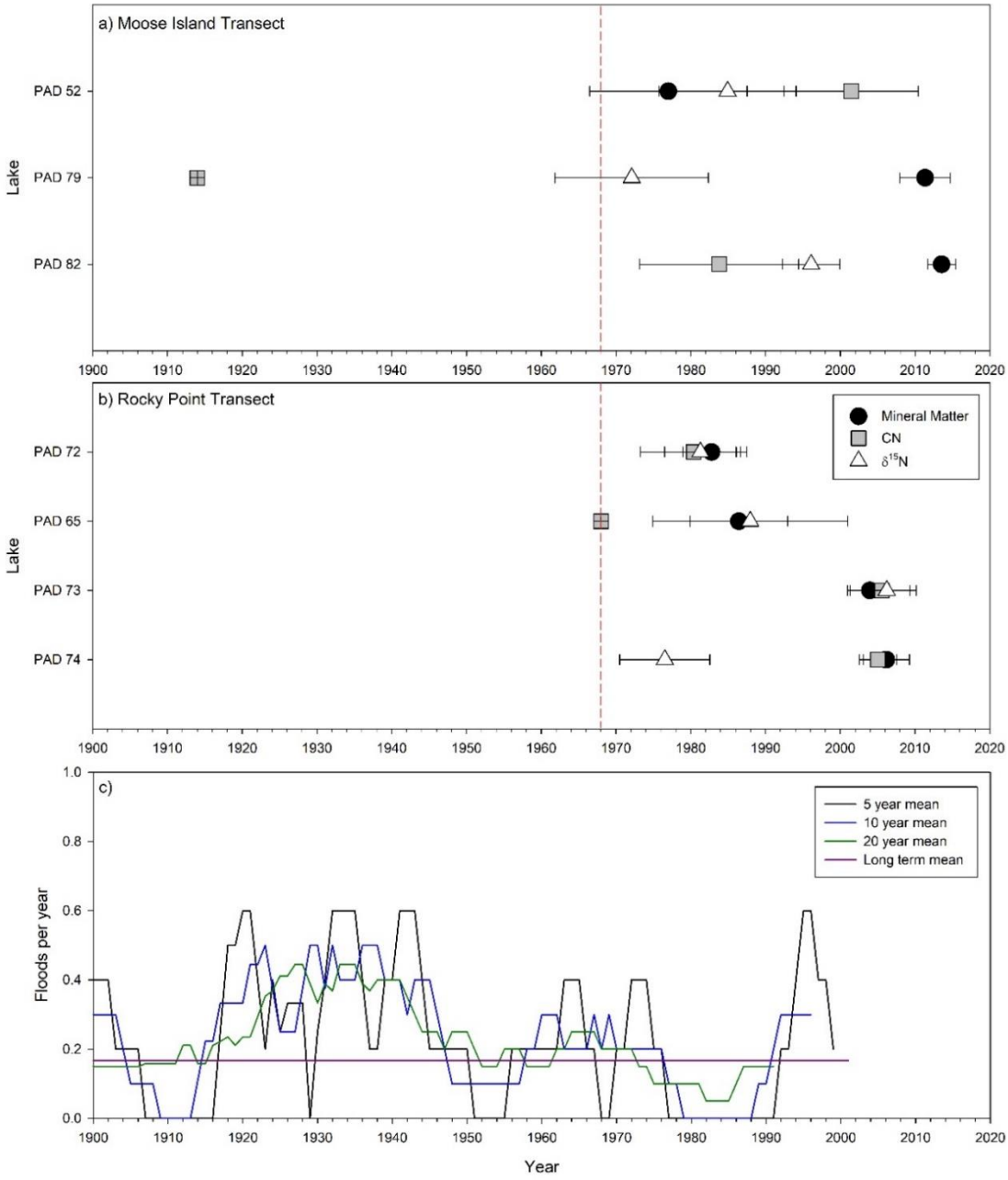

Figure 4.1. Figure depicts the timing of the breakpoints and their associated 95% confidence intervals (CI) for each proxy (mineral matter content, organic carbon to nitrogen ratio (C/N), and $\delta^{15}N$). Panel a) includes three lakes at the Moose Island transect by distance from the Peace River (PAD 52, PAD 79, PAD 82). Panel b) includes four lakes along the Rocky Point transect by distance from the Peace River (PAD 72, PAD 65, PAD 73, PAD 74). Each breakpoint is represented by a point with mineral matter represented by a black circle, C/N represented by a gray square, and $\delta^{15}N$ represented by a white triangle. 95% CIs are presented as bars around each breakpoint. Additionally, two breakpoint values (C/N for PAD 79 and PAD 65) were not accurately representative of change based on visual assessments, so instead a visual estimation of the main point of change was used and is represented by a gray square with a cross. Panel c) depicts the 5- (black line), 10- (blue line), 20- (green line) year means and the long term (purple line) mean of flood frequency from historic and Traditional Knowledge records, as compiled by Timoney et al. (1997).

4.2 Assessing the cause of recent decline in $\delta^{15}N$ in the floodplain lake sediment records

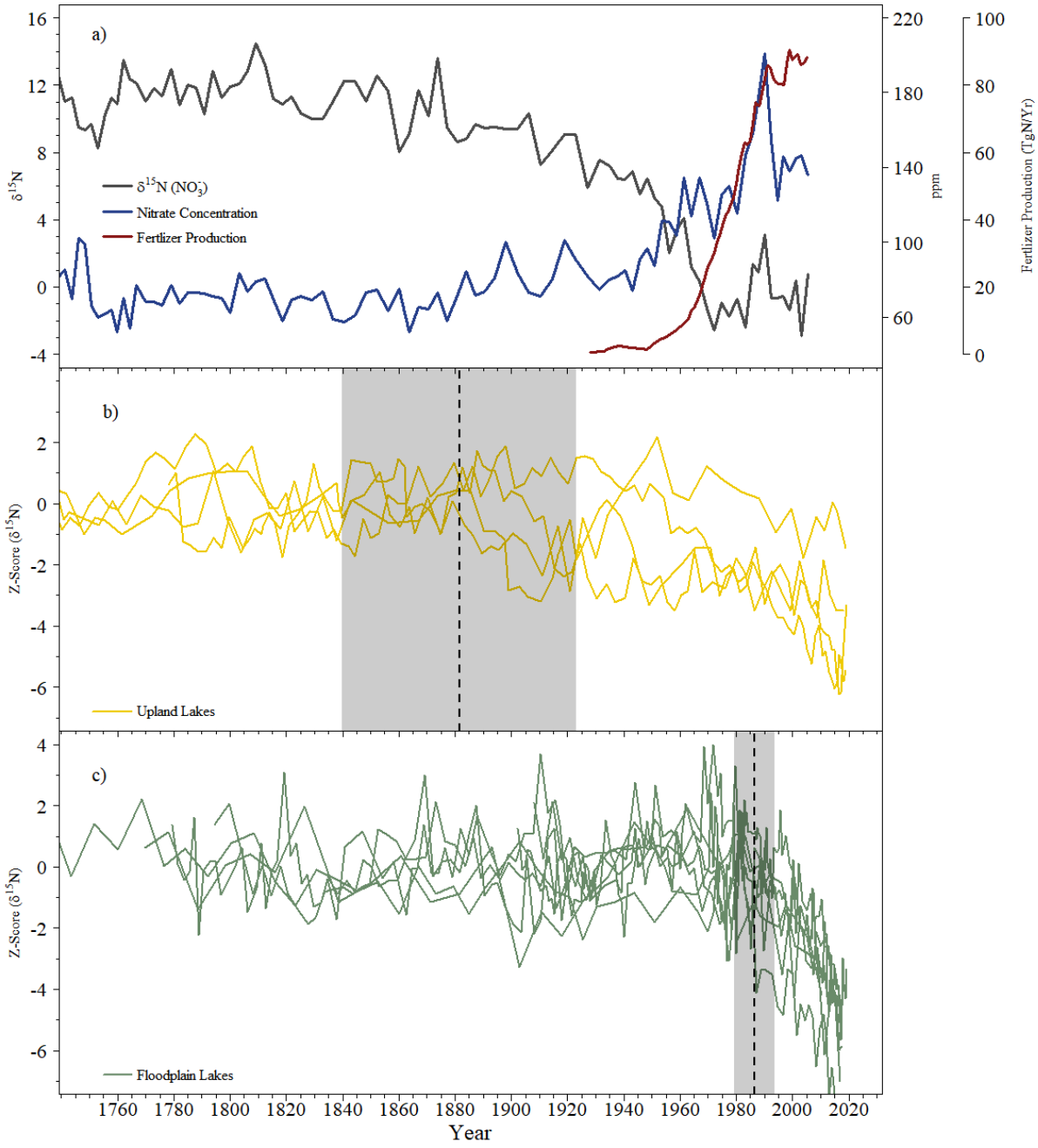

Figure 4.2. Panel a) depicts the $\delta^{15}N$ of nitrate (NO_3^-; gray line) and the nitrate (NO_3^-) concentration (blue line) from the Greenland Summit Ice Core (Hastings et al., 2009) as well as the Global Fertilizer Production (red line; Holland et al., 2005). Panel b) displays the Z-scores of $\delta^{15}N$ data (yellow lines) in sediment cores from four upland lakes adjacent to the PAD (sites AC1, AC3, AC5 and PC4; data from Brown, 2022). Panel c) displays the Z-scores of $\delta^{15}N$ data (green lines) for the seven dated floodplain lakes along the Moose Island and Rocky Point transects (PAD 52, PAD 65, PAD 72, PAD 73, PAD 74, PAD 78, and PAD 82). Average breakpoint analysis results for each set of lakes are indicated with vertical black dashed lines and the average 95% confidence intervals for the breakpoint are shaded in gray.

Analysis of nitrogen stable isotope composition in sediment cores is not widely used to reconstruct past changes in hydrological processes, but this variable was included in my thesis because I observed a fairly consistent trend towards lower $\delta^{15}N$ values since the late ~1980s at all lakes, which is consistent with the direction of change in $\delta^{15}N$ of materials deposited via atmospheric transport as a consequence of human alteration of the nitrogen cycle (Holtgrieve et al., 2011) as presented below.

To investigate possible causes for the observed recent declines in $\delta^{15}N$ values from the sediment records in this study, $\delta^{15}N$ data were standardized using z-scores for the sediment records from the seven lakes with established chronologies (PAD 52, PAD 65, PAD 72, PAD 73, PAD 74, PAD 79, PAD 82; hereafter referred to as floodplain lakes; Figure 4.2c). Temporal changes at the upland lakes were compared to z-scores of $\delta^{15}N$ in sediment cores from four upland lakes adjacent to the PAD which are outside the reach of floodwaters and are assumed to receive deposition of N almost exclusively via atmospheric pathways (AC1, AC3, AC5 and PC4; obtained from Brown, 2022; Figure 4.2b). The upland lakes identified with 'AC' are located adjacent to the southern Athabasca Sector, whereas the lake with 'PC' is adjacent to the northern Peace Sector. For sediment cores from the floodplain and upland lakes, z-scores were calculated using the mean and standard deviation of $\delta^{15}N$ values in samples deposited before ~1900. Pre-1900 was used to represent baseline $\delta^{15}N$ values and assumed to be before the onset of anthropogenic influence of atmospheric deposition of reactive nitrogen (Holtgrieve et al., 2011). The sediment cores from PAD 72 and PAD 82 did not extend to before ~1900, and instead the mean and standard deviation of the data prior to the $\delta^{15}N$ breakpoint for each lake record were used (~1981 and ~1996,

respectively; Table C1). The $\delta^{15}N$ breakpoint and 95% confidence interval (CI) of the upland lakes and floodplain lakes were averaged for each group of lakes (Figure 4.2b & c).

On average, decline of $\delta^{15}N$ in sediments of the floodplain lakes began ~1987 [95% CI 1979,1994] (Figure 4.2c), which is about a century later than occurred at the upland lakes (average ~1882, 95% CI 1840, 1923; Figure 4.2b). The onset of the declining trend in $\delta^{15}N$ at the upland lakes aligns with the initial rise in atmospheric nitrate concentration and decline in $\delta^{15}N$ of nitrate recorded in the Greenland Summit ice core (Hastings et al., 2009; Figure 4.2a & b). Similar decline in $\delta^{15}N$ has been observed in sediment cores from remote lakes in other regions and has been attributed to rising emissions from fossil fuel combustion and other industrial activities after possible influence from diagenetic processes was ruled out as unlikely (Holtgrieve et al., 2011). The century delay in decline of $\delta^{15}N$ in sediments of the floodplain lakes likely identifies that river floodwaters continued to dominate supply of N and masked signals of decline in $\delta^{15}N$ in materials deposited from the atmosphere until ~1987. Decline of $\delta^{15}N$ at the floodplain lakes did not coincide with decline of C/N ratios at most floodplain lakes (except at PAD 72 and PAD 73) and sedimentation rates differed markedly among the floodplain lakes. Thus, diagenetic processes are unlikely to account for the relatively consistent timing of decline in $\delta^{15}N$ (e.g., Holtgrieve et al., 2011). Instead, the observed average onset of decline in $\delta^{15}N$ in ~1987 likely reflects when influence of Peace River floodwaters decreased sufficiently at these flood-prone lakes to reveal a measurable decline in $\delta^{15}N$ supplied via atmospheric pathways. Another consideration for the cause of this trend is nitrogen oxide (NOx) emissions from the Athabasca Oil Sands Region (AOSR), located ~200 km to the south of the study sites. However, prior work in this region identified that the $\delta^{15}N$ signature in the AOSR region ranges from -4.9 to 6.3‰ (Proemse et al.,

2013). While NOx emissions from oil sands development are a concern in the region, the wide range in the recorded $\delta^{15}N$ values from the AOSR suggests these records would not necessarily cause a trend to lower $\delta^{15}N$ values, as was observed in our records.

Chapter 5 – Conclusions, Implications and Recommendation

5.1 Key findings and implications

After analysis of sediment cores collected from lakes PAD 52 and PAD 65 displayed evidence consistent with reduced influence of river floodwaters coincident with or shortly after the onset of Peace River flow regulation in 1968 (Faber, 2020), I investigated if this pattern is widespread among lakes in lesser-studied areas of the northern portion of the Peace Sector of the PAD adjacent to the Peace River. Sediment cores were collected from twelve flood-prone lakes at varying distances from the Peace River (up to 9.7 km) along two transects (Moose Island and Rocky Point), and analyzed for mineral matter content, C/N ratio and nitrogen isotope composition to assess for directional change to reduced influence of floodwaters beginning in 1968. High mineral matter content of sediment demonstrates that all lakes in both transects have been prone to strong influence of floodwaters. However, declines in mineral matter content, C/N ratios and $\delta^{15}N$ were observed in upper strata of all sediment cores, identifying reduction in influence of Peace River floodwaters. Breakpoint analysis was conducted on stratigraphic records from the seven lakes where a reliable chronology could be generated, and only three of the twenty-one breakpoints and their 95% CIs coincided with the onset of river regulation in 1968 (mineral matter content at PAD 52, C/N at PAD 65, $\delta^{15}N$ at PAD 79). Significant breakpoints were detected for all the other variables at the seven lakes with dated cores, but they occurred several years to decades after onset of Peace River flow regulation. The sole exception is for C/N ratios at PAD 79, which declined at ~1914 and remained relatively constant thereafter. These findings do not provide strong support for widely held notion that the ice-jam flood regime of the Lower Peace River and perched lake drying at the PAD began in 1968 due to effects of the W.A.C. Bennett Dam. Instead, climatic shifts to lower snowpack and warmer temperatures since at least the mid-

1970s appear to be a main driver for reduced river floodwater influence at these flood-prone lakes (Prowse & Conly, 1998; Beltaos et al., 2006; Lamontagne et al., 2021). However, it is not possible to discount that climatic trends during the past couple of decades may have caused the river flow regime to pass a threshold and delay effects of the W.A.C. Bennett Dam. Application of a mixing model based on metal concentrations in the sediment cores from six of the study lakes (PAD 52, PAD 65, PAD 72, PAD 74, PAD 79, PAD 82) infers marked decline of sediment input from the Peace River between ~1890 and 1930 (Kay et al., 2021; Kay, 2022), which was not captured by the variables measured within this thesis research and identifies a strong role of climate long before anthropogenic alteration of the Peace River flow regime. Thus, the variables reported in this thesis may not be the most sensitive to hydrological changes at these highly flood-prone lakes, but they appear to have captured well signals of declining influence of floodwaters during more recent decades.

Regardless of the cause of decline in influence of river floodwaters to lakes within 10 km of the Peace River, drawdown of lake and river water levels is a key concern for the Indigenous Peoples who rely on adequate water levels for transportation and access to the delta's natural resources (MCFN, 2014; Straka et al., 2018). Application of models that quantify influence of factors that promote ice-jam flood formation predict that flood frequency is likely to decrease in future years to decades (DeBeer et al., 2016; Lamontange et al., 2021), with negative consequences for ecosystem function and Indigenous land users (Wolfe et al., 2012; MCFN, 2014; Straka et al., 2018; Timoney, 2021). A federal Action Plan for Wood Buffalo National Park intends to increase water abundance in the PAD but, based on the data generated in this thesis, actions must address effects of climate change and not solely attempt to mitigate perceived effects of the W.A.C. Bennett Dam (WBNP, 2019).

5.2 Recommendations for Future Research

In the future, breakpoint analyses could be performed in more complex ways to account for possibility of multiple breakpoints. Alternately, General Additive Models, and associated first derivative testing, could be explored to assess if they identify the onset of trends in stratigraphic variables with improved statistical rigor (Simpson, 2018). Analyses could be conducted on grain size distributions of the sediment cores from the study lakes along both transects to provide further insight into changes in the sediment source and mechanisms for sediment transport (Sly, 1989). For example, mean grain size of sediment has been used to track flood events in flood-prone oxbow lakes in the PAD (e.g., Wolfe et al., 2006). Analysis of sediment cores by X-ray fluorescence (XRF) can provide a wealth of information about changes in elemental composition of mineral-rich sediment (Davies et al., 2015), which can be used to track changes in source of sediment and influence of river floodwaters as was done at oxbow lakes upstream of the PAD (Stratton, 2022; Girard, 2022). XRF detectors can be placed on core scanning infrastructure to allow for high-resolution scanning of sediment cores (e.g., < 1-mm intervals), which permit generation of fine temporal resolution of stratigraphic profiles. The element count data provided by XRF can be used to delineate flood events using profiles of single elements (e.g., Si, Al, K, Ca, Ti, Rb) and ratios of elements (e.g., Zr/Fe, Fe/Ca, Zr/Ti), and variations in grain-size can be inferred from counts of Zr, Si, Ti or ratios such as Al/Si, Fe/Si, Fe/Ti, Ti/K (Davies et al., 2015). These above analyses may be used to also compare to results from metal concentration mixing model results of Kay (2022) and provide information to help further discern the relative roles of Peace River flow regulation and climate change on the decline in flood influence of lakes in the Peace Sector of the PAD.

References

Appleby, P.G. (2001). Chronostratigraphic techniques in recent sediments. In J. P. Smol (Ed), Tracking Environmental Change Using Lake Sediments: Basin Analysis, Coring, and Chronological Techniques, Developments in Paleoenvironmental Research, *1*: 171–203.

Appleby, P.G., & Oldfield, F. (1978). The Calculation of Lead-210 Dates Assuming a Constant Rate of Supply of Unsupported 210Pb to the Sediment. *CATENA, 5*: 1-8.

Beltaos, S. (2014). Comparing the impacts of regulation and climate on ice-jam flooding of the Peace- Athabasca Delta. *Cold Regions Science and Technology, 108*: 49-58.

Beltaos, S. (2018). The 2014 ice-jam flood of the Peace-Athabasca Delta: Insights from numerical modelling. *Cold Regions Science and Technology, 155*: 367-380

Beltaos, S. & Peters, D. L. (2020). Naturalized flow regime of the regulated Peace River, Canada, during the spring breakup of the ice cover. *Cold Regions Science and Technology, 172*: 103005.

Beltaos, S., Prowse, T. D., & Carter, T. (2006). Ice regime of the lower Peace River and ice-jam flooding of the Peace-Athabasca Delta. *Hydrological Processes, 20*: 4009-4029.

Brown, K. C. (2022). Evaluating the role of local climate change on reduced freshwater availability at the Peace-Athabasca Delta using paleolimnology. MSc Thesis, University of Waterloo

Davies, S. J., Lamb, H. F., & Roberts, S. J. (2015). Micro-XRF core scanning in paleolimnology: recent developments. In: Croudace IW, Rothwell RG (eds) Micro-XRF studies of sediment cores. Springer Science, New York, 189–226.

DeBeer, C.M., Wheater, H. S., Carey, S. K., & Chun, K. P. (2016). Recent climatic, cryospheric, and hydrological changes over the interior of western Canada: a review and synthesis. *Hydrology and Earth System Science, 20*: 1573-1598.

Faber, J. A., Reconstructing hydrologic conditions and metals supplied by the Peace River to the Peace-Athabasca Delta. (2020). Wilfrid Laurier University, MSc Thesis, Wilfrid Laurier University.

Flett, L., Bill L., Crozier, J., & Surrendi, D. (1996). A report of wisdom synthesized from the Traditional Knowledge Component Studies. Northern River Basins Study, Synthesis Report No. 12. Alberta Environmental Protection: Edmonton, Canada.

Girard, C. L. (2022). Paleohydrology of the Wabasca River and relations with flood regimes at the downstream Peace-Athabasca Delta. MSc Thesis, University of Waterloo.

Glew J., Smol J. P., & Last W. M. (2001). Sediment core collection and extrusion. In: Last WM, Smol JP (eds) Tracking environmental change using lake sediments: basin analysis, coring, and chronological techniques, Developments in Paleoenvironmental Research. *Kluwer Academic Publishers*, Dordrecht, *1:* 73–105.

Hasting, M.G., Jarvis, J.C., & Steig, E.J. (2009). Anthropogenic impacts on nitrogen isotopes of ice-core nitrate. *Science. 324* (5932): 1228.

Heiri, O. (2001). Loss on ignition as a method for estimating organic and carbonate content in sediments: Reproducibility and comparability of results. *Journal of Paleolimnology, 25*(1): 101-110.

Holland, A., Lee-Taylor, J., Nevison, C., & Sulzman, J. (2005). Global N Cycle: Fluxes and N2O Mixing Ratios Originating from Human Activity (data set available at www.daac.ornl.gov, doi:10.3334/ORNLDAAC/797; Distributed Active Archive Center, Oak Ridge National Laboratory, Oak Ridge, TN).

Holtgrieve, G. W., Schindler, D. E., Hobbs, W. O., Leavitt, P. R., Ward, E. J., Bunting, L., Chen, G., Finney, B. P., Gregory-Eaves, I., Holgrem, S., Lisac, M. J., Lisi, P. J., Nydick, K., Rogers, L. A., Saros, J. E., Selbie, D. T., Shapely, M. D., Walsh, P. B., & Wolfe, A. P. (2011). A coherent signature of anthropogenic nitrogen deposition to remote watersheds of the northern hemisphere. *Science, 334:* 1545.

International Union for Conservation of Nature and the World Heritage Center (IUNC/WHC). (2017). Reactive Monitoring Mission to Wood Buffalo National Park, Canada. Technical Report, 28-30.

IPCC. (2013). Climate Change 2013: The physical science basis. Contribution from Working Group 1 to the fourth assessment report of the Inter-Governmental Panel on Climate Change, in IPCC Fourth Assessment Report.

Johnston, J.W., Köster, D., Wolfe, B.B., Hall, R.I., Edwards, T.W.D., Endres, A.L., Martin, M.E., Wiklund, J.A., & Light, C. (2010). Quantifying Lake Athabasca (Canada) water level during the 'Little Ice Age' highstand from palaeolimnological and geophysical analyses of a transgressive barrier-beach complex. *The Holocene, 20*(5): 801-911.

Kay, M. L. (2022). Development and application of paleolimnological analyses to disentangle the roles of natural processes and anthropogenic activities on contaminant deposition and hydrological conditions across a northern delta. PhD Thesis, University of Waterloo.

Kay, M. L., Swanson, H. K., Burbank, J., Owca, T. J., MacDonald, L. A., Savage, C. A. M., Remmer, C. R., Neary, L. K., Wiklund, J. A., Wolfe B. B., & Hall, R. I. (2021). A Bayesian mixing model framework for quantifying temporal variation in source of sediment to lakes across broad hydrological gradients of floodplains. *Limnology and Oceanography: Methods, 19:* 540 – 551.

Kay M.L., Wiklund, J.A., Remmer, C.R., Neary, L. K., Brown, K., Ghosh, A., MacDonald, E., Thomson, K., Vucic, J. M., Wesenberg, K., Hall R. I., & Wolfe, B. B. (2019). Bi-directional hydrological changes in perched basins of the Athabasca Delta (Canada) in recent decades caused by natural processes. *Environmental Research Communications, 1*(8): 11001.

Lamontagne, J. R., Jasek, M., & Smith, J. D. (2021). Coupling physical understanding and statistical modeling to estimate ice jam flood frequency in the northern Peace-Athabasca Delta under climate change. *Cold Regions Science and Technology,* 192: 103383.

Leng, M. J., Lamb, A. L., Marshall, J. D. Wolfe, B. B., Jones, M. D., Holmes, J. A., & Arrowsmith, C. (2006). Developments in Paleoenvironmental Research Vol 10: 4 Isotopes in Lake Sediments. Published by Springer, Dordrecht.

McGowan, S., Leavitt, P. R., Hall, R. I., Wolfe, B. B., Edwards, T. W. D., Karst-Riddoch, T., Vardy, & S. R. (2011). Interdecadal declines in flood frequency increase primary production in lakes of a northern river delta. *Global Change Biology, 12:* 1212-1224.

Meyers, P.A. & Teranes, J.L. (2001). Sediment Organic Matter. In: Last, W.M., Smol, J.P. (Eds.), Tracking Environmental Change using Lake Sediments, Vol. 2: Physical and Chemical Techniques. *Kluwer Academic Publishers,* Dordrecht.

Mikisew Cree First Nation (MCFN). (2014). Petition to the World Heritage Committee requesting Inclusion of Wood Buffalo National Park on the List of World Heritage in Danger. 1-18.

Mikutta, R., Kleber, M., Kaiser, K., & Jahn, R. (2005). Review: Organic matter removal from soils using hydrogen peroxide, sodium hypochlorite, and disodium peroxodisulfate. *Soil Science Society of America Journal, 69*: 120-135.

Muggeo, V.M.R. (2008) Segmented: an R package to fit regression models with broken-line relationships. *R News,* 8(1): 20–25

Neary, L.K., Remmer, C.R., Krist, J., Wolfe, B.B., & Hall, R.I. (2021). A new lake classification scheme for the Peace-Athabasca Delta (Canada) characterizes hydrological processes that cause lake-level variation. *Journal of Hydrology: Regional Studies, 38*: 100948.

Ormerod, S. J., Dobson, M., Hildrew, A. G., & Townsend C. R. (2010). Multiple stressors in freshwater ecosystems. *Freshwater Biology, 55*(Suppl. 1): 1-4.

Peace-Athabasca Delta Project Group (PADPG). (1973). Peace-Athabasca Delta Project. Technical Report, 2, 75.

Peace-Athabasca Delta Technical Studies (PADTS). (1996). Final Report PADTS Steering Committee Fort Chipewyan Alberta 106.

Peters, D. L., & Prowse, T. D. (2001). Regulation effects on the lower Peace River, Canada. *Hydrological Processes, 15*(16): 3181-3194.

Peters, D.L., Prowse, T.D., Marsh, P., Lafleur, P.M., & Buttle, J.M. (2006). Persistence of water within perched basins of the Peace-Athabasca Delta, Northern Canada. *Wetlands Ecology and Management, 14:* 221-243.

Proemse, B. C., Mayer, B., Fenn, M. E., & Ross, C. S. (2013). A multi-isotope approach for estimating industrial contributions to atmospheric nitrogen deposition in the Athabasca oil sands region in Alberta, Canada. *Environmental Pollution. 182:* 80-91.

Prowse, T. D., & Conly, F. M. (1998). Impacts of climatic variability and flow regulation on ice-jam flooding of a northern delta. *Hydrological Processes, 12*(10-11): 1589–1610.

Prowse, T.D. & Conly, F.M. (2002). A review of hydroecological results of the Northern River Basins Study, Canada. Part 2. Peace-Athabasca Delta. *River Research and Applications, 18*: 447-460.

Prowse, T. D., & Lalonde, V. (1996). Open-water and ice-jam flooding of a northern delta. *Nordic Hydrology. 27*: 85-100.

Prowse, T.D., Peters, D.L., Baltaos, S., D.L., Pietroniro, Romolo, L.A., Toyra, J., & Leconte, R. (2002). Restoring Ice-jam Floodwater to a Drying Delta Ecosystem. *Water International, 27*(1): 59 – 69.

Remmer, C. R., Klemt, W. H., Wolfe, B. B., & Hall, R. I. (2018). Inconsequential effects of flooding in 2014 on lakes in the Peace-Athabasca Delta (Canada) due to long-term drying. *Limnology and Oceanography, 63*(4): 1502-1518.

Remmer, C. R., Owca, T., Neary, L., Wiklund, J. A., Kay, M. L., Wolfe, B. B., & Hall, R. I. (2020). Delineating extent and magnitude of river flooding to lakes across a northern delta using water isotope tracers. *Hydrological Processes, 303-320*.

Schindler, D.W. & Donahue, W.F. (2006). An impending water crisis in Canada's western prairie provinces. *Proceedings of the National Academy of Science of the United States of America, 103*(19): 7210-7216.

Schindler, D.W. & Smol, J. P. (2006). Cumulative Effects of Climate Warming and Other Human activities on Freshwaters of Arctic and Subarctic North America. *Ambio, 35* (4): 160 – 168.

Simpson, G.L. (2018). Modelling palaeoecological time series using generalized additive models. *Frontiers in Ecology and Evolution,* 6.

Sinnatamby, R.N., Yi, Y., Sokal, M.A., Clogg-Wright, K.P., Asada, T., Vardy, S.R., Karst-Riddoch, T.L., Last, W.M., Johnston, J.W., Hall, R.I., Wolfe, B.B., & Edwards, T.W.D. (2010). Historical and paleolimnological evidence for expansion of Lake Athabasca (Canada) during the Little Ice Age. *Journal of Paleolimnology, 43*: 705-717.

Sly, P. G. (1989). Sediment dispersion: part 1, fine sediments and significance of the silt/clay ratio. *Hydrobiologia, 176/177*: 99-110

Smol, J. P. (2010). The power of the past: using sediments to track the effects of multiple stressors on lake ecosystems. *Freshwater Biology, 55* (Suppl. 1): 34-59.

Stevenson, M. A., McGowan, S., Anderson, N. J., Foy, R. H., Leavitt, P. R., McElarney, Y. R., Engstrom, D. R., & Pla-Rabés, S. (2016). Impacts of forestry planting on primary production in upland lakes from north-west Ireland. *Global Change Biology, 22:* 1490-1504.

Straka, J.R., Antoine, A., Bruno, R., Campbell, D., Campbell, R., Campbell, R., Cardinal, J., Gibot, G., Gray, Q.Z., Irwin, S., Kindopp, R., Ladouceur, R., Ladouceur, W., Lankshear, J., Maclean, B., Macmillan, S., Marcel, F., Marten, G., Marten, L., McKinnon, J., Patterson, L.D., Voyageur, C., Voyageur, M., Whiteknife, G.S., & Wiltzen, L. (2018). "We Used to Say Rats Fell from the Sky After a Flood": Temporary Recovery of Muskrat Following Ice Jams in the Peace-Athabasca Delta. *Arctic, 71*(2): 218-228.

Stratton, M. S. (2022). Investigating the role of the Smoky River watershed on past ice-jam flood regimes at the Peace-Athabasca delta via analysis of oxbow lake sediment cores. MSc Thesis, University of Waterloo.

Telford, J.V.K., Kay, M.L., Van der Heide, H.C., Wiklund, J.A., Owca, T.J., Faber, J.A., Wolfe, B.B. & Hall, R.I. (2020). Building upon open-barrel corer and sectioning systems to foster the continuing legacy of John Glew. *Journal of Paleolimnology, 65*: 271-277.

Timoney, K. P. (2002). A dying delta? A case study of a wetland paradigm. *Wetlands, 22*: 282–300.

Timoney, K. P. (2006). Landscape cover change in the Peace-Athabasca Delta, 1927-2001. *Wetlands*, 26: 765-778.

Timoney, K. P. (2013). The Peace-Athabasca Delta: Portrait of a Dynamic Ecosystem. Edmonton, University of Alberta Press

Timoney, K. P. (2021). Flooding in the Peace-Athabasca Delta: climatic and hydrologic change and variation over the past 120 years. *Climatic Change, 169*:34 1-26.

Timoney, K. P., Peterson, G., Fargey, P., Peterson, M., McCanny, S., & Wein, R. (1997). Spring Ice-Jam Flooding of the Peace-Athabasca Delta: Evidence of a Climatic Oscillation. *Climatic Change. 35*: 463 – 483.

Vannini, P., & Vannini, A. (2019). The exhaustion of Wood Buffalo National Park: Mikisew Cree First Nation experiences and perspectives. *International Review of Qualitative Research*, *12*: 278-303.

Wiklund, J.A., Bozinovski, N., Hall, R.I., & Wolfe, B.B. (2010). Epiphytic diatoms as flood indicators. *Journal of Paleolimnology*, *44*(1), 25-42.

Wiklund, J.A., Hall, R.I., & Wolfe, B.B. (2012). Timescales of hydrolimnological change in floodplain lakes of the Peace-Athabasca Delta, northern Alberta, Canada. *Ecohydrology*, *5*: 351-367.

Wood Buffalo National Park (WBNP). (2019). Action Plan, 1-90.

Wolfe, A. P., Baron, J. S., & Cornett, R. J. (2001). Anthropogenic nitrogen deposition induces rapid ecological changes in alpine lakes of the Colorado Front Range (USA). *Journal of Paleolimnology*, 25: 1-7.

Wolfe, B.B., Edwards, T.W.D., Hall, R.I. & Johnston, J.W. (2011). A 5200-year record of freshwater availability for regions in western North America fed by high-elevation runoff. *Geophysical Research Letters, 38*: L11404.

Wolfe, B. B., Hall, R. I., Last, W. M., Edwards, T. W., English, M. C., Karst-Riddoch, T. L., Paterson, A., Palmini, R. (2006). Reconstruction of multi-century flood histories from oxbow lake sediments, Peace-Athabasca Delta, Canada. *Hydrological Processes, 20*, 4131-4153.

Wolfe, B. B., Hall, R. I., Edwards, W. D., Jarvis, S. R., Sinnatamby, R. N., Yi, Y., & Johnston, J. W. (2008a). Climate-driven shifts in quantity and seasonality of the river discharge over the past 1000 years from the hydrographic apex of North America. *Geophysical Research Letters, 35(*24), L24402.

Wolfe, B. B., Hall, R. I., Edwards, T. W., Vardy, S. R., Falcone, M. D., Sjunneskog, C., Sylvestre et al. (2008b). Hydroecological responses of the Athabasca Delta, Canada, to changes in river flow and climate during the 20th century. *Ecohydrology, 1*(2), 131-148.

Wolfe, B. B., Hall, R. I., Edwards, T. W., & Johnston, J. W. (2012). Developing temporal hydroecological perspectives to inform stewardship of a northern floodplain landscape subject to multiple stressors: Paleolimnological investigations of the Peace–Athabasca Delta. *Environmental Reviews*, *20*(3), 191-210.

Wolfe, B. B., Hall, R. I., Wiklund, J.A., & Kay, M.L. (2020). Response to Commentary by Beltaos and Peters on: "Past variation in Lower Peace River ice-jam flood frequency" by Wolfe et al. (2020). *Environmental Reviews. 28* (4).

Wolfe, B. B., Karst-Riddoch, T. L., Vardy, S. R., Falcone, M. D., Hall, R. I., & Edwards, T. W. D.(2005). Impacts of climate and river flooding on the hydro-ecology of a floodplain basin, Peace-Athabasca Delta, Canada since A.D. 1700. *Quaternary Research, 64* (2), 147-162.

Appendices

Appendix A - Geochronology radioisotope and CRS-inferred ^{210}Pb

Table A.1 Activity measurements of ^{210}Pb, ^{226}Ra and ^{137}Cs (Bq/kq), CRS age model dates (year) and the total, organic and inorganic matter dry mass sedimentation rates (g/cm^2/yr) for the PAD 52 sediment core (C-1). The interpolated ^{210}Pb values shaded in orange. Midpoint depth is the middle value that the sediment interval spans (the interval 0 - 1-cm is represented by a midpoint depth of 0.5-cm). The linear extrapolated CRS age values are shaded in gray. Values are from Faber (2020).

Midpoint Depth	**CRS Dates**	**CRS Error**	**Total Sed.**	**Organic Matter Sed.**	**Inorganic Matter Sed.**	**^{210}Pb**	**^{210}Pb Error**	**^{226} Ra**	**^{226} Ra error**	**^{137}Cs**	**^{137}Cs error**
(cm)		± 2 sigma	(g/cm^2/yr)	(g/cm^2/yr)	(g/cm^2/yr)	(Bq/kg)	(1 std. dev.)	(Bq/kg)	(1 std. dev.)	(Bq/kg)	(1 std. dev.)
0.5	2016.79	0.62	0.0523	0.0213	0.031	8.8675	0.7785	1.5065	0.2735	0.2236	0.0741
1.5	2014.88	1.09	0.0503	0.0141	0.0362	9.9612	0.8961	1.4951	0.2751	0.1294	0.0741
2.5	2013.11	1.47	0.0606	0.0221	0.0385	8.1255	0.6989	1.8413	0.2493	0.195	0.0648
3.5	2011.26	2.03	0.0709	0.0203	0.0506	8.4756	0.6965	1.8526	0.25	0.2	0.0639
4.5	2008.9	2.76	0.0839	0.0231	0.0608	8.382	0.606	2.0338	0.2465	0.2329	0.0564
5.5	2005.27	4.25	0.1036	0.0267	0.0769	7.7232	0.6058	2.1478	0.2671	0.1499	0.0546
6.5	2000.75	5.79	0.1302	0.0285	0.1017	7.0579	0.6094	2.5403	0.3569	0.3471	0.0611
7.5	1995.83	8	0.1107	0.0202	0.0905	6.5623	0.8211	1.8257	0.2953	0.2815	0.0796
8.5	1991.72	9.21	0.0951	0.0259	0.0692	4.1368	0.3636	2.452	0.2484	0.2488	0.037
9.5	1987.81	11.68	0.0813	0.0163	0.065	4.5806	0.4758	2.285	0.2484	0.2674	0.0488
10.5	1983.26	13.75	0.0695	0.0149	0.0546	3.3457	0.3722	2.1147	0.2086	0.3411	0.0411
11.5	1979.7	14.98	0.097	0.0195	0.0774	3.2169	0.4688	2.5813	0.2658	0.2646	0.0509
12.5	1976.99	15.34	0.1444	0.0175	0.1269	2.9914	0.3247	2.6471	0.2186	0.2952	0.0355
13.5	1974.11	15.98	0.1485	0.0121	0.1363	3.1943	0.4073	2.704	0.2668	0.5325	0.0493
14.5	1970.02	16.89	0.1609	0.0208	0.1401	2.6853	0.3454	2.1144	0.2143	0.5052	0.0434
15.5	1962.6	20.68	0.2171	0.0241	0.193	3.0135	0.3731	1.9504	0.2096	0.514	0.0447
16.5	1952.99	21.07	0.317	0.029	0.2881	2.785	0.3162	2.1576	0.1996	0.3401	0.0361
17.5	1943.6		0.2809	0.0294	0.2515	2.9788	0.3673	1.7958	0.1852	0.1866	0.0373
18.5	1934.41		0.2508	0.0576	0.1932	2.7707	0.337	2.4731	0.2128	0.0627	0.0301

19.5	1925.58		0.1301	0.0138	0.1163	2.4368	0.3708	1.8899	0.2239	-0.0127	0.2439
20.5	1918.04		0.0708	0.0109	0.0599	2.501	0.5194				
21.5	1910.61		0.0663	0.0092	0.0571	2.5664	0.3638	2.1159	0.2222	-0.0066	0.0319
22.5	1902.82		0.0666	0.0083	0.0583	2.678	0.5092				
23.5	1893.07		0.0734	0.0122	0.0611	2.7927	0.3562	2.2414	0.2079	-0.0036	0.0135
24.5	1881.57		0.0791	0.0157	0.0634	2.7831	0.4961				
25.5	1871.29					2.7735	0.3452	2.6288	0.2355	-0.0328	0.0602
26.5	1860.63					2.8361	0.508				
27.5	1849.97					2.8996	0.3727	2.6987	0.2796	-0.0223	0.1109
28.5	1838.41					2.6375	0.3034	2.369	0.2031		
29.5	1826.27					2.5429	0.3541	2.8073	0.2409	-0.0315	0.0671
30.5	1815.95					2.6407	0.498				
31.5	1807.09					2.5143	0.3645	2.0528	0.1996	-0.0642	0.0494
32.5	1798.27					2.6407	0.498				
33.5	1788.54					2.7713	0.3394	2.067	0.2016	-0.0132	0.3688
34.5	1777.98					2.96	0.5237				
35.5	1769.47					3.1571	0.3989	2.1002	0.211	-0.0365	0.0761

Table A.2. Activity measurements of ^{210}Pb, ^{226}Ra and ^{137}Cs (Bq/kq), CRS age model dates (year) and the total, organic and inorganic matter dry mass sedimentation rates (g/cm^2/yr) for the PAD 65 sediment core (C-1). The interpolated ^{210}Pb values shaded in orange. Midpoint depth is the middle value that the sediment interval spans (the interval 0 - 1-cm is represented by a midpoint depth of 0.5-cm). The linear extrapolated CRS age values are shaded in gray. Values are from Faber (2020).

Midpoint Depth	**CRS Dates**	**CRS Error**	**Total Sed.**	**Organic Matter Sed.**	**Inorganic Matter Sed.**	**^{210}Pb**	**^{210}Pb Error**	**^{226} Ra**	**^{226} Ra error**	**^{137}Cs**	**^{137}Cs error**
(cm)		± 2 sigma	(g/cm^2/yr)	(g/cm^2/yr)	(g/cm^2/yr)	(Bq/kg)	(1 std. dev.)	(Bq/kg)	(1 std. dev.)	(Bq/kg)	(1 std. dev.)
0.5	2016	0.31	0.0523	0.0213	0.031	10.7435	0.9436	2.6924	0.569	0.3556	0.1554
1.5	2014.51	0.72	0.0503	0.0141	0.0362	10.728	0.9617	2.6083	0.4861	0.3127	0.151
2.5	2012.45	1.01	0.0606	0.0221	0.0385	8.4477	0.5517	2.1139	0.2264	0.3839	0.068
3.5	2010.2	1.45	0.0709	0.0203	0.0506	7.3066	0.7002				
4.5	2007.81	1.85	0.0839	0.0231	0.0608	6.2732	0.4312	2.3009	0.2238	0.3477	0.0587
5.5	2005.23	2.42	0.1036	0.0267	0.0769	5.2791	0.5507				
6.5	2002.73	2.85	0.1302	0.0285	0.1017	4.3961	0.3426	2.2161	0.2193	0.4182	0.0525
7.5	2000.61	3.26	0.1107	0.0202	0.0905	4.627	0.6132				
8.5	1998.49	3.73	0.0951	0.0259	0.0692	4.8659	0.5086				
9.5	1996.22	4.24	0.0813	0.0163	0.065	5.1128	0.6324				
10.5	1993.17	5.14	0.0695	0.0149	0.0546	5.368	0.3759	2.2624	0.2003	0.6387	0.0571
11.5	1989.12	6.19	0.097	0.0195	0.0774	4.4894	0.5657				
12.5	1984.8	7.16	0.1444	0.0175	0.1269	3.7123	0.4227	2.5505	0.2918	0.5317	0.0861
13.5	1981.14	7.81	0.1485	0.0121	0.1363	3.4137	0.4816				
14.5	1978.2	8.65	0.1609	0.0208	0.1401	3.1314	0.2307	2.3018	0.1684	1.2147	0.0464
15.5	1975.63	9.1	0.2171	0.0241	0.193	3.0938	0.3498				
16.5	1973.55	9.45	0.317	0.029	0.2881	3.0565	0.263	2.6977	0.1951	1.422	0.0582
17.5	1971.72	9.57	0.2809	0.0294	0.2515	2.8629	0.3593				
18.5	1969.74	9.97	0.2508	0.0576	0.1932	2.6776	0.2449	2.2729	0.1861	0.5743	0.0474
19.5	1966.71	10.72	0.1301	0.0138	0.1163	2.8978	0.3628				
20.5	1959.93	14.1	0.0708	0.0109	0.0599	3.1297	0.2677	1.9428	0.1674	0.6302	0.0484
21.5	1950.95	16.19	0.0663	0.0092	0.0571	3.0747	0.4516				
22.5	1943.85	18.32	0.0666	0.0083	0.0583	3.0204	0.3637				
23.5	1937.02	17.98	0.0734	0.0122	0.0611	2.9667	0.4392				

24.5	1930.39	19.48	0.0791	0.0157	0.0634	2.9136	0.2462	2.5172	0.1879	0.2446	0.0419
25.5	1925.51					2.8704	0.4314				
26.5	1920.75					2.8276	0.3542				
27.5	1915.42					2.7853	0.4363				
28.5	1909.28					2.7434	0.2547	2.5109	0.1886	0.0662	0.0358
29.5	1903.01					2.712	0.3334				
30.5	1897.06					2.6809	0.2152	2.6667	0.1983	-0.0195	0.1164
31.5	1890.8					2.6536	0.3779				
32.5	1884.82					2.6264	0.3106				
33.5	1879.27					2.5995	0.3828				
34.5	1873.32					2.5727	0.2239	2.2593	0.1739	-0.0576	0.049
35.5	1867.04					2.5475	0.3875				
36.5	1860.16					2.5226	0.3163				
37.5	1852.51					2.4977	0.3872				
38.5	1845.27					2.4731	0.2234	1.8942	0.1619	-0.0621	0.0479
39.5	1838.28					2.3284	0.3809				
40.5	1830.77					2.1894	0.3084				
41.5	1823.22					2.0561	0.3746				
42.5	1816					1.9283	0.2126	1.8867	0.1677	-0.0588	0.0495
43.5	1808.43					2.0993	0.3956				
44.5	1800.25					2.2802	0.3337				
45.5	1791.98					2.4712	0.4212				
46.5	1784.12					2.6726	0.2571	2.5049	0.1851	-0.0102	0.1906
47.5	1776.58					2.4858	0.33				
48.5	1768.6					2.3079	0.2069	3.0583	0.1977	0.002	0.0048
49.5	1759.98					2.2755	0.2905				
50.5	1751.74					2.2434	0.204	2.2862	0.1789	-0.0018	0.0056
51.5	1743.32					2.2366	0.2891				
52.5	1734.55					2.2298	0.2048	2.2064	0.1707	-0.027	0.07

53.5	1726.16

Table A.3. Activity measurements of ^{210}Pb, ^{226}Ra and ^{137}Cs (Bq/kq), CRS age model dates (year) and the total, organic and inorganic matter dry mass sedimentation rates (g/cm^2/yr) for the PAD 72 sediment core (C-1). The interpolated ^{210}Pb values shaded in orange. Midpoint depth is the middle value that the sediment interval spans (the interval 0 - 1-cm is represented by a midpoint depth of 0.5-cm). The linear extrapolated CRS age values are shaded in gray.

Midpoint Depth	**CRS Dates**	**CRS Error**	**Total Sed.**	**Organic Matter Sed.**	**Inorganic Matter Sed.**	**^{210}Pb**	**^{210}Pb Error**	**^{226} Ra**	**^{226} Ra error**	**^{137}Cs**	**^{137}Cs error**
(cm)		± 2 sigma	(g/cm^2/yr)	(g/cm^2/yr)	(g/cm^2/yr)	(Bq/kg)	(1 std. dev.)	(Bq/kg)	(1 std. dev.)	(Bq/kg)	(1 std. dev.)
0.25	2018.18	0.09	0.0631	0.0216	0.0415	6.8076	0.4684	1.3703	0.2306	0.1451	0.0824
0.75	2017.81	0.13	0.0384	0.0124	0.026	10.5535	0.699	1.7232	0.389	0.1573	0.1181
1.25	2017.12	0.26	0.0373	0.0111	0.0262	10.8423	0.6531	1.8643	0.3008	0.2541	0.1052
1.75	2016.2	0.37	0.0366	0.0121	0.0244	10.8534	0.9447				
2.25	2015.23	0.5	0.036	0.0104	0.0255	10.8645	0.6826	2.0642	0.3597	0.2134	0.1064
2.75	2014.05	0.69	0.0449	0.0144	0.0305	8.693	0.8972				
3.25	2012.97	0.8	0.0572	0.0158	0.0414	6.832	0.5823	1.6848	0.3112	0.1234	0.0943
3.75	2012.04	0.92	0.0592	0.0143	0.0449	6.6444	0.7299				
4.25	2010.94	1.08	0.0613	0.012	0.0493	6.4602	0.4401	1.9309	0.2422	0.3122	0.0686
4.75	2009.66	1.25	0.0586	0.011	0.0476	6.5821	0.6288				
5.25	2008.37	1.41	0.0559	0.0102	0.0457	6.7056	0.449	2.1192	0.2702	0.2651	0.0762
5.75	2007.05	1.61	0.0702	0.0127	0.0575	5.8321	0.5609				
6.25	2005.79	1.77	0.0903	0.0154	0.0749	5.038	0.3361	2.4243	0.234	0.3056	0.0563
6.75	2004.52	1.98	0.0853	0.0152	0.0702	5.0237	0.545				
7.25	2003.03	2.22	0.0801	0.012	0.0681	5.0094	0.429	2.2844	0.2273	0.3085	0.0671
7.75	2001.46	2.46	0.0826	0.0126	0.0701	4.8313	0.539				
8.25	1999.96	2.69	0.0857	0.0132	0.0725	4.6574	0.3264	2.3493	0.1858	0.2489	0.0468
8.75	1998.43	2.94	0.0776	0.0111	0.0665	4.749	0.4566				
9.25	1996.65	3.28	0.0701	0.01	0.0601	4.8418	0.3193	2.2756	0.1841	0.3408	0.0481
9.75	1994.69	3.62	0.0732	0.0112	0.062	4.5038	0.4445				
10.25	1992.57	4.05	0.0769	0.0102	0.0667	4.1819	0.3092	1.8629	0.1774	0.3722	0.0501
10.75	1990.54	4.39	0.0852	0.0117	0.0735	3.8593	0.4198				
11.25	1988.9	4.71	0.0972	0.0137	0.0835	3.5538	0.2839	1.7517	0.1708	0.4062	0.0485
11.75	1987.3	5.06	0.0924	0.0119	0.0805	3.5247	0.3774				

12.25	1985.48	5.5	0.0874	0.0099	0.0775	3.4957	0.2487	2.0429	0.162	0.5629	0.0414
12.75	1984.01	5.7	0.1901	0.0256	0.1645	2.9494	0.3478				
13.25	1983.28	5.75	0.5885	0.0427	0.5458	2.4632	0.2431	2.2665	0.1844	0.4575	0.046
13.75	1982.84	5.74	0.6622	0.0464	0.6158	2.498	0.3261				
14.25	1982.44	5.76	0.751	0.0467	0.7043	2.533	0.2174	2.5793	0.173	0.2633	0.036
14.75	1982	5.75	0.566	0.0433	0.5227	2.6137	0.3252				
15.25	1981.3	5.79	0.435	0.0289	0.406	2.696	0.2419	2.444	0.184	0.3501	0.0423
15.75	1980.67	5.8	0.5419	0.0519	0.49	2.561	0.3392				
16.25	1980.36	5.82	0.7024	0.0805	0.6219	2.4306	0.2377	2.4688	0.1877	0.4946	0.0451
16.75	1980.04	5.88	0.3082	0.0485	0.2598	2.6969	0.3418				
17.25	1979.28	6.1	0.1602	0.0223	0.1379	2.9819	0.2455	2.3376	0.1781	0.5593	0.0468
17.75	1978.07	6.32	0.1434	0.0188	0.1246	2.9205	0.3449				
18.25	1976.64	6.65	0.1278	0.0146	0.1132	2.8599	0.2423	2.0047	0.1699	0.6253	0.0464
18.75	1974.87	6.98	0.1146	0.0134	0.1012	2.9075	0.3367				
19.25	1972.84	7.46	0.1015	0.0121	0.0894	2.9555	0.2338	2.4162	0.165	0.5919	0.0424
19.75	1970.96	7.65	0.1608	0.0186	0.1422	2.9024	0.3388				
20.25	1969.77	7.74	0.2883	0.0317	0.2565	2.85	0.2452	2.5854	0.1795	0.6743	0.0474
20.75	1968.88	7.69	0.2351	0.0244	0.2107	2.664	0.3277				
21.25	1967.75	7.9	0.1915	0.0208	0.1707	2.4864	0.2175	2.1098	0.1573	0.7648	0.0436
21.75	1966.48	8.12	0.1485	0.0172	0.1313	2.4799	0.3044				
22.25	1964.76	8.58	0.1162	0.0132	0.1029	2.4735	0.213	1.8999	0.1504	0.7191	0.0425
22.75	1962.64	8.98	0.1102	0.0123	0.098	2.4609	0.3068				
23.25	1960.61	9.45	0.1043	0.0123	0.0919	2.4484	0.2209	1.8885	0.1588	0.802	0.0469
23.75	1958.68	9.66	0.1351	0.0154	0.1197	2.4346	0.2904				
24.25	1957.06	9.9	0.1813	0.0207	0.1606	2.4207	0.1886	2.1353	0.165	0.6868	0.0372
24.75	1954.92	10.45	0.0869	0.0095	0.0773	2.6789	0.2874				
25.25	1950.4	12.35	0.0449	0.0049	0.04	2.9548	0.2169	1.946	0.1496	0.4572	0.0369
25.75	1945.66	13	0.0694	0.0084	0.061	2.7882	0.2817				
26.25	1943.02	13.41	0.1364	0.0164	0.12	2.628	0.1797	2.3811	0.1549	0.3061	0.0297

26.75	1940.41	13.73	0.0721	0.0088	0.0632	2.6805	0.3097				
27.25	1934.96	16.02	0.0397	0.0046	0.0351	2.7337	0.2521	2.0134	0.1597	0.3551	0.0432
27.75	1929.74					2.5254	0.3515				
28.25	1926.73					2.3281	0.2449	2.4668	0.181	0.1661	0.0429
28.75	1923.69					2.3537	0.3189				
29.25	1920.8					2.3796	0.2043	2.325	0.162	0.0598	0.0305
29.75	1917.78					2.2108	0.2843				
30.25	1914.48					2.0502	0.1977	1.858	0.1466	0.0081	0.0157
30.75	1911.38					2.2319	0.2957				
31.25	1908.08					2.4241	0.2199	2.5742	0.1722	0.0523	0.0308

Table A.4. Activity measurements of ^{210}Pb, ^{226}Ra and ^{137}Cs (Bq/kq), CRS age model dates (year) and the total, organic and inorganic matter dry mass sedimentation rates (g/cm^2/yr) for the PAD 73 sediment core (C-1). The interpolated ^{210}Pb values shaded in orange. Midpoint depth is the middle value that the sediment interval spans (the interval 0 - 1-cm is represented by a midpoint depth of 0.5-cm). The linear extrapolated CRS age values are shaded in gray.

Midpoint Depth	**CRS Dates**	**CRS Error**	**Total Sed.**	**Organic Matter Sed.**	**Inorganic Matter Sed.**	**^{210}Pb**	**^{210}Pb Error**	**^{226} Ra**	**^{226} Ra error**	**^{137}Cs**	**^{137}Cs error**
(cm)		± 2 sigma	(g/cm^2/yr)	(g/cm^2/yr)	(g/cm^2/yr)	(Bq/kg)	(1 std. dev.)	(Bq/kg)	(1 std. dev.)	(Bq/kg)	(1 std. dev.)
0.25	2017.91	0.56	0.0736	0.0163	0.0573	4.9318	0.7666	2.0782	0.2197	0.5269	0.0841
0.75	2017.15	0.71	0.0605	0.0143	0.0462	5.2502	0.9722	1.8749	0.2121	0.4008	0.1018
1.25	2016.38	1.03	0.0509	0.0127	0.0383	5.9096	1.2596	1.9769	0.3087	0.3335	0.1419
1.75	2015.5	1.38	0.0547	0.0147	0.04	5.5318	1.7349				
2.25	2014.55	1.71	0.0592	0.0186	0.0406	5.1704	1.1931	1.9688	0.2352	0.2031	0.1416
2.75	2013.52	2.11	0.065	0.0153	0.0497	5.0414	1.5027				
3.25	2012.5	2.39	0.0719	0.0163	0.0557	4.9146	0.9136	2.4433	0.2604	0.273	0.1072
3.75	2011.48	2.71	0.0783	0.0154	0.0628	4.5822	1.1267				
4.25	2010.34	3.06	0.0856	0.0163	0.0693	4.2651	0.6594	2.3171	0.2317	0.5716	0.0728
4.75	2009.3	3.32	0.1176	0.0236	0.0941	3.7767	0.8248				
5.25	2008.51	3.55	0.1722	0.0367	0.1354	3.3271	0.4954	2.4192	0.2298	0.4932	0.0506
5.75	2007.57	3.99	0.1649	0.0292	0.1357	3.3532	0.6952				
6.25	2006.5	4.29	0.1561	0.0254	0.1308	3.3794	0.4877	2.4352	0.2324	0.4566	0.051
6.75	2005.2	4.86	0.1349	0.021	0.1139	3.3335	0.6814				
7.25	2003.6	5.34	0.115	0.0191	0.0959	3.2881	0.476	2.1058	0.2031	0.6025	0.0503
7.75	2002.13	5.79	0.1507	0.0229	0.1279	3.1222	0.6891				
8.25	2001.12	6.02	0.2073	0.0304	0.1769	2.9619	0.4983	2.3636	0.2271	0.6709	0.0547
8.75	2000.27	6.33	0.1281	0.022	0.1061	3.1419	0.7009				
9.25	1998.91	6.88	0.0835	0.0131	0.0704	3.329	0.4929	1.9191	0.1887	0.6854	0.0534
9.75	1997.34	7.34	0.1009	0.0168	0.0841	3.5867	0.698				
10.25	1996.19	7.65	0.126	0.0206	0.1054	3.8574	0.4943	2.1336	0.2061	0.6305	0.0528
10.75	1995.25	7.98	0.164	0.0265	0.1375	3.3389	0.6792				
11.25	1994.51	8.16	0.2198	0.0369	0.1829	2.869	0.4659	2.4112	0.2286	0.7173	0.0504
11.75	1993.95	8.35	0.2202	0.0378	0.1824	2.9154	0.7903				

12.25	1993.34	8.56	0.2202	0.0322	0.188	2.9622	0.6384				
12.75	1992.68	8.77	0.2199	0.034	0.1859	3.0096	0.7733				
13.25	1991.95	9.03	0.2193	0.0323	0.187	3.0574	0.4364	2.632	0.2453	0.4757	0.0418
13.75	1991.17	9.26	0.1895	0.0298	0.1597	2.9614	0.7547				
14.25	1990.27	9.58	0.1645	0.0231	0.1414	2.8675	0.6157				
14.75	1989.31	9.86	0.1424	0.0218	0.1206	2.7755	0.7535				
15.25	1988.25	10.3	0.1242	0.0209	0.1033	2.6856	0.4343	2.0118	0.1919	0.4282	0.0413
15.75	1986.92	10.82	0.09	0.0127	0.0774	3.1006	0.6559				
16.25	1985.03	11.79	0.0665	0.0085	0.058	3.5563	0.4915	2.3966	0.228	0.4017	0.0482
16.75	1980.87	13.62	0.0678	0.0051	0.0628	3.3832	0.6752				
17.25	1976.53	14.87	0.0621	0.0077	0.0544	3.2158	0.4628	2.2587	0.2153	0.4047	0.0472
17.75	1974.02	15.91	0.059	0.0086	0.0504	3.3119	0.6988				
18.25	1971.31	17.5	0.0569	0.0059	0.051	3.41	0.5235	2.5162	0.2408	0.7587	0.0574
18.75	1968.71	18.36	0.0813	0.0111	0.0702	3.1497	0.6796				
19.25	1966.99	18.99	0.1304	0.0153	0.1151	2.903	0.4334	2.5712	0.2402	0.4806	0.0419
19.75	1965.11	20.16	0.0702	0.0093	0.061	3.0819	0.6022				
20.25	1960.56	24.68	0.0403	0.0045	0.0358	3.2681	0.4181	2.3125	0.2169	0.3398	0.0397
20.75	1955.6	25.18	0.0883	0.0099	0.0784	3.0634	0.5701				
21.25	1953.59	24.35	0.3531	0.0339	0.3192	2.8675	0.3876	2.9074	0.2675	0.0989	0.0364
21.75	1952.54	22.92	0.2272	0.0267	0.2005	2.8465	0.5394				
22.25	1950.95	22.68	0.1521	0.0168	0.1353	2.8256	0.375	2.6515	0.2442	0.0412	0.0384
22.75	1949.03	20	0.1588	0.0148	0.144	2.9528	0.5362				
23.25	1946.97	16.52	0.1668	0.0126	0.1542	3.0838	0.3832	2.9431	0.2703	0.0446	0.0377
23.75	1944.23					2.871	0.6635				
24.25	1940.82					2.6683	0.5416				
24.75	1937					2.4753	0.6631				
25.25	1933.28					2.2918	0.3827	2.8231	0.2599	0.0337	0.0419
25.75	1929.8										
26.25	1926.11										

26.75	1922.51							
27.25	1919.16						0.0085	0.2242
27.75	1916.09							
28.25	1913.26							
28.75	1910.31							
29.25	1907.54							
29.75	1904.89							
30.25	1902.05	2.2605	0.3727	2.0875	0.1945	-0.0166	0.0198	
30.75	1899.13							
31.25	1895.96							
31.75	1892.42							
32.25	1889.35							
32.75	1886.64							
33.25	1883.52							
33.75	1879.98							
34.25	1876.47							
34.75	1873.08							
35.25	1869.45							
35.75	1866.17							
36.25	1862.84	2.4773	0.4002	2.5808	0.2392	-0.0193	0.0231	
36.75	1859							
37.25	1855.61							
37.75	1852.71							
38.25	1849.69							
38.75	1846.66							
39.25	1843.66							
39.75	1840.28							
40.25	1836.78							
40.75	1833.62							

41.25	1830.45
41.75	1827.59
42.25	1824.39
42.75	1820.71
43.25	1817.78
43.75	1814.7
44.25	1811.38
44.75	1808.16
45.25	1804.32
45.75	1799.66
46.25	1794.47

Table A.5. Activity measurements of ^{210}Pb, ^{226}Ra and ^{137}Cs (Bq/kq), CRS age model dates (year) and the total, organic and inorganic matter dry mass sedimentation rates (g/cm^2/yr) for the PAD 74 sediment core (C-1). The interpolated ^{210}Pb values shaded in orange. Midpoint depth is the middle value that the sediment interval spans (the interval 0 - 1-cm is represented by a midpoint depth of 0.5-cm). The linear extrapolated CRS age values are shaded in gray.

Midpoint Depth	**CRS Dates**	**CRS Error**	**Total Sed.**	**Organic Matter Sed.**	**Inorganic Matter Sed.**	**^{210}Pb**	**^{210}Pb Error**	**^{226} Ra**	**^{226} Ra error**	**^{137}Cs**	**^{137}Cs error**
(cm)		± 2 sigma	(g/cm^2/yr)	(g/cm^2/yr)	(g/cm^2/yr)	(Bq/kg)	(1 std. dev.)	(Bq/kg)	(1 std. dev.)	(Bq/kg)	(1 std. dev.)
0.25	2017.67	0.31	0.0391	0.0099	0.0292	10.5383	0.5945	1.4349	0.2824	0.2073	0.1033
0.75	2016.56	0.45	0.0448	0.0093	0.0355	9.2682	0.6027	1.6658	0.3259	0.1422	0.1091
1.25	2015.73	0.6	0.0612	0.0118	0.0493	7.5801	0.5482	2.1506	0.3971	0.439	0.1164
1.75	2014.84	0.8	0.0708	0.0178	0.053	6.4745	0.6813				
2.25	2013.93	0.96	0.0826	0.0148	0.0677	5.482	0.4045	1.6778	0.2346	0.2178	0.0715
2.75	2013.13	1.1	0.0741	0.0138	0.0603	6.0431	0.5657				
3.25	2012.15	1.33	0.0669	0.0127	0.0542	6.6412	0.3955	2.1756	0.2483	0.1634	0.0627
3.75	2010.99	1.55	0.0773	0.0186	0.0587	5.9174	0.5501				
4.25	2009.92	1.77	0.0907	0.013	0.0777	5.2481	0.3824	2.1841	0.2585	0.3709	0.0729
4.75	2008.63	2.12	0.0913	0.0119	0.0794	5.1706	0.52				
5.25	2006.79	2.61	0.0905	0.0108	0.0797	5.0939	0.3524	2.2597	0.2505	0.3442	0.0621
5.75	2004.84	3.04	0.121	0.0144	0.1066	4.4572	0.4504				
6.25	2003.42	3.31	0.1719	0.0209	0.151	3.8759	0.2804	2.5549	0.2074	0.3563	0.0476
6.75	2002.38	3.57	0.2248	0.0273	0.1975	3.605	0.3846				
7.25	2001.55	3.75	0.305	0.0382	0.2668	3.347	0.2632	2.6492	0.2195	0.3419	0.0449
7.75	2000.72	4	0.2048	0.0243	0.1805	3.6665	0.3886				
8.25	1999.38	4.42	0.1421	0.0196	0.1225	4.0058	0.2859	2.5832	0.1921	0.437	0.0487
8.75	1997.73	4.83	0.122	0.0191	0.1029	3.747	0.3731				
9.25	1995.89	5.39	0.1052	0.0141	0.0911	3.4997	0.2397	1.7672	0.1612	0.3988	0.0428
9.75	1993.85	5.95	0.1071	0.0145	0.0927	3.6271	0.3655				
10.25	1991.69	6.63	0.1095	0.0153	0.0942	3.7576	0.2759	1.994	0.1742	0.2224	0.0457
10.75	1989.76	7.1	0.1262	0.0201	0.1061	3.4886	0.3512				
11.25	1988.14	7.64	0.1514	0.0202	0.1312	3.2327	0.2172	2.2484	0.1621	0.3186	0.0367
11.75	1986.47	8.13	0.1733	0.021	0.1523	3.2934	0.3338				

12.25	1985.14	8.47	0.2014	0.0295	0.172	3.3549	0.2534	2.7178	0.1961	0.4601	0.0479
12.75	1984.08	8.8	0.211	0.0306	0.1804	3.3629	0.3624				
13.25	1983.04	9.12	0.2211	0.0289	0.1923	3.3709	0.259	2.8278	0.2547	0.4615	0.0485
13.75	1981.94	9.42	0.2722	0.0261	0.246	3.1912	0.3428				
14.25	1980.83	9.65	0.3396	0.0417	0.2979	3.0179	0.2245	2.6877	0.1833	0.3513	0.0415
14.75	1979.83	9.93	0.2609	0.0332	0.2277	2.7618	0.304				
15.25	1978.58	10.39	0.2039	0.0272	0.1767	2.5205	0.2049	2.0038	0.153	0.3971	0.0387
15.75	1977.17	10.71	0.2402	0.0286	0.2117	2.7636	0.3182				
16.25	1975.99	10.96	0.2893	0.0347	0.2546	3.0219	0.2434	2.6884	0.1987	0.4343	0.047
16.75	1975.06	11	0.4065	0.0547	0.3518	2.9587	0.3337				
17.25	1974.45	11.02	0.6074	0.0701	0.5372	2.8964	0.2282	2.9594	0.2043	0.5593	0.0458
17.75	1973.58	11.17	0.2712	0.0266	0.2446	2.9238	0.336				
18.25	1971.67	11.89	0.1391	0.0153	0.1239	2.9514	0.2466	2.3308	0.1923	0.7249	0.0519
18.75	1969.66	12.1	0.2133	0.0265	0.1868	2.9579	0.3496				
19.25	1968.56	12.15	0.3745	0.0428	0.3317	2.9644	0.2479	2.7611	0.2061	0.8327	0.0546
19.75	1967.32	12.48	0.1695	0.0197	0.1498	2.9678	0.3334				
20.25	1964.58	13.74	0.0868	0.0103	0.0765	2.9713	0.223	2.1596	0.1692	0.5874	0.0446
20.75	1961.87	14.12	0.1602	0.0233	0.1368	2.689	0.2844				
21.25	1960.71	14.1	0.3968	0.0607	0.3361	2.4252	0.1765	2.5537	0.1677	0.4347	0.0352
21.75	1959.93	14.17	0.2556	0.0392	0.2164	2.356	0.2624				
22.25	1958.75	14.5	0.1717	0.0273	0.1444	2.2882	0.1942	1.9579	0.1622	0.5399	0.0443
22.75	1956.82	15.07	0.1146	0.018	0.0966	2.4937	0.2978				
23.25	1953.92	16.28	0.077	0.0115	0.0655	2.7112	0.2258	2.058	0.1683	0.3873	0.0426
23.75	1951.16	16.53	0.1324	0.0164	0.116	2.5528	0.2969				
24.25	1949.52	16.09	0.2821	0.0383	0.2438	2.4007	0.1927	2.5389	0.1778	0.3699	0.0374
24.75	1948.27	16.13	0.1601	0.0279	0.1322	2.5851	0.2762				
25.25	1946.56	16.71	0.0976	0.0178	0.0798	2.7787	0.1979	2.3775	0.1742	0.4362	0.0379
25.75	1944.91	16.6	0.1658	0.0275	0.1383	2.79	0.2943				
26.25	1943.93	16.11	0.3338	0.0499	0.2839	2.8014	0.2178	2.6956	0.2048	0.312	0.0426

26.75	1942.69	16.31	0.1029	0.0205	0.0823	2.9319	0.2969				
27.25	1938.04	18.57	0.0421	0.0065	0.0356	3.0663	0.2018	2.2913	0.1726	0.0643	0.0299
27.75	1932.08	19.57	0.0503	0.0069	0.0435	2.945	0.2874				
28.25	1928.12					2.8268	0.2047	2.5073	0.1662	0.0252	0.0234
28.75	1925.33					2.7944	0.2862				
29.25	1922.94					2.7622	0.2001	2.6048	0.1755	0.0012	0.003
29.75	1920.41					2.747	0.2879				
30.25	1917.92					2.7319	0.207	3.0263	0.199	-0.0269	0.0644
30.75	1915.42					2.7109	0.2901				
31.25	1912.9					2.69	0.2033	3.1612	0.1765	-0.0117	0.587
31.75	1910.38					2.7925	0.296				
32.25	1907.98					2.8976	0.2151	2.8719	0.1777	0.0061	0.0119
32.75	1905.58										
33.25	1903.39										
33.75	1900.65										
34.25	1897.46										
34.75	1894.93										
35.25	1892.97										
35.75	1890.54										
36.25	1887.51					2.713	0.1664	2.2946	0.1465	0.0626	0.0233
36.75	1884.81										
37.25	1881.83										
37.75	1878.39										
38.25	1875.36										
38.75	1872.27										
39.25	1869.06										
39.75	1865.67										
40.25	1862.27					2.3973	0.1866	2.3912	0.165	-0.0053	0.0268
40.75	1859.37										

41.25	1856.1			
41.75	1852.98			
42.25	1850.2			
42.75	1847.2			
43.25	1844.27			
43.75	1841.38			
44.25	1838.3	2.3727	0.1826	
44.75	1834.72			

Table A.6. Activity measurements of ^{210}Pb, ^{226}Ra and ^{137}Cs (Bq/kq), CRS age model dates (year) and the total, organic and inorganic matter dry mass sedimentation rates (g/cm^2/yr) for the PAD 79 sediment core (C-1). The interpolated ^{210}Pb values shaded in orange. Midpoint depth is the middle value that the sediment interval spans (the interval 0 - 1-cm is represented by a midpoint depth of 0.5-cm). The linear extrapolated CRS age values are shaded in gray.

Midpoint Depth (cm)	**CRS Dates**	**CRS Error** ± 2 sigma	**Total Sed.** (g/cm^2/yr)	**Organic Matter Sed.** (g/cm^2/yr)	**Inorganic Matter Sed.** (g/cm^2/yr)	**^{210}Pb** (Bq/kg)	**^{210}Pb Error** (1 std. dev.)	**^{226} Ra** (Bq/kg)	**^{226} Ra error** (1 std. dev.)	**^{137}Cs** (Bq/kg)	**^{137}Cs error** (1 std. dev.)
1	2019.46	0.17	0.0559	0.0157	0.0403	7.4058	2.3187	3.2072	0.6944	0.0394	0.1749
2.5	2018.79	1.52	0.0533	0.0113	0.042	8.7098	2.3187				
3.25	2017.59	1.71	0.0492	0.0075	0.0417	10.1586	1.0097	5.5789	0.229	0.2029	0.1124
3.75	2016.24	2.07	0.0504	0.0086	0.0418	10.0082	1.0097				
4.25	2014.73	2.39	0.0512	0.0103	0.0409	9.8593	0.791	5.8151	0.1746	0.1266	0.0665
4.75	2013.3	2.73	0.0543	0.0091	0.0452	9.0992	0.791				
5.25	2011.71	3.2	0.0583	0.0081	0.0502	8.3792	0.6564	5.1278	0.1453	0.0679	0.0504
5.75	2009.96	3.74	0.0773	0.0097	0.0676	7.4501	0.6564				
6.25	2008.49	4.14	0.1076	0.0116	0.096	6.5923	0.5648	5.0143	0.1417	0.0586	0.05
6.75	2007.32	4.52	0.1286	0.0163	0.1123	6.1355	0.5648				
7.25	2006.32	4.83	0.1575	0.0184	0.1391	5.7004	0.5204	4.6977	0.1345	0.0955	0.0501
7.75	2005.01	5.42	0.0924	0.0117	0.0807	6.3944	0.5204				
8.25	2002.88	6.3	0.0569	0.0071	0.0498	7.1427	0.6242	4.5856	0.1499	0.2273	0.0612
8.75	2000.18	7.35	0.0628	0.0072	0.0555	6.3648	0.6242				
9.25	1997.51	8.36	0.0696	0.0077	0.0619	5.6455	0.4408	3.877	0.1037	0.3323	0.0477
9.75	1995.16	9.26	0.0625	0.0069	0.0556	5.7992	0.4408				
10.25	1993.1	10.15	0.0569	0.008	0.0489	5.9556	0.6347	4.0885	0.1495	0.352	0.0738

10.75	1991.07	11.15	0.0538	0.0079	0.0459	5.8951	0.6347				
11.25	1988.41	12.83	0.0506	0.0063	0.0442	5.8349	0.5439	3.9839	0.1282	0.4426	0.0688
11.75	1986.06	13.59	0.1047	0.0113	0.0934	4.9964	0.5439				
12.25	1984.93	13.89	0.313	0.0294	0.2837	4.2423	0.4816	3.9841	0.1281	0.2328	0.0582
12.75	1983.76	14.48	0.1613	0.0185	0.1427	4.6775	0.4816				
13.25	1981.93	15.64	0.0907	0.0109	0.0798	5.1414	0.5033	4.3126	0.1314	0.4364	0.067
13.75	1980.59	15.81	0.306	0.0336	0.2724	4.7177	0.5033				
14.25	1980.28	15.74	2.7443	0.2845	2.4598	4.3179	0.4878	4.2927	0.1331	0.2437	0.0585
14.75	1980.21	15.66	1.886	0.1923	1.6937	4.2162	0.4878				
15.25	1980.13	15.65	1.3502	0.1226	1.2277	4.1162	0.4773	4.2671	0.131	0.0583	0.0504
15.75	1980.02	15.56	1.3596	0.1259	1.2336	4.0874	0.4773				
16.25	1979.91	15.54	1.3682	0.1222	1.246	4.0588	0.4805	4.3045	0.1338	0.1059	0.0519
16.75	1979.79	15.4	1.3505	0.1162	1.2344	3.9672	0.4805				
17.25	1979.65	15.37	1.3312	0.117	1.2142	3.877	0.3851	3.9382	0.111	0.071	0.0416
17.75	1979.45	14.85	1.3385	0.0974	1.2411	3.556	0.3851				
18.25	1979.24	14.77	1.3409	0.1075	1.2334	3.2533	0.4253	3.7325	0.1279	0.1763	0.0532
18.75	1979.09	14.55	1.3216	0.1109	1.2107	3.3277	0.4253				
19.25	1978.94	14.46	1.3021	0.1123	1.1898	3.4032	0.4687	3.9369	0.1302	0.2976	0.0621
19.75	1978.64	14.31	0.4315	0.0384	0.3932	4.0489	0.4687				
20.25	1978.04	14.53	0.19	0.0177	0.1722	4.7715	0.541	4.4285	0.2124	0.8181	0.0951
20.75	1977.38	14.59	0.2455	0.0226	0.2229	4.7011	0.541				
21.25	1976.86	14.69	0.3274	0.0294	0.298	4.6314	0.4844	4.4405	0.1348	0.8326	0.0922

21.75	1976.58	14.54	1.2341	0.1443	1.0898	4.0657	0.4745	4.7666	0.143	1.0646	0.1091
22.25	1975.37	15.49	0.0804	0.0099	0.0704	4.5133	0.4739	3.7492	0.1227	1.6771	0.1515
22.75	1973.97	15.59	0.2739	0.0277	0.2461	4.9482	0.4981	4.7392	0.1475	1.396	0.1312
23.25	1973.49	15.61	0.3465	0.0331	0.3134	4.7524	0.5424	4.5899	0.1484	1.122	0.1176
23.75	1973.08	15.03	0.5819	0.0503	0.5316	4.562	0.5424				
24.25	1972.81	14.88	1.0971	0.0975	0.9996	4.3768	0.4884	4.5969	0.1371	0.6522	0.0784
24.75	1972.47	13.92	0.5293	0.0432	0.4861	4.2646	0.4884				
25.25	1971.77	13.63	0.2904	0.0221	0.2683	4.1544	0.4836	3.9694	0.1263	0.44	0.0672
25.75	1971.18	13.33	0.5065	0.0465	0.46	4.0562	0.4836				
26.25	1970.95	13.04	1.0356	0.0915	0.9441	3.9597	0.4781	4.7416	0.1441	0.5291	0.0763
26.75	1970.14	13.3	0.0988	0.0097	0.0891	4.9273	0.5057	4.4057	0.134	0.7172	0.0842
27.25	1965.84	15.63	0.0251	0.0032	0.0219	6.0763	0.6063	4.1122	0.1424	1.0343	0.1125
27.75	1960.99	16.72	0.0233	0.0032	0.0201	5.8142	0.6324	4.1208	0.1535	0.684	0.0985
28.25	1958.83	17.04	0.0772	0.0129	0.0643	4.947	0.5777	4.4755	0.1516	0.2662	0.0712
28.75	1957.13	16.86	0.0861	0.0111	0.075	4.8026	0.5777				
29.25	1955.35	16.65	0.0976	0.0107	0.0869	4.661	0.4597	4.3254	0.1727	0.0902	0.0486
29.75	1951.73	16.97	0.0358	0.004	0.0318	5.3391	0.4597				
30.25	1948.64					6.0799	0.5281	4.3184	0.13	0.0058	0.0285
30.75	1947.72					5.5935	0.5281				
31.25	1946.67					5.1337	0.5362	4.592	0.1448	0.0358	0.0535
31.75	1945.29					5.1692	0.5362				
32.25	1943.98					5.2049	0.5615	4.8419	0.1527	0.0423	0.0555

32.75	1942.78						
33.25	1941.47						
33.75	1940.25						
34.25	1939.14						
34.75	1938.05						
35.25	1936.82						
35.75	1935.54						
36.25	1933.73	4.3456	0.4715	3.9693	0.2115	0.0322	0.0433
36.75	1931.75						
37.25	1930.32						
37.75	1929.22						
38.25	1928.25						
38.75	1927.26						
39.25	1926.37						
39.75	1925.6						
40.25	1924.74						
40.75	1923.63						
41.25	1922.29						
41.75	1920.89						
42.25	1919.65						
42.75	1918.58						
43.25	1917.31						

43.75	1915.48								
44.25	1913.07				3.7917	0.5159	4.3514	0.1411	-0.0543	0.0605
44.75	1910.55								
45.25	1907.64								
45.75	1904.54								
46.25	1901.69								
46.75	1898.97								
47.25	1896.14								
47.75	1893.14								
48.25	1890.49								
48.75	1887.86								
49.25	1885.01								
49.75	1882.04								
50.25	1879.02								
50.75	1876.51								
51.25	1874.16								
51.75	1871.65								
52.25	1869.06								
52.75	1866.71								
53.25	1864.77								
53.75	1862.81								
54.25	1860.86								

54.75	1858.2
55.25	1854.32
56	1847.13
56.75	1840.83
57.25	1837.76
57.75	1834.76
58.25	1832.35
58.75	1829.83
59.25	1827.4
59.75	1825.43
60.25	1823.54
60.75	1821.69
61.25	1819.15
61.75	1816.59
62.25	1814.74
62.75	1812.79
63.25	1811.01
63.75	1809.37
64.25	1807.79
64.75	1806.09
65.25	1804.09
65.75	1801.52

66.25	1798.8
66.75	1796.63
67.25	1794.65
67.75	1792.62
68.25	1790.64
68.75	1788.94
69.25	1787.35
69.75	1785.7
70.25	1783.7
70.75	1781.47
71.25	1779.52

Table A.7. Activity measurements of ^{210}Pb, ^{226}Ra and ^{137}Cs (Bq/kq), CRS age model dates (year) and the total, organic and inorganic matter dry mass sedimentation rates (g/cm^2/yr) for the PAD 82 sediment core (C-1). The interpolated ^{210}Pb values shaded in orange. Midpoint depth is the middle value that the sediment interval spans (the interval 0 - 1-cm is represented by a midpoint depth of 0.5-cm). The linear extrapolated CRS age values are shaded in gray.

Midpoint Depth	**CRS Dates**	**CRS Error**	**Total Sed.**	**Organic Matter Sed.**	**Inorganic Matter Sed.**	**^{210}Pb**	**^{210}Pb Error**	**^{226} Ra**	**^{226} Ra error**	**^{137}Cs**	**^{137}Cs error**
(cm)		± 2 sigma	(g/cm^2/yr)	(g/cm^2/yr)	(g/cm^2/yr)	(Bq/kg)	(1 std. dev.)	(Bq/kg)	(1 std. dev.)	(Bq/kg)	(1 std. dev.)
0.25	2019.50	0.07	0.1471	0.0292	0.1179	8.5288	2.6025	4.2417	0.5577	0.0059	0.0428
0.75	2019.32	0.38	0.1374	0.0211	0.1163	8.7929	2.6025				
1.25	2018.86	0.48	0.1276	0.0150	0.1126	9.0625	0.8647	4.1760	0.2240	-0.0106	0.4634
1.75	2018.31	0.63	0.1980	0.0206	0.1774	7.2367	0.8647				
2.25	2017.77	0.83	0.3351	0.0325	0.3026	5.6743	0.6265	3.8768	0.1905	0.0543	0.0579
2.75	2017.09	1.05	0.1811	0.0191	0.1620	7.2158	0.6265				
3.25	2016.08	1.25	0.1074	0.0133	0.0941	9.0141	0.8724	3.6380	0.1998	0.0421	0.0716
3.75	2015.08	1.42	0.1556	0.0181	0.1375	7.1036	0.8724				
4.25	2014.37	1.55	0.2444	0.0251	0.2193	5.4843	0.5633	3.2649	0.1709	0.0218	0.0480
4.75	2013.66	1.73	0.2388	0.0201	0.2187	5.5656	0.5633				
5.25	2012.94	1.87	0.2329	0.0237	0.2092	5.6477	0.5633	3.4187	0.1678	0.0041	0.0264
5.75	2012.34	2.00	0.3417	0.0332	0.3084	4.9540	0.5633				
6.25	2011.94	2.07	0.5381	0.0411	0.4970	4.3196	0.4847	3.3902	0.1620	-0.0181	0.0685
6.75	2011.60	2.19	0.5706	0.0490	0.5216	4.3612	0.4847				
7.25	2011.26	2.28	0.6053	0.0532	0.5521	4.4031	0.4889	3.5943	0.1702	0.0163	0.0410
7.75	2010.83	2.41	0.2489	0.0274	0.2215	5.8945	0.4889				
8.25	2010.03	2.62	0.1240	0.0140	0.1100	7.6897	0.8821	3.8466	0.2346	0.0591	0.1007
8.75	2008.97	2.88	0.1565	0.0160	0.1404	6.5675	0.8821				
9.25	2008.00	3.07	0.2026	0.0171	0.1855	5.5603	0.5418	3.3574	0.1619	0.0765	0.0508
9.75	2007.39	3.19	0.7597	0.0593	0.7004	4.1844	0.5418				
10.25	2007.19	3.26	8.4188	0.5557	7.8631	3.0566	0.3891	3.2222	0.1496	0.0389	0.0408
10.75	2007.15	3.33	8.4901	0.5728	7.9173	3.4035	0.3891				
11.25	2007.12	3.35	8.5656	0.6398	7.9258	3.7757	0.4601	3.6309	0.1702	0.0689	0.0486
11.75	2006.94	3.49	0.8897	0.0602	0.8295	4.3862	0.4601				
12.25	2006.25	3.71	0.2401	0.0202	0.2199	5.0592	0.5625	3.2954	0.1667	0.1138	0.0589

12.75	2005.17	3.96	0.2017	0.0139	0.1878	5.4556	0.5625				
13.25	2004.04	4.21	0.1700	0.0167	0.1534	5.8722	0.5890	3.5437	0.1750	0.2494	0.0656
13.75	2002.91	4.47	0.1468	0.0165	0.1303	6.0121	0.5890				
14.25	2001.69	4.78	0.1274	0.0117	0.1157	6.1541	0.5595	3.2565	0.1586	0.3235	0.0640
14.75	2000.27	5.16	0.1016	0.0108	0.0908	6.6988	0.5595				
15.25	1998.78	5.54	0.0814	0.0095	0.0719	7.2747	0.7452	3.1269	0.1836	0.4375	0.0984
15.75	1997.46	5.87	0.1141	0.0123	0.1018	6.3574	0.7452				
16.25	1996.44	6.12	0.1706	0.0166	0.1539	5.5206	0.6037	3.6975	0.1865	0.4109	0.0818
16.75	1995.70	6.30	0.2100	0.0213	0.1887	5.0403	0.6037				
17.25	1995.08	6.48	0.2657	0.0221	0.2436	4.5886	0.4793	3.4705	0.1645	0.2826	0.0591
17.75	1994.35	6.74	0.2107	0.0197	0.1910	4.8626	0.4793				
18.25	1993.45	7.04	0.1683	0.0151	0.1532	5.1474	0.5774	3.4613	0.1754	0.5468	0.0827
18.75	1992.62	7.26	0.2628	0.0223	0.2405	4.5781	0.5774				
19.25	1992.05	7.39	0.4521	0.0361	0.4160	4.0524	0.4785	3.4565	0.1658	0.2012	0.0570
19.75	1991.60	7.52	0.5442	0.0398	0.5044	3.8079	0.4785				
20.25	1991.10	7.67	0.6636	0.0381	0.6255	3.5734	0.4544	3.1786	0.1535	0.0361	0.0444
20.75	1990.70	7.72	0.9035	0.0599	0.8436	3.9554	0.4544				
21.25	1990.47	7.76	1.2895	0.0999	1.1896	4.3637	0.5185	4.1656	0.1948	0.2662	0.0655
21.75	1990.28	7.81	0.8850	0.0679	0.8171	3.9541	0.5185				
22.25	1989.97	7.93	0.6322	0.0355	0.5967	3.5710	0.3920	3.1715	0.1451	0.1414	0.0432
22.75	1989.58	7.98	1.1919	0.0728	1.1191	3.3608	0.3920				
23.25	1989.32	7.99	2.6883	0.1516	2.5367	3.1591	0.3434	3.0674	0.1377	0.1825	0.0403
23.75	1989.00	8.06	0.9068	0.0501	0.8566	3.5178	0.3434				
24.25	1988.33	8.30	0.4031	0.0231	0.3799	3.9028	0.4378	3.3035	0.1540	0.3345	0.0561
24.75	1987.73	8.39	0.6686	0.0486	0.6200	3.6978	0.4378				
25.25	1987.46	8.43	1.2639	0.1007	1.1631	3.5000	0.3789	3.3160	0.1493	0.4236	0.0555
25.75	1987.16	8.52	0.7537	0.0572	0.6965	3.6662	0.3789				
26.25	1986.69	8.67	0.4808	0.0329	0.4479	3.8375	0.3971	3.3626	0.1519	0.4627	0.0582
26.75	1986.08	8.85	0.4218	0.0298	0.3920	3.8529	0.3971				

27.25	1985.26	9.12	0.3700	0.0199	0.3502	3.8684	0.4323	3.2741	0.1526	0.1389	0.0447
27.75	1984.34	9.27	0.5206	0.0294	0.4912	3.5694	0.4323				
28.25	1983.63	9.38	0.7745	0.0356	0.7389	3.2863	0.3467	3.0183	0.1351	0.2515	0.0425
28.75	1983.22	9.32	1.5600	0.0822	1.4778	3.2914	0.3467				
29.25	1983.06	9.30	3.9690	0.2798	3.6892	3.2966	0.3953	3.3575	0.1527	0.8649	0.0852
29.75	1982.99	9.26	3.9993	0.2728	3.7265	3.1994	0.3953				
30.25	1982.92	9.23	4.0311	0.2839	3.7472	3.1041	0.3729	3.1203	0.1441	0.6796	0.0726
30.75	1982.68	9.17	1.0963	0.0678	1.0285	3.4317	0.3729				
31.25	1981.64	9.29	0.4366	0.0226	0.4140	3.7816	0.4450	3.3266	0.1577	0.6481	0.0749
31.75	1980.45	9.42	0.5366	0.0331	0.5034	3.3551	0.3702	3.0039	0.1385	1.2852	0.1150
32.25	1980.10	9.35	309.1400	22.8831	286.2569	3.4028	0.3972	3.4022	0.1558	2.5743	0.2168
32.75	1980.02	9.35	1.6197	0.1250	1.4947	3.4175	0.4202	3.3036	0.1563	2.2176	0.1904
33.25	1979.62	9.45	0.5277	0.0299	0.4977	3.5214	0.4128	3.1736	0.1475	0.9287	0.0912
33.75	1978.68	9.57	0.3345	0.0209	0.3136	3.6585	0.4128				
34.25	1977.45	9.88	0.2203	0.0132	0.2071	3.7992	0.4362	3.0134	0.1432	1.1724	0.1105
34.75	1976.31	10.13	0.2509	0.0193	0.2316	3.9537	0.4474	3.2902	0.1564	1.2757	0.1203
35.25	1974.74	10.74	0.1299	0.0107	0.1192	4.4634	0.4864	3.2216	0.1555	1.4289	0.1315
35.75	1973.09	11.02	0.2132	0.0178	0.1954	3.9648	0.4864				
36.25	1972.09	11.18	0.4106	0.0277	0.3828	3.5048	0.3329	3.1505	0.1375	0.7881	0.0738
36.75	1970.79	11.47	0.2178	0.0158	0.2019	3.7641	0.3329				
37.25	1967.90	12.54	0.1244	0.0064	0.1180	4.0358	0.4500	2.9566	0.1432	0.1987	0.0519
37.75	1965.80	12.34	2.3669	0.1522	2.2147	3.0583	0.3756	3.2410	0.1481	0.4116	0.0561
38.25	1965.09	12.67	0.2095	0.0159	0.1936	3.6568	0.4329	3.0945	0.1466	0.7992	0.0838
38.75	1963.19	13.47	0.1044	0.0091	0.0953	4.7718	0.5280	3.6873	0.1777	0.9873	0.1064
39.25	1961.05	14.05	0.1328	0.0115	0.1212	4.2857	0.4749	3.4977	0.1644	0.7871	0.0847
39.75	1959.06	14.83	0.1124	0.0103	0.1021	4.3383	0.4886	3.4568	0.1654	0.4888	0.0705
40.25	1957.23	15.33	0.1518	0.0140	0.1378	3.9638	0.4331	3.3551	0.1828	0.3968	0.0584
40.75	1955.52	16.00	0.1049	0.0104	0.0945	4.1543	0.4331				
41.25	1952.90	17.45	0.0736	0.0066	0.0670	4.3509	0.4954	3.2218	0.1591	0.1678	0.0582

41.75	1950.06	18.25	0.1040	0.0092	0.0948	4.0528	0.4954				
42.25	1948.11	18.78	0.1632	0.0132	0.1500	3.7686	0.4297	3.3420	0.1552	0.0451	0.0438
43.25	1943.66	18.76	0.1116	0.0101	0.1015	3.6825	0.4293	3.0869	0.1467	0.0813	0.0443
44.25	1939.85	18.43	1.0543	0.0764	0.9779	3.5227	0.3972	3.5535	0.1609	0.1015	0.0440
44.75	1939.27	17.60	0.2693	0.0233	0.2460	3.5122	0.3972				
45.25	1937.14	18.21	0.1024	0.0089	0.0935	3.5016	0.3825			0.0373	0.0375
45.75	1933.28	18.43	0.0759	0.0062	0.0698	3.6458	0.3825				
46.25	1928.52	20.06	0.0551	0.0043	0.0508	3.7938	0.3926	3.0681	0.1412	-0.0006	0.0076
46.75	1925.57										
47.25	1924.75										
47.75	1923.74										
48.25	1922.61					3.1394	0.4014	3.1023	0.1455	-0.0378	0.0486
48.75	1921.47										
49.25	1920.39										
49.75	1919.49										
50.25	1918.63					3.5652	0.3629	3.2865	0.1468	0.0069	0.0249
50.75	1917.52										
51.25	1916.32										
51.75	1915.23										
52.25	1914.25										
52.75	1913.27										
53.25	1912.30									0.0017	
53.75	1911.32										
54.25	1910.23										
54.75	1909.18										
55.25	1908.11										
55.75	1906.89										
56.25	1905.75										
56.75	1904.80										

57.25	1903.92
57.75	1903.03
58.25	1902.14
58.75	1901.29

Appendix B - Loss-on-sequential heating, and C&N elemental and isotope composition data

Table B.1. Loss-on-sequential heating, and organic carbon and nitrogen elemental and isotopic data for PAD 52 which includes water content (%H_2O), organic matter content (%OM), mineral matter content with carbonates (%MM IC), mineral matter content excluding carbonates (%MM EC), calcium carbonate content (%$CaCO_3$), organic carbon (%C), nitrogen content (%N), carbon to nitrogen ratio (C/N), organic carbon isotope composition ($\delta^{13}C$), nitrogen isotope composition ($\delta^{15}N$) and the respective depth (in cm).

Depth (cm)	%H2O	%OM	%MM IC	%MM EC	%$CaCO_3$	%C	%N	C/N	$\delta^{13}C$	$\delta^{15}N$
0	92.43	32.76	67.24	53.51	13.73	17.29	2.20	7.85	-24.62	-1.26
1	90.44	28.51	71.49	62.50	8.99	16.59	2.14	7.74	-25.16	-0.53
2	92.42	25.37	74.63	67.52	7.10	15.28	1.88	8.12	-25.70	-0.67
3	90.72	21.12	78.88	66.86	12.02	14.69	1.76	8.37	-26.05	-1.04
4	88.17	22.58	77.42	67.19	10.23	13.43	1.57	8.58	-26.40	-0.29
5	78.58	15.64	84.36	73.48	10.89	12.02	1.35	8.90	-26.29	-0.21
6	77.42	15.77	84.23	72.61	11.62	9.50	1.01	9.39	-26.24	-0.16
7	79.69	15.20	84.80	74.00	10.80	8.30	0.88	9.42	-26.33	0.36
8	75.17	14.44	85.57	75.89	9.68	6.94	0.74	9.39	-26.35	0.42
9	71.68	12.58	87.42	77.63	9.79	6.34	0.69	9.21	-26.07	0.24
10	65.21	11.90	88.10	79.67	8.44	5.86	0.63	9.33	-25.98	0.73
11	57.26	8.41	91.59	83.97	7.62	4.45	0.47	9.47	-26.23	0.75
12	44.50	6.18	93.82	87.72	6.10	3.61	0.37	9.75	-26.03	0.58
13	50.30	7.40	92.60	86.91	5.69	3.83	0.38	9.97	-25.87	0.49
14	48.18	7.64	92.36	88.28	4.08	2.79	0.28	10.00	-26.40	0.65
15	46.28	8.73	91.27	84.76	6.51	3.84	0.38	10.02	-26.06	0.96
16	46.26	8.01	91.99	86.04	5.95	3.88	0.41	9.56	-26.55	0.56
17	49.03	11.37	88.63	82.13	6.50	4.86	0.51	9.59	-26.69	0.85
18	48.61	10.84	89.16	82.23	6.92	5.62	0.58	9.76	-26.80	0.41
19	48.64	12.74	87.26	80.36	6.91	6.28	0.63	9.91	-26.71	0.21
20	66.04	21.51	78.49	69.98	8.51	11.18	1.16	9.65	-25.60	-0.08
21	47.24	10.70	89.30	82.75	6.56	6.49	0.64	10.21	-25.76	0.12
22	53.89	14.93	85.07	73.29	11.78	4.19	0.39	10.81	-26.10	-0.33

23	37.26	7.61	92.39	86.46	5.93	3.09	0.27	11.41	-26.48	0.65
24	41.69	8.42	91.58	84.13	7.45	4.24	0.39	10.82	-26.62	0.27
25	44.82	12.37	87.63	80.18	7.45	4.21	0.40	10.61	-26.94	0.20
26	42.84	9.87	90.13	82.56	7.57	4.26	0.41	10.42	-26.50	0.57
27	41.49	8.56	91.44	84.15	7.30	3.87	0.38	10.20	-27.00	0.35
28	39.34	7.82	92.18	85.90	6.29	3.40	0.32	10.56	-27.17	0.20
29	40.92	8.26	91.74	86.35	5.39	3.82	0.37	10.25	-27.13	0.98
30	40.10	8.61	91.39	85.68	5.70	4.09	0.40	10.29	-27.05	0.44
31	42.97	10.30	89.70	85.14	4.56	3.55	0.34	10.46	-27.26	0.59
32	46.60	10.26	89.74	83.68	6.06	4.07	0.39	10.38	-27.19	0.50
33	44.48	10.07	89.93	85.04	4.89	4.58	0.45	10.13	-27.38	0.14
34	47.17	10.87	89.13	83.86	5.27	4.83	0.48	10.08	-27.55	0.77
35	50.83	11.04	88.96	84.16	4.80	4.70	0.46	10.14	-27.61	0.64

Table B.2. Loss-on-sequential heating, data for PAD 64 which includes water content (%H_2O), mineral matter content excluding carbonates (%MM EC), and the respective depths (in cm).

Depth (cm)	%H2O	%MM EC
0	81.89	84.29
1	69.93	87.8
2	77.81	83.79
3	65.82	77.05
4	63.39	85.73
5	66.77	85.47
6	62.98	87.01
7	44.07	86.46
8	45.91	88.36
9	56.84	88.54
10	66.45	88.14
11	66.82	84.29
12	76.5	83.04
13	65.93	81.93
14	56.92	84.83
15	58.68	88.32
16	54.03	87.05
17	45.93	89.15
18	40.74	89.86
19	38.97	90.21
20	41.94	89.7
21	54.04	89.58
22	47.36	89.61
23	44.61	88.96
24	52.77	89.69
25	54.4	89.42

26	46.98	89.4
27	42.82	89.59
28	44.68	89.29
29	47.02	89.13
30	48.89	89.93
31	49.42	90.17
32	34.36	91.6
33	41.11	90.61
34	51.04	89.15
35	39.21	90.2
36	45.89	88.92
37	55.66	88.26
38	57.45	88.32
39	40.65	89.19
40	48.9	89.12
41	46.84	89.95
42	46.66	89.28
43	38.39	89.84
44	39.24	90.8
45	39.48	90.44
46	42	90.27
47	46.86	90.15
48	51.4	89.11
49	50.44	88.76
50	50.95	89.23
51	51.18	89.46
52	52.88	89.76
53	47.14	89.03
54	52.96	89.07

55	49.89	89.08
56	50.95	89.82
57	45.35	90.12
58	38.23	90.37

Table B.3. Loss-on-sequential heating, and organic carbon and nitrogen elemental and isotopic data for PAD 65 which includes water content (%H_2O), organic matter content (%OM), mineral matter content with carbonates (%MM IC), mineral matter content excluding carbonates (%MM EC), calcium carbonate content (%$CaCO_3$), organic carbon (%C), nitrogen content (%N), carbon to nitrogen ratio (C/N), organic carbon isotope composition ($\delta^{13}C$), nitrogen isotope composition ($\delta^{15}N$) and the respective depth (in cm).

Depth (cm)	%H2O	%OM	%MM IC	%MM EC	%$CaCO_3$	%C	%N	C/N	$\delta^{13}C$	$\delta^{15}N$
0	94.79	40.68	59.32	47.42	11.89					
1	92.18	32.25	67.75	55.15	12.60					
2	87.09	28.64	71.36	64.49	6.87					
3	85.04	27.53	72.47	63.48	8.99	13.25	1.35	9.81	-26.45	-1.47
4	82.60	25.74	74.26	65.12	9.14					
5	79.08	21.92	78.08	68.87	9.21	9.71	0.95	10.23	-25.93	-0.89
6	77.54	18.26	81.74	72.94	8.81	8.45	0.84	10.03	-26.39	-0.67
7	82.32	27.23	72.77	64.01	8.76	11.64	1.23	9.46	-26.15	-1.49
8	83.85	20.00	80.00	69.02	10.98	11.32	1.28	8.83	-26.03	-0.83
9	83.40	21.48	78.52	71.59	6.93	11.25	1.24	9.10	-25.06	-1.29
10	80.79	20.15	79.85	69.86	9.99	10.20	1.09	9.34	-25.18	-0.82
11	66.56	12.11	87.89	79.73	8.16	5.28	0.54	9.87	-25.72	-0.28
12	53.11	8.17	91.83	86.76	5.07	4.54	0.42	10.70	-24.72	-0.36
13	65.67	12.95	87.05	78.48	8.57	5.11	0.50	10.28	-25.45	0.04
14	64.30	11.10	88.90	81.13	7.77	4.45	0.46	9.70	-25.92	-0.89
15	60.48	9.14	90.86	82.88	7.99	4.48	0.46	9.69	-26.20	-0.37
16	55.64	16.71	83.29	76.07	7.23	4.54	0.44	10.29	-26.52	-0.11
17	61.98	10.63	89.37	83.15	6.22	6.53	0.58	11.19	-27.19	-0.73
18	59.08	15.41	84.59	78.39	6.20	7.59	0.66	11.50	-27.32	-0.90
19	60.01	113.41	-13.41	-20.48	7.08	8.55	0.73	11.76	-27.43	-0.73
20	57.51	12.45	87.55	82.32	5.23	7.64	0.65	11.73	-27.36	-0.50
21	62.17	16.65	83.35	77.73	5.63	8.49	0.71	11.97	-27.21	-0.81
22	68.16	19.81	80.19	74.93	5.25	9.20	0.77	12.00	-27.67	-0.55
23	64.53	21.42	78.58	74.19	4.39	10.44	0.85	12.28	-27.90	-0.63
24	67.81	19.99	80.01	75.15	4.87	10.65	0.87	12.19	-28.01	-0.68

25	68.98	21.54	78.46	73.86	4.60	10.09	0.81	12.41	-27.66	-0.97
26	61.63	15.94	84.06	78.35	5.71	8.13	0.67	12.19	-27.41	-0.59
27	64.53	18.09	81.91	76.76	5.15	7.26	0.60	12.16	-27.35	-0.53
28	50.86	12.32	87.68	81.95	5.73	7.35	0.61	12.01	-27.43	-0.34
29	59.94	16.54	83.46	77.84	5.62	7.88	0.66	11.92	-29.66	-0.08
30	60.67	18.44	81.56	76.83	4.73	9.55	0.76	12.64	-27.34	-0.30
31	61.34	17.45	82.55	77.43	5.12	9.24	0.76	12.09	-27.13	-0.50
32	64.35	19.92	80.08	74.55	5.52	10.47	0.84	12.51	-27.29	-0.74
33	62.25	19.13	80.87	75.95	4.93	9.53	0.78	12.28	-27.09	-0.49
34	58.75	17.52	82.48	76.48	6.00	8.72	0.70	12.37	-27.06	-0.56
35	60.16	16.32	83.68	77.61	6.06	7.55	0.61	12.43	-27.24	-0.30
36	53.56	14.24	85.76	79.24	6.51	7.00	0.58	12.07	-27.12	-0.74
37	54.25	15.50	84.50	77.84	6.66	7.68	0.64	11.99	-27.22	-0.45
38	54.33	14.33	85.67	78.05	7.62	7.99	0.65	12.32	-27.06	-0.53
39	54.50	15.07	84.93	76.92	8.01	7.83	0.65	11.98	-27.07	-0.43
40	53.29	16.06	83.94	77.10	6.84	8.03	0.67	11.96	-27.13	-0.34
41	54.45	16.36	83.64	76.74	6.89	7.63	0.64	12.01	-27.12	-0.66
42	55.34	17.21	82.79	75.51	7.28	7.95	0.65	12.27	-27.15	-0.45
43	54.29	14.76	85.24	78.11	7.12	7.21	0.59	12.21	-27.12	-0.01
44	51.70	13.94	86.06	78.48	7.58	6.67	0.55	12.22	-26.89	-0.10
45	52.82	12.98	87.02	80.38	6.64	6.65	0.54	12.33	-27.12	-0.40
46	51.16	14.20	85.80	79.40	6.40	6.89	0.57	12.08	-27.02	-0.15
47	58.83	17.10	82.90	76.39	6.51	7.16	0.58	12.41	-26.98	-0.31
48	49.38	12.22	87.78	81.59	6.19	6.74	0.55	12.27	-27.23	0.30
49	49.40	11.58	88.42	82.35	6.07	6.29	0.51	12.27	-27.09	-0.15
50	51.55	15.10	84.90	79.47	5.43	6.12	0.51	12.06	-27.06	0.08
51	51.76	13.26	86.74	80.68	6.07	5.79	0.47	12.30	-26.96	-0.39
52	52.11	13.41	86.59	80.40	6.19	5.36	0.45	11.92	-26.85	0.23
53	52.79	13.89	86.11	79.95	6.16	6.72	0.55	12.30	-26.82	-0.13

Table B.4. Loss-on-sequential heating data for PAD 66 which includes mineral matter content excluding carbonates (%MM EC), and the respective depth (in cm).

Depth (cm)	%MM EC
0	86.71
1	88.86
2	91.29
3	89.7
4	89.41
5	88.89
6	89.08
7	89.47
8	89.75
9	89.67
10	88.7
11	88.91
12	88.56
13	88.25
14	88.57
15	88.87
16	88.39
17	88.57
18	87.55
19	88.23
20	89.72
21	89.5
22	90.23
23	90.47
24	90.26
25	90.26

26	90.73
27	90.05
28	89.66
29	89.35
30	
31	89.17
32	88.95
33	89.05
34	89.03
35	88.36
36	89.14

Table B.5. Loss-on-sequential heating, and organic carbon and nitrogen elemental and isotopic data for PAD 72 which includes water content (%H_2O), organic matter content (%OM), mineral matter content with carbonates (%MM IC), mineral matter content excluding carbonates (%MM EC), calcium carbonate content (%$CaCO_3$), organic carbon (%C), nitrogen content (%N), carbon to nitrogen ratio (C/N), organic carbon isotope composition ($\delta^{13}C$), nitrogen isotope composition ($\delta^{15}N$) and the respective depth (in cm).

Depth (cm)	%H2O	%OM	%MM IC	%MM EC	%$CaCO_3$	%C	%N	C/N	$\delta^{13}C$	$\delta^{15}N$
0	96.83	34.16	65.84	57.39	8.45	18.63	2.19	8.49	-25.84	-1.82
0.5	96.30	32.32	67.68	58.75	8.93					
1	92.58	29.79	70.21	57.91	12.30	20.11	2.14	9.40	-24.98	-2.03
1.5	90.92	33.22	66.78	54.13	12.65	17.82	1.99	8.97	-25.79	-1.85
2	89.65	29.02	70.98	58.46	12.52	18.34	1.98	9.24	-25.51	-1.80
2.5	88.20	32.07	67.93	58.08	9.86	16.75	1.83	9.15	-26.06	-1.58
3	87.70	27.60	72.40	62.41	9.99	14.88	1.60	9.30	-26.34	-1.77
3.5	86.98	24.17	75.83	63.17	12.66	14.70	1.54	9.53	-26.09	-1.39
4	84.21	19.56	80.44	68.92	11.53	13.21	1.35	9.76	-26.01	-1.26
4.5	84.35	18.75	81.25	70.96	10.29	10.78	1.11	9.75	-25.91	-1.34
5	82.77	18.31	81.69	68.27	13.42	11.42	1.17	9.74	-25.52	-1.58
5.5	79.36	18.08	81.92	68.36	13.56	11.19	1.17	9.56	-25.80	-1.28
6	76.24	17.09	82.91	69.97	12.94	10.38	1.09	9.51	-25.75	-1.20
6.5	76.15	17.77	82.23	70.27	11.96	9.52	1.03	9.28	-25.84	-1.30
7	75.19	15.00	85.00	71.21	13.78	9.07	0.99	9.17	-25.70	-1.20
7.5	73.86	15.23	84.77	70.99	13.78	9.75	1.05	9.25	-25.64	-1.39
8	74.45	15.36	84.64	71.09	13.54	9.92	1.06	9.36	-25.64	-1.01
8.5	73.58	14.30	85.70	72.16	13.55	8.93	0.96	9.32	-25.80	-0.98
9	72.17	14.20	85.80	72.29	13.51	9.12	0.97	9.44	-25.81	-1.26
9.5	72.85	15.34	84.66	72.53	12.13	8.86	0.93	9.48	-25.56	-1.22
10	65.40	13.27	86.73	75.45	11.29	8.68	0.90	9.61	-25.64	-1.02
10.5	67.40	13.75	86.25	75.33	10.93	8.24	0.86	9.54	-25.56	-0.99
11	69.03	14.07	85.93	74.59	11.34	8.11	0.85	9.58	-25.58	-0.99
11.5	68.28	12.89	87.11	76.79	10.32	3.88	0.40	9.59	-25.61	-1.13
12	65.25	11.33	88.67	81.01	7.67	3.52	0.35	10.02	-25.51	-0.45

12.5	65.85	13.45	86.55	77.88	8.67	6.55	0.67	9.86	-25.82	-0.43
13	48.81	7.26	92.74	87.17	5.57	4.75	0.46	10.38	-25.59	-0.36
13.5	49.09	7.01	92.99	87.38	5.61	4.53	0.44	10.41	-25.81	-0.42
14	48.94	6.21	93.79	88.35	5.44	3.65	0.34	10.88	-25.89	-0.45
14.5	51.44	7.65	92.35	86.91	5.43	3.64	0.34	10.77	-25.88	-0.38
15	48.26	6.65	93.35	88.15	5.20	2.68	0.23	11.43	-25.89	-0.02
15.5	57.71	9.59	90.41	83.25	7.16	4.44	0.41	10.78	-25.65	-0.48
16	64.67	11.46	88.54	81.99	6.55	6.27	0.57	10.93	-25.00	-0.56
16.5	69.78	15.73	84.27	78.53	5.74	7.62	0.68	11.26	-25.70	-0.89
17	66.63	13.93	86.07	79.47	6.60	7.83	0.69	11.35	-25.86	-0.48
17.5	65.41	13.08	86.92	80.67	6.25	6.34	0.61	10.34	-25.47	-0.42
18	59.74	11.44	88.56	81.20	7.36	6.49	0.62	10.41	-25.32	-0.61
18.5	59.58	11.72	88.28	80.76	7.52	6.84	0.65	10.50	-25.10	-0.68
19	54.62	11.92	88.08	80.08	8.00	6.05	0.58	10.43	-25.28	-0.38
19.5	57.29	11.54	88.46	81.74	6.72	6.18	0.60	10.29	-25.39	-0.40
20	57.88	11.00	89.00	81.68	7.32	5.92	0.58	10.18	-25.41	-0.38
20.5	54.75	10.38	89.62	81.76	7.85	5.61	0.55	10.18	-25.63	-0.38
21	58.64	10.85	89.15	82.24	6.91	5.60	0.54	10.44	-25.67	-0.26
21.5	62.78	11.58	88.42	82.32	6.09	5.44	0.53	10.17	-25.88	-0.24
22	57.26	11.38	88.62	81.95	6.67	4.95	0.50	9.90	-25.95	-0.33
22.5	53.79	11.12	88.88	81.91	6.97	5.45	0.55	9.94	-25.61	-0.36
23	58.49	11.84	88.16	80.63	7.53	6.19	0.62	10.04	-25.31	-0.30
23.5	54.30	11.40	88.60	80.18	8.43	5.24	0.52	10.13	-25.68	-0.14
24	58.77	11.41	88.59	81.08	7.52	5.68	0.56	10.15	-25.48	-0.51
24.5	55.28	10.98	89.02	81.99	7.03	6.04	0.59	10.25	-25.10	-0.37
25	51.55	10.95	89.05	81.07	7.98	5.64	0.55	10.19	-25.49	-0.21
25.5	55.28	12.11	87.89	79.92	7.96	5.84	0.57	10.27	-25.27	-0.36
26	58.39	12.04	87.96	80.74	7.22	5.97	0.58	10.23	-25.35	-0.23
26.5	56.85	12.27	87.73	79.63	8.10	5.07	0.50	10.21	-25.23	-0.24

27	56.54	11.55	88.45	79.98	8.47	4.79	0.46	10.38	-25.49	-0.26
27.5	47.85	8.69	91.31	83.55	7.76	5.84	0.57	10.30	-25.31	-0.38
28	48.11	9.18	90.82	83.84	6.98	4.96	0.47	10.45	-25.23	-0.57
28.5	47.85	9.59	90.41	84.19	6.22	5.03	0.49	10.21	-25.32	-0.45
29	43.65	9.08	90.92	84.85	6.07	5.34	0.52	10.35	-25.25	-0.19
29.5	47.07	10.15	89.85	83.54	6.31	5.19	0.51	10.19	-25.30	-0.32
30	46.55	9.84	90.16	83.27	6.89	5.22	0.50	10.44	-25.36	0.03
30.5	46.64	9.89	90.11	83.57	6.54	5.09	0.51	10.07	-25.31	-0.31
31	46.17	9.31	90.69	82.76	7.92	4.74	0.47	10.07	-25.42	0.03

Table B.6. Loss-on-sequential heating, and organic carbon and nitrogen elemental and isotopic data for PAD 73 which includes water content (%H_2O), organic matter content (%OM), mineral matter content with carbonates (%MM IC), mineral matter content excluding carbonates (%MM EC), calcium carbonate content (%$CaCO_3$), organic carbon (%C), nitrogen content (%N), carbon to nitrogen ratio (C/N), organic carbon isotope composition ($\delta^{13}C$), nitrogen isotope composition ($\delta^{15}N$) and the respective depth (in cm).

Depth (cm)	%H2O	%OM	%MM IC	%MM EC	%$CaCO_3$	%C	%N	C/N	$\delta^{13}C$	$\delta^{15}N$
0	93.29	22.19	77.81	69.13	8.67	14.93	1.42	10.52	-26.10	-1.30
0.5	91.85	23.59	76.41	64.90	11.51	15.75	1.57	10.06	-26.24	-1.43
1	88.26	24.88	75.12	64.20	10.92	15.04	1.52	9.88	-26.03	-1.21
1.5	90.02	26.83	73.17	63.22	9.95	14.00	1.44	9.75	-26.28	-1.24
2	86.54	31.39	68.61	60.11	8.50	12.88	1.30	9.90	-26.39	-1.05
2.5	85.73	23.60	76.40	67.60	8.81	12.06	1.20	10.05	-26.12	-1.06
3	83.73	22.65	77.35	68.23	9.13	10.77	1.06	10.16	-26.71	-0.91
3.5	82.56	19.71	80.29	72.93	7.36	10.49	0.97	10.78	-26.69	-0.92
4	81.71	19.02	80.98	73.23	7.75	10.24	1.00	10.26	-26.66	-0.56
4.5	78.87	20.04	79.96	74.10	5.86	10.57	0.92	11.43	-26.81	-0.69
5	77.44	21.34	78.66	73.30	5.36	9.81	0.87	11.24	-26.89	-0.69
5.5	74.15	17.72	82.28	77.83	4.45	9.46	0.84	11.28	-26.74	-0.73
6	72.52	16.24	83.76	79.23	4.53	7.92	0.70	11.27	-26.57	-0.52
6.5	69.51	15.53	84.47	79.54	4.93	9.35	0.79	11.85	-26.82	-0.64
7	69.32	16.58	83.42	78.61	4.80	8.11	0.70	11.52	-26.89	-0.57
7.5	63.90	15.16	84.84	80.47	4.36	7.11	0.63	11.27	-27.08	-0.29
8	71.14	14.68	85.32	80.93	4.39	7.47	0.65	11.48	-26.91	-0.82
8.5	72.12	17.20	82.80	78.48	4.33	8.05	0.71	11.36	-27.07	-0.26
9	69.92	15.67	84.33	79.89	4.44	8.56	0.74	11.63	-26.79	-0.80
9.5	71.91	16.62	83.38	78.36	5.01	8.28	0.74	11.27	-26.98	-0.51
10	76.16	16.34	83.66	78.28	5.38	8.54	0.76	11.25	-26.91	-0.56
10.5	68.37	16.14	83.86	80.01	3.85	8.12	0.72	11.23	-27.07	-0.49
11	76.53	16.81	83.19	79.21	3.98	8.05	0.70	11.53	-27.13	-0.52
11.5	72.48	17.16	82.84	78.74	4.10	8.12	0.71	11.42	-27.02	-0.56
12	72.69	14.61	85.39	80.95	4.44	7.86	0.69	11.34	-26.96	-0.48

12.5	67.38	15.47	84.53	80.61	3.92	8.18	0.70	11.62	-26.75	-0.40
13	66.48	14.72	85.28	80.75	4.53	7.87	0.68	11.52	-26.70	-0.42
13.5	70.57	15.70	84.30	79.33	4.97	8.06	0.69	11.64	-26.77	-0.53
14	68.16	14.04	85.96	80.53	5.43	7.20	0.63	11.44	-26.65	-0.51
14.5	72.23	15.29	84.71	79.34	5.37	7.36	0.66	11.12	-26.48	-0.35
15	74.15	16.86	83.14	79.27	3.88	7.55	0.67	11.28	-26.42	-0.34
15.5	69.47	14.08	85.92	81.09	4.83	7.97	0.70	11.45	-26.66	-0.61
16	68.09	12.79	87.21	82.16	5.05	8.52	0.78	10.89	-25.71	-0.78
16.5	51.05	7.46	92.54	87.53	5.01	4.52	0.37	12.09	-25.76	-0.15
17	65.24	12.47	87.53	82.03	5.49	6.33	0.56	11.22	-25.33	-0.67
17.5	68.90	14.59	85.41	78.66	6.75	6.23	0.60	10.37	-25.34	-0.75
18	64.28	10.39	89.61	82.89	6.72	5.95	0.55	10.79	-25.80	-0.52
18.5	67.61	13.62	86.38	79.99	6.38	6.42	0.59	10.88	-25.92	-0.46
19	62.46	11.74	88.26	83.14	5.12	5.64	0.54	10.49	-26.20	-0.22
19.5	68.75	13.19	86.81	78.44	8.37	5.80	0.54	10.74	-26.36	-0.04
20	56.07	11.14	88.86	84.16	4.69	4.97	0.45	11.02	-26.70	-0.24
20.5	52.52	11.22	88.78	84.45	4.32	5.13	0.45	11.44	-26.91	-0.15
21	47.77	9.59	90.41	85.93	4.47	4.73	0.39	12.02	-26.71	-0.24
21.5	53.14	11.75	88.25	84.36	3.89	4.80	0.40	12.03	-26.85	0.00
22	50.88	11.02	88.98	85.20	3.79	4.20	0.35	11.95	-26.88	0.05
22.5	50.25	9.31	90.69	86.49	4.20	5.12	0.43	11.84	-27.14	-0.19
23	45.16	7.54	92.46	88.53	3.93	5.10	0.43	11.76	-27.13	-0.15
23.5	45.37	8.92	91.08	86.70	4.38	3.35	0.29	11.50	-26.95	0.33
24	45.89	9.31	90.69	86.28	4.41	3.13	0.26	12.07	-26.45	-0.26
24.5	42.67	7.72	92.28	87.68	4.60	4.15	0.36	11.58	-26.30	-0.19
25	45.24	9.54	90.46	86.22	4.24	4.72	0.37	12.86	-26.15	-0.21
25.5	47.33	10.49	89.51	84.47	5.03	3.48	0.28	12.50	-26.36	-0.21
26	40.40	8.91	91.09	87.23	3.86	4.42	0.35	12.59	-26.13	-0.24
26.5	45.98	10.23	89.77	84.99	4.77	5.09	0.40	12.83	-26.01	-0.16

27	51.16	13.50	86.50	81.86	4.64	5.03	0.40	12.50	-25.87	-0.44
27.5	59.69	19.05	80.95	77.24	3.71	6.27	0.53	11.77	-25.51	-0.63
28	50.09	12.69	87.31	82.13	5.18	7.16	0.61	11.81	-25.17	-0.23
28.5	51.06	13.69	86.31	81.48	4.83	6.84	0.58	11.79	-25.17	-0.46
29	53.64	15.27	84.73	80.29	4.44	7.20	0.63	11.50	-25.26	-0.36
29.5	52.13	13.32	86.68	82.21	4.47	7.12	0.61	11.75	-25.46	-0.41
30	50.14	13.65	86.35	81.75	4.60	7.45	0.63	11.83	-25.72	-0.36
30.5	50.29	12.95	87.05	82.48	4.57	7.05	0.58	12.08	-26.11	-0.28
31	49.74	12.66	87.34	82.24	5.09	6.99	0.58	12.10	-26.18	-0.41
31.5	51.30	15.83	84.17	79.49	4.68	7.40	0.63	11.76	-26.11	-0.30
32	53.05	14.71	85.29	80.17	5.11	8.59	0.70	12.27	-25.71	-0.40
32.5	50.00	13.73	86.27	80.36	5.91	6.87	0.58	11.81	-25.98	-0.09
33	45.92	11.09	88.91	83.11	5.81	5.77	0.50	11.55	-25.86	-0.31
33.5	46.37	11.35	88.65	83.25	5.39	5.68	0.50	11.47	-25.98	-0.15
34	50.22	10.08	89.92	84.35	5.56	4.55	0.40	11.34	-26.05	-0.12
34.5	42.29	9.52	90.48	84.67	5.81	4.24	0.38	11.16	-25.88	0.18
35	43.41	10.45	89.55	84.71	4.84	6.74	0.61	11.10	-25.39	-0.24
35.5	45.77	12.31	87.69	83.07	4.61	6.36	0.56	11.30	-25.45	-0.25
36	43.90	10.96	89.04	84.82	4.22	5.79	0.51	11.32	-25.77	-0.26
36.5	44.76	10.61	89.39	84.82	4.57	5.38	0.47	11.55	-25.75	-0.12
37	48.21	13.08	86.92	82.13	4.79	6.32	0.54	11.78	-26.06	-0.06
37.5	47.76	12.86	87.14	82.43	4.71	7.01	0.58	12.03	-26.14	-0.03
38	49.95	14.30	85.70	81.12	4.58	6.98	0.59	11.76	-26.20	-0.44
38.5	49.05	14.85	85.15	80.48	4.67	7.46	0.63	11.82	-26.10	-0.47
39	49.03	13.59	86.41	81.31	5.10	7.45	0.64	11.62	-26.14	-0.52
39.5	48.70	13.04	86.96	82.03	4.94	6.98	0.58	12.02	-26.35	-0.47
40	47.80	12.94	87.06	82.04	5.01	6.88	0.59	11.61	-26.00	-0.48
40.5	48.69	12.92	87.08	82.25	4.83	7.21	0.62	11.59	-25.89	-0.50
41	51.19	14.63	85.37	80.24	5.13	7.62	0.65	11.70	-25.80	-0.70

41.5	48.89	13.45	86.55	81.03	5.52	7.32	0.63	11.69	-25.91	-0.75
42	46.88	12.92	87.08	81.75	5.33	7.14	0.61	11.80	-25.98	-0.65
42.5	46.71	12.71	87.29	82.26	5.03	6.28	0.54	11.54	-26.09	-0.52
43	49.09	13.57	86.43	82.26	4.17	6.91	0.57	12.15	-26.36	-0.31
43.5	49.39	14.01	85.99	81.31	4.67	6.91	0.56	12.29	-26.26	-0.53
44	46.04	12.17	87.83	83.47	4.37	6.14	0.49	12.42	-27.03	-0.31
44.5	46.70	12.60	87.40	82.59	4.81	6.37	0.52	12.27	-26.70	-0.52
45	35.10	7.63	92.37	88.01	4.36	4.22	0.33	12.93	-27.20	-0.21
45.5	30.85	6.47	93.53	89.32	4.21	3.25	0.25	13.06	-27.39	0.17
46	39.36	8.51	91.49	87.36	4.13	2.53	0.19	13.15	-27.08	0.01

Table B.7. Loss-on-sequential heating, and organic carbon and nitrogen elemental and isotopic data for PAD 74 which includes water content (%H_2O), organic matter content (%OM), mineral matter content with carbonates (%MM IC), mineral matter content excluding carbonates (%MM EC), calcium carbonate content (%$CaCO_3$), organic carbon (%C), nitrogen content (%N), carbon to nitrogen ratio (C/N), organic carbon isotope composition ($\delta^{13}C$), nitrogen isotope composition ($\delta^{15}N$) and the respective depth (in cm).

Depth (cm)	%H2O	%OM	%MM IC	%MM EC	%$CaCO_3$	%C	%N	C/N	$\delta^{13}C$	$\delta^{15}N$
0	95.15	25.40	74.60	63.81	10.79	13.63	1.66	8.22	-30.04	-1.04
0.5	91.84	20.72	79.28	70.09	9.19	11.98	1.40	8.58	-29.95	-1.06
1	86.32	19.32	80.68	71.02	9.66	10.20	1.11	9.21	-29.52	-0.75
1.5	86.60	25.18	74.82	66.98	7.84	10.23	1.08	9.51	-29.02	-0.75
2	85.05	17.96	82.04	72.00	10.04	9.58	1.00	9.55	-29.35	-0.67
2.5	85.75	18.58	81.42	72.12	9.30	10.05	1.03	9.72	-29.03	-0.85
3	83.18	18.95	81.05	71.51	9.54	10.95	1.12	9.80	-28.95	-0.76
3.5	81.48	24.05	75.95	67.23	8.71	9.79	1.01	9.66	-28.77	-0.58
4	78.99	14.36	85.64	75.75	9.89	8.91	0.89	9.99	-28.32	-0.63
4.5	73.36	13.04	86.96	78.65	8.31	7.24	0.72	10.09	-27.81	-0.48
5	66.62	11.96	88.04	81.46	6.58	6.23	0.61	10.24	-27.45	-0.60
5.5	59.67	11.93	88.07	81.95	6.12	6.13	0.57	10.69	-26.95	-0.56
6	64.06	12.14	87.86	81.73	6.13	5.81	0.56	10.40	-27.18	-0.37
6.5	61.47	12.14	87.86	81.80	6.06	5.66	0.54	10.55	-27.02	-0.35
7	59.09	12.53	87.47	81.43	6.05	5.60	0.54	10.34	-27.35	-0.20
7.5	58.52	11.87	88.13	82.48	5.65	5.88	0.55	10.66	-27.19	-0.08
8	60.74	13.77	86.23	80.31	5.92	6.25	0.59	10.60	-27.35	-0.35
8.5	63.79	15.66	84.34	78.24	6.10	7.02	0.64	10.95	-27.26	-0.27
9	59.76	13.42	86.58	80.36	6.22	7.54	0.70	10.81	-27.10	-0.42
9.5	57.67	13.52	86.48	80.64	5.85	5.69	0.53	10.80	-27.16	-0.14
10	59.17	13.96	86.04	80.77	5.26	5.52	0.49	11.16	-27.12	-0.17
10.5	62.68	15.95	84.05	78.98	5.07	5.71	0.53	10.73	-26.97	-0.50
11	54.44	13.32	86.68	82.27	4.41	5.21	0.52	10.03	-27.40	0.02
11.5	55.22	12.12	87.88	81.42	6.45	5.61	0.54	10.36	-27.24	0.08
12	57.54	14.63	85.37	79.53	5.84	6.84	0.65	10.51	-27.10	-0.49

12.5	57.53	14.49	85.51	79.30	6.21	7.22	0.69	10.42	-26.91	-0.25
13	55.23	13.06	86.94	81.18	5.76	6.31	0.60	10.59	-26.84	-0.16
13.5	49.15	9.61	90.39	84.95	5.44	5.08	0.48	10.67	-27.22	0.28
14	49.65	12.28	87.72	83.42	4.30	5.04	0.46	10.97	-27.08	0.04
14.5	49.98	12.74	87.26	82.72	4.54	4.87	0.44	11.00	-27.34	0.54
15	53.52	13.32	86.68	82.46	4.22	4.83	0.44	10.96	-27.05	0.23
15.5	48.35	11.90	88.10	83.32	4.78	4.99	0.46	10.86	-27.21	0.23
16	47.72	11.99	88.01	83.27	4.74	4.75	0.44	10.81	-27.48	0.21
16.5	50.04	13.47	86.53	82.30	4.23	4.68	0.43	10.92	-27.19	0.14
17	48.44	11.55	88.45	83.41	5.05	5.44	0.50	10.89	-27.04	0.50
17.5	47.04	9.80	90.20	84.35	5.85	4.69	0.42	11.15	-26.91	0.37
18	49.80	10.96	89.04	83.24	5.79	3.74	0.35	10.78	-27.67	0.66
18.5	50.64	12.40	87.60	83.04	4.56	4.24	0.39	10.97	-27.50	0.33
19	48.85	11.42	88.58	84.31	4.27	5.28	0.47	11.15	-27.79	0.65
19.5	49.53	11.65	88.35	83.57	4.78	5.41	0.49	10.97	-27.60	0.11
20	48.25	11.84	88.16	83.29	4.86	5.87	0.53	10.99	-27.42	0.16
20.5	53.59	14.57	85.43	80.81	4.62	6.01	0.54	11.16	-27.46	0.33
21	54.29	15.29	84.71	79.09	5.62	6.00	0.54	11.02	-27.47	0.16
21.5	54.63	15.32	84.68	79.55	5.13	6.13	0.55	11.06	-27.45	-0.04
22	53.66	15.88	84.12	79.09	5.03	6.62	0.58	11.40	-27.46	0.14
22.5	56.16	15.71	84.29	80.23	4.06	5.88	0.53	11.13	-27.26	0.18
23	56.81	14.95	85.05	78.32	6.73	6.00	0.54	11.10	-27.51	0.14
23.5	51.43	12.37	87.63	82.09	5.54	7.34	0.65	11.25	-27.60	0.43
24	48.90	13.58	86.42	82.10	4.32	6.27	0.55	11.39	-27.59	0.07
24.5	61.06	17.40	82.60	73.63	8.97	6.87	0.61	11.22	-27.69	0.23
25	63.61	18.24	81.76	75.35	6.40	6.72	0.61	11.07	-27.74	0.00
25.5	59.50	16.59	83.41	77.43	5.99	6.99	0.64	10.94	-27.78	-0.03
26	56.85	14.95	85.05	80.17	4.88	7.14	0.65	11.07	-28.09	0.19
26.5	65.11	19.96	80.04	74.29	5.74	7.70	0.71	10.83	-27.84	0.00

27	56.14	15.54	84.46	78.31	6.15	7.08	0.64	10.99	-27.52	-0.07
27.5	53.72	13.66	86.34	79.89	6.45	6.73	0.60	11.14	-27.61	0.04
28	57.01	16.42	83.58	78.13	5.44	5.95	0.55	10.91	-27.31	-0.22
28.5	46.75	11.98	88.02	83.87	4.14	5.84	0.54	10.86	-27.17	0.03
29	48.65	12.50	87.50	82.88	4.62	4.80	0.44	10.80	-26.68	-0.14
29.5	48.71	12.69	87.31	82.59	4.72	4.39	0.40	10.92	-26.69	-0.02
30	38.86	9.59	90.41	86.68	3.73	4.78	0.43	11.09	-26.71	-0.33
30.5	47.00	11.66	88.34	82.86	5.47	4.76	0.43	11.14	-26.71	0.19
31	48.00	12.56	87.44	82.78	4.66	5.17	0.47	11.05	-27.04	0.13
31.5	45.34	11.52	88.48	83.91	4.56	5.70	0.51	11.18	-27.03	-0.33
32	49.06	14.35	85.65	80.81	4.84	7.20	0.62	11.55	-27.62	-0.41
32.5	46.62	12.69	87.31	83.04	4.27	4.59	0.41	11.21	-26.98	0.02
33	43.25	10.92	89.08	85.25	3.82	5.46	0.48	11.35	-26.84	-0.40
33.5	39.30	9.41	90.59	86.54	4.05	4.53	0.40	11.18	-25.06	-0.35
34	40.21	10.61	89.39	84.55	4.84	4.69	0.42	11.06	-26.46	-0.25
34.5	45.81	12.41	87.59	83.63	3.96	4.38	0.39	11.32	-26.68	-0.12
35	48.25	11.24	88.76	83.96	4.80	4.85	0.43	11.37	-26.64	-0.13
35.5	42.35	9.09	90.91	85.52	5.39	3.88	0.36	10.90	-26.50	-0.19
36	38.76	7.61	92.39	86.87	5.52	3.53	0.33	10.86	-26.41	0.32
36.5	37.71	7.95	92.05	86.98	5.06	4.42	0.39	11.24	-26.46	0.15
37	37.55	7.90	92.10	86.83	5.27	3.09	0.27	11.57	-26.53	-0.06
37.5	33.51	6.33	93.67	89.07	4.60	3.81	0.35	10.94	-26.66	0.01
38	39.47	9.20	90.80	85.55	5.25	3.96	0.36	10.90	-26.35	0.00
38.5	36.44	10.67	89.33	84.12	5.20	3.82	0.34	11.22	-26.35	-0.08
39	37.15	8.52	91.48	86.48	5.01	3.25	0.29	11.12	-26.39	0.49
39.5	35.86	7.67	92.33	86.63	5.69	4.03	0.36	11.14	-26.34	0.12
40	37.70	8.89	91.11	85.63	5.48	4.12	0.38	10.74	-26.20	0.02
40.5	38.98	8.72	91.28	85.54	5.74	3.86	0.36	10.86	-26.14	-0.11
41	35.85	7.76	92.24	86.48	5.76	4.49	0.41	10.90	-25.91	-0.11

41.5	39.18	9.20	90.80	84.82	5.98	4.31	0.39	10.99	-25.92	-0.14
42	40.25	10.64	89.36	82.81	6.55	4.85	0.44	10.97	-25.66	-0.03
42.5	38.22	9.30	90.70	85.12	5.58	4.76	0.44	10.88	-25.91	0.01
43	38.26	9.22	90.78	85.18	5.60	4.30	0.40	10.77	-25.92	-0.17
43.5	39.22	9.04	90.96	85.49	5.47	4.67	0.43	10.74	-25.55	-0.11
44	40.61	9.47	90.53	85.06	5.47	4.72	0.43	10.95	-25.51	-0.18
44.5	39.35	9.49	90.51	84.31	6.20	4.59	0.41	11.28	-25.94	-0.08

Table B.8. Loss-on-sequential heating data for PAD 78 which includes water content (%H_2O), organic matter content (%OM), mineral matter content with carbonates (%MM IC), mineral matter content excluding carbonates (%MM EC), calcium carbonate content (%$CaCO_3$), and the respective depth (in cm).

Depth (cm)	%H2O	%OM	%MM IC	%MM EC	%$CaCO_3$
0	89.08	21.64	78.36	73.09	5.26
0.5	71.2	18.93	81.07	76.30	4.77
1	69.32	19.45	80.55	75.75	4.80
1.5	67.36	18.63	81.37	76.23	5.14
2	66.75	18.55	81.45	76.27	5.18
2.5	67.34	18.31	81.69	76.40	5.28
3	66.6	19.09	80.91	75.60	5.30
3.5	66.7	19.03	80.97	75.66	5.31
4	62.55	18.67	81.33	75.66	5.67
4.5	59.56	17.79	82.21	76.70	5.51
5	61.67	18.58	81.42	76.10	5.33
5.5	60.76	18.40	81.60	75.82	5.78
6	63.16	19.34	80.66	74.99	5.67
6.5	60.55	18.21	81.79	76.06	5.73
7.5	56.44	17.74	82.26	76.96	5.30
8	55.8	17.25	82.75	77.55	5.20
8.5	56.88	18.02	81.98	76.70	5.28
9	57.33	16.43	83.57	78.21	5.36
9.5	54.9	16.89	83.11	77.46	5.65
10	52.29	16.53	83.47	78.03	5.44
10.5	50.82	15.89	84.11	78.24	5.87
11	49.32	16.05	83.95	78.16	5.79
11.5	51.66	15.86	84.14	78.58	5.56
12	45.57	14.14	85.86	80.77	5.09
12.5	48.04	15.63	84.37	78.71	5.66

13	46.31	15.08	84.92	79.12	5.80
13.5	46.04	14.93	85.07	79.01	6.06
14	46.68	15.25	84.75	78.68	6.07
14.5	48.37	14.56	85.44	79.48	5.96
15	47.39	14.53	85.47	79.42	6.04
15.5	45.79	14.22	85.78	79.61	6.17
16	45.92	13.85	86.15	80.09	6.06
16.5	44.57	13.96	86.04	79.91	6.13
17					
17.5	45.14	13.66	86.34	80.38	5.96
18	47.22	14.73	85.27	79.87	5.40
18.5	45.98	15.18	84.82	79.20	5.62
19	44.28	14.33	85.67	80.42	5.25
19.5	44.5	13.96	86.04	80.49	5.56
20	46.61	15.23	84.77	78.91	5.86
20.5	45.94	14.97	85.03	79.63	5.40
21	45.05	14.72	85.28	79.73	5.55
21.5	44.22	15.23	84.77	79.51	5.26
22	45.28	15.49	84.51	78.78	5.73
22.5	44.56	15.29	84.71	79.09	5.62
23	44.07	15.65	84.35	78.84	5.50
23.5	43.55	14.58	85.42	80.15	5.27
24	40.37	13.02	86.98	81.58	5.40
24.5	41.15	13.15	86.85	82.01	4.84
25	40.9	13.04	86.96	81.41	5.55
25.5	40.99	13.48	86.52	80.89	5.63
26	41.88	13.35	86.65	81.39	5.26
26.5	41.79	12.96	87.04	81.53	5.51
27	41.79	12.52	87.48	81.71	5.77

27.5	40.83	11.50	88.50	82.56	5.94
28	41.31	11.86	88.14	82.38	5.76
28.5	40.94	11.82	88.18	82.68	5.50
29	40.59	11.52	88.48	82.71	5.76
29.5	40.25	11.48	88.52	83.04	5.48
30	40.39	11.46	88.54	83.01	5.53
30.5	41.03	11.37	88.63	83.32	5.31
31	38.4	10.47	89.53	84.35	5.18
31.5	39.43	10.77	89.23	83.83	5.39
32	40.31	11.51	88.49	82.90	5.59
32.5	40.51	10.96	89.04	83.57	5.47
33	40.2	11.24	88.76	82.96	5.79
33.5	40.79	11.74	88.26	82.57	5.69
34	39.93	11.14	88.86	82.90	5.96
34.5	39.22	13.57	86.43	80.54	5.89
35	39	11.53	88.47	82.37	6.11
35.5	39.26	11.04	88.96	82.80	6.16
36	38.35	10.64	89.36	82.80	6.56
36.5	38.96	10.79	89.21	82.93	6.29
37	38.32	10.51	89.49	82.91	6.58
37.5	37.72	10.20	89.80	83.67	6.12
38	38.63	10.79	89.21	82.68	6.53
38.5	38.79	10.59	89.41	83.72	5.69

Table B.9. Loss-on-sequential heating, and organic carbon and nitrogen elemental and isotopic data for PAD 79 which includes water content (%H_2O), organic matter content (%OM), mineral matter content with carbonates (%MM IC), mineral matter content excluding carbonates (%MM EC), calcium carbonate content (%$CaCO_3$), organic carbon (%C), nitrogen content (%N), carbon to nitrogen ratio (C/N), organic carbon isotope composition ($\delta^{13}C$), nitrogen isotope composition ($\delta^{15}N$) and the respective depth (in cm).

Depth (cm)	%H2O	%OM	%MM IC	%MM EC	%$CaCO_3$	%C	%N	C/N	$\delta^{13}C$	$\delta^{15}N$
0	99.63	31.25	68.75	61.95	6.80					
0.5	99.57	24.32	75.68	66.49	9.19					
1	99.79	34.78	65.22	50.43	14.78					
1.5	99.58	21.62	78.38	76.54	1.84					
2	96.38	23.38	76.62	69.85	6.77					
2.5	90.46	19.11	80.89	74.98	5.91					
3	86.76	15.20	84.80	78.09	6.71					
3.5	86.47	17.03	82.97	76.44	6.53					
4	85.69	20.14	79.86	73.66	6.20	6.66	0.67	10.01	-31.33	-0.61
4.5	85.93	16.75	83.25	77.10	6.15	4.82	0.58	8.27	-31.93	-0.17
5	80.85	13.82	86.18	79.79	6.39	4.00	0.49	8.17	-31.88	0.21
5.5	76.72	12.54	87.46	81.13	6.33	3.87	0.46	8.38	-31.54	0.09
6	73.62	10.78	89.22	82.43	6.80	3.31	0.39	8.43	-31.01	0.28
6.5	75	12.71	87.29	80.77	6.52	3.81	0.46	8.33	-31.61	-0.30
7	71.09	11.68	88.32	82.08	6.24	3.38	0.40	8.55	-30.75	-0.06
7.5	71.21	12.67	87.33	81.56	5.77	3.62	0.43	8.50	-31.02	0.21
8	72.67	12.53	87.47	81.15	6.33					
8.5	71.02	11.52	88.48	82.29	6.19					
9	70.97	11.04	88.96	82.33	6.62	3.61	0.43	8.37	-30.58	0.64
9.5	71.09	11.10	88.90	82.15	6.74	3.41	0.40	8.56	-29.87	0.34
10	77.11	14.11	85.89	78.46	7.44					
10.5	78.88	14.65	85.35	77.77	7.58	5.58	0.73	7.68	-31.92	0.42
11	72.71	12.52	87.48	80.34	7.14	4.30	0.51	8.45	-30.29	0.49
11.5	68.82	10.76	89.24	82.79	6.45	3.60	0.41	8.71	-29.43	0.69
12	60.57	9.38	90.62	84.83	5.79					

12.5	62.12	11.50	88.50	83.29	5.21					
13	65.71	12.02	87.98	81.85	6.13					
13.5	67.15	10.98	89.02	82.21	6.80					
14	71.14	10.37	89.63	83.09	6.54					
14.5	72.43	10.20	89.80	83.02	6.79					
15	74.93	9.08	90.92	83.39	7.53	2.12	0.24	9.03	-27.47	0.13
15.5	73.16	9.26	90.74	83.87	6.87	1.83	0.21	8.56	-27.07	0.00
16	72.8	14.37	85.63	35.16	50.47					
16.5	68.54	8.60	91.40	84.41	6.99	1.61	0.17	9.25	-26.84	1.14
17	65.56	8.79	91.21	84.88	6.33					
17.5	53.65	7.28	92.72	89.80	2.93	1.52	0.14	11.06	-26.66	1.02
18	54.6	8.02	91.98	86.62	5.36	1.83	0.18	10.23	-27.19	1.44
18.5	63.09	8.39	91.61	85.50	6.11	1.88	0.19	10.00	-27.07	1.98
19	64.79	8.62	91.38	84.55	6.82	1.75	0.19	8.99	-27.23	0.96
19.5	66.48	8.89	91.11	84.18	6.93	1.89	0.21	9.07	-27.47	1.54
20	68.55	9.34	90.66	84.22	6.44					
20.5	71.81	9.21	90.79	83.90	6.89	1.70	0.20	8.47	-27.39	1.11
21	70.85	8.98	91.02	83.86	7.16	1.42	0.17	8.50	-27.32	1.18
21.5	65.97	11.69	88.31	79.97	8.34	2.43	0.27	9.14	-29.03	-0.11
22	69.4	12.35	87.65	79.35	8.31	2.70	0.32	8.44	-29.04	0.98
22.5	69.31	10.13	89.87	81.82	8.05	1.97	0.24	8.26	-28.26	1.22
23	70.1	9.56	90.44	83.95	6.50	1.67	0.21	7.89	-27.60	0.65
23.5	66.47	8.65	91.35	84.78	6.56	1.70	0.19	8.75	-26.84	1.75
24	65.91	8.89	91.11	85.07	6.04					
24.5	59.14	8.17	91.83	85.97	5.86	1.68	0.17	9.81	-26.60	1.96
25	56.61	7.61	92.39	86.34	6.05	2.30	0.18	12.91	-26.42	1.15
25.5	69.13	9.18	90.82	83.53	7.29	1.61	0.20	8.11	-27.03	2.05
26	68.76	8.84	91.16	84.25	6.92	1.70	0.20	8.32	-27.14	2.15
26.5	69.85	9.78	90.22	82.91	7.32	2.45	0.30	8.09	-28.96	1.13

27	76.03	12.85	87.15	77.72	9.42	5.08	0.63	8.09	-30.24	0.77
27.5	76.5	13.63	86.37	78.08	8.29					
28	75.73	16.67	83.33	74.33	9.00					
28.5	73.92	12.88	87.12	79.03	8.09	4.89	0.59	8.34	-30.51	0.82
29	66.95	10.98	89.02	82.51	6.52	2.36	0.27	8.66	-28.25	1.38
29.5	67.12	11.23	88.77	82.42	6.35	3.88	0.44	8.85	-30.05	1.44
30	75.62	13.41	86.59	78.58	8.01	5.47	0.66	8.29	-30.84	1.13
30.5	76.48	16.44	83.56	76.60	6.96	6.50	0.79	8.23	-31.08	0.91
31	72.17	15.07	84.93	77.59	7.35	5.82	0.67	8.64	-30.80	1.22
31.5	70.62	12.90	87.10	80.12	6.98	4.27	0.50	8.63	-30.18	1.53
32	69.05	11.44	88.56	80.69	7.87					
32.5	68.35	11.42	88.58	81.76	6.83	3.03	0.36	8.43	-29.55	0.93
33	69.95	13.96	86.04	77.95	8.10	3.66	0.44	8.37	-30.99	0.93
33.5	70.54	13.25	86.75	77.74	9.01	3.80	0.47	8.09	-31.46	0.21
34	72.81	12.52	87.48	77.78	9.70	3.50	0.41	8.56	-30.72	0.69
34.5	71.54	11.11	88.89	80.96	7.93	2.51	0.30	8.35	-29.38	0.78
35	70.68	10.22	89.78	82.27	7.51	2.24	0.26	8.45	-28.43	1.20
35.5	69.58	9.82	90.18	83.51	6.68	2.08	0.24	8.62	-28.00	1.30
36	58.12	7.72	92.28	86.41	5.87	1.82	0.18	10.31	-27.23	1.78
36.5	63.7	8.53	91.47	84.41	7.06	2.28	0.23	10.12	-27.92	0.86
37	68.97	9.76	90.24	83.09	7.16	2.84	0.31	9.15	-28.99	0.64
37.5	74.55	13.93	86.07	78.37	7.70	4.78	0.56	8.50	-30.61	1.08
38	75.92	15.66	84.34	76.26	8.07	6.58	0.79	8.37	-31.40	0.71
38.5	76.74	19.32	80.68	73.72	6.95	7.82	0.89	8.78	-32.14	1.11
39	78.64	18.72	81.28	73.09	8.19	8.66	1.02	8.47	-32.36	1.19
39.5	80.33	18.51	81.49	73.60	7.89	7.01	0.84	8.35	-32.46	0.85
40	75.82	15.39	84.61	77.25	7.35					
40.5	69.71	11.59	88.41	81.87	6.54	4.32	0.50	8.72	-29.53	1.35
41	70.51	12.34	87.66	81.02	6.64	4.28	0.49	8.74	-29.88	1.31

41.5	70.75	12.74	87.26	80.72	6.54	4.30	0.49	8.76	-30.52	0.97
42	72.96	14.40	85.60	77.92	7.67	4.94	0.59	8.39	-31.21	0.82
42.5	74.97	12.83	87.17	78.88	8.29					
43	66.93	9.43	90.57	83.95	6.61	2.50	0.27	9.25	-28.22	1.72
43.5	52.43	9.13	90.87	85.66	5.21	2.66	0.26	10.14	-28.16	2.05
44	48.65	9.92	90.08	85.11	4.97	2.85	0.27	10.47	-27.85	1.88
44.5	47.52	10.55	89.45	84.73	4.71	3.93	0.31	12.74	-28.23	2.66
45	52.51	12.23	87.77	83.09	4.69	3.30	0.31	10.53	-28.13	1.59
45.5	49.47	7.98	92.02	86.14	5.88	3.65	0.33	11.13	-27.92	1.59
46	44.89	9.42	90.58	85.15	5.43	2.99	0.29	10.46	-27.91	1.22
46.5	46.4	9.54	90.46	85.23	5.23	3.38	0.30	11.42	-27.70	1.32
47	45.65	9.82	90.18	85.11	5.07	3.50	0.31	11.30	-27.64	1.04
47.5	46.32	9.67	90.33	85.04	5.29	3.23	0.29	11.04	-27.94	1.31
48	44.83	9.77	90.23	85.16	5.07					
48.5	46.63	9.66	90.34	84.78	5.56	2.95	0.27	10.77	-27.82	1.82
49	49.36	9.74	90.26	84.41	5.85	2.95	0.28	10.61	-27.98	1.31
49.5	45.48	9.15	90.85	85.22	5.62	3.08	0.29	10.69	-27.87	1.66
50	47.35	9.49	90.51	84.81	5.71	3.55	0.30	11.86	-27.89	1.01
50.5	48.14	10.90	89.10	83.91	5.19	3.30	0.30	10.85	-27.91	1.41
51	47.89	9.93	90.07	84.58	5.49	3.17	0.29	10.96	-28.00	1.06
51.5	49.88	10.52	89.48	83.61	5.86	3.32	0.32	10.52	-28.07	1.07
52	49.94	10.41	89.59	83.92	5.67	3.32	0.32	10.43	-28.09	1.72
52.5	54.58	9.83	90.17	84.11	6.06	3.03	0.29	10.28	-28.25	1.13
53	59.84	10.32	89.68	83.06	6.61	2.65	0.27	9.69	-28.08	1.12
53.5	61.51	9.55	90.45	83.35	7.10	2.71	0.27	9.99	-28.17	0.51
54	58.13	9.36	90.64	84.57	6.07	2.38	0.24	10.09	-27.77	0.79
54.5	33.83	30.51	69.49	65.47	4.02	2.26	0.21	10.64	-27.58	1.22
55	44.68	8.23	91.77	86.72	5.06	2.16	0.21	10.47	-27.26	1.00
55.5	39.01	8.38	91.62	87.06	4.56	2.25	0.21	10.83	-27.09	1.63

56.5	38.95	8.84	91.16	86.78	4.38	2.47	0.23	10.90	-27.07	1.42
57	40.65	9.13	90.87	86.39	4.49	3.07	0.25	12.41	-27.10	0.44
57.5	47.57	9.60	90.40	85.60	4.80	2.80	0.24	11.50	-27.08	0.98
58	54.64	9.18	90.82	85.42	5.40	2.32	0.23	10.22	-27.19	0.66
58.5	48.54	8.74	91.26	86.18	5.08	2.57	0.23	11.05	-27.26	0.61
59	51.71	9.00	91.00	86.02	4.98	2.24	0.21	10.51	-27.17	1.05
59.5	58.74	9.49	90.51	84.94	5.57	2.48	0.23	10.86	-27.38	0.92
60	61.24	9.32	90.68	84.84	5.84	1.75	0.20	8.79	-26.90	1.47
60.5	58.69	8.82	91.18	85.49	5.70	1.79	0.19	9.69	-26.98	1.30
61	45.23	7.67	92.33	87.68	4.65	1.54	0.15	9.95	-27.06	2.42
61.5	51.97	8.58	91.42	86.15	5.27	2.06	0.21	10.03	-27.65	1.22
62	54	9.27	90.73	85.34	5.39	2.56	0.27	9.33	-28.63	1.09
62.5	61.29	11.54	88.46	81.97	6.49	3.35	0.38	8.93	-30.33	0.59
63	63.09	9.97	90.03	83.22	6.81	2.47	0.28	8.94	-28.96	1.47
63.5	63.97	10.29	89.71	83.27	6.43	2.16	0.25	8.66	-28.46	0.86
64	63.06	9.83	90.17	83.82	6.35					
64.5	60.77	10.64	89.36	83.38	5.98	2.55	0.25	10.24	-27.62	0.54
65	53.75	10.86	89.14	84.08	5.06	2.93	0.25	11.52	-27.69	1.41
65.5	44.03	9.32	90.68	86.28	4.40	2.47	0.22	11.08	-27.54	1.13
66	50.94	11.89	88.11	83.03	5.08	2.84	0.25	11.45	-27.93	0.91
66.5	56.64	14.03	85.97	80.56	5.41	2.33	0.23	9.93	-28.41	0.78
67	55.93	11.27	88.73	83.71	5.03	2.55	0.22	11.76	-27.20	1.23
67.5	57.01	9.69	90.31	84.67	5.64	1.96	0.20	9.61	-27.48	1.22
68	60.06	9.25	90.75	85.01	5.74	1.82	0.20	9.11	-27.33	1.10
68.5	62.84	9.50	90.50	85.12	5.37	1.79	0.21	8.62	-27.20	0.23
69	62.37	10.01	89.99	84.54	5.45	1.85	0.22	8.59	-27.15	1.81
69.5	62.32	9.60	90.40	84.27	6.13	1.75	0.21	8.50	-26.87	1.08
70	53.36	10.06	89.94	84.73	5.22	1.84	0.20	9.22	-27.13	0.97
70.5	54.59	10.65	89.35	84.24	5.11	2.25	0.23	9.89	-27.76	1.18

71	56.97	10.82	89.18	83.48	5.70	2.23	0.23	9.57	-27.88	1.72

Table B.10. Loss-on-sequential heating data for PAD 80 which includes water content (%H_2O), organic matter content (%OM), mineral matter content with carbonates (%MM IC), mineral matter content excluding carbonates (%MM EC), calcium carbonate content (%$CaCO_3$), and the respective depth (in cm).

Depth (cm)	%H2O	%OM	%MM IC	%MM EC	%$CaCO_3$
0	85.8	15.21	84.79	80.78	4.01
0.5	73.62	16.78	83.22	79.43	3.79
1	75.53	17.85	82.15	78.76	3.39
1.5	69.8	20.05	79.95	76.50	3.45
2	71	19.32	80.68	76.84	3.84
2.5	66.79	18.72	81.28	77.66	3.63
3	63.34	17.61	82.39	78.23	4.15
3.5	62.85	18.17	81.83	77.66	4.16
4	65.15	18.03	81.97	78.28	3.68
4.5	62.12	16.79	83.21	79.36	3.85
5	61.56	16.12	83.88	80.04	3.84
5.5	58.86	16.24	83.76	79.75	4.01
6	56.41	16.29	83.71	79.79	3.92
6.5	60.91	16.41	83.59	80.00	3.59
7	60.24	17.65	82.35	78.71	3.64
7.5	65.03	19.26	80.74	76.58	4.16
8	60.85	16.78	83.22	78.92	4.30
8.5	58.2	18.26	81.74	78.03	3.71
9	57.83	15.74	84.26	80.87	3.40
9.5	55.53	17.36	82.64	78.53	4.12
10	57.84	17.16	82.84	78.98	3.87
10.5	58.2	16.60	83.40	79.25	4.15
11	55.37	17.35	82.65	78.75	3.89
11.5	54.4	14.43	85.57	81.71	3.86
12	51.23	15.91	84.09	80.48	3.61

12.5	50.85	14.86	85.14	81.58	3.55
13	49.85	14.28	85.72	82.28	3.44
13.5	57.18	15.86	84.14	80.26	3.88
14	57.92	16.13	83.87	79.87	3.99
14.5	58.06	16.47	83.53	79.61	3.92
15	59.4	17.90	82.10	78.26	3.84
15.5	51.41	13.60	86.40	81.96	4.43
16	52.85	15.28	84.72	81.25	3.47
16.5	52.18	15.96	84.04	80.21	3.82
17	48.98	12.99	87.01	83.13	3.89
17.5	50.19	14.65	85.35	81.53	3.82
18	48.65	13.90	86.10	82.44	3.66
18.5	50.55	14.52	85.48	82.29	3.19
19	49.68	14.06	85.94	82.14	3.80
19.5	46.99	13.43	86.57	82.73	3.83
20	42.42	10.90	89.10	85.15	3.95
20.5	43.85	10.65	89.35	85.35	4.01
21	45.35	11.77	88.23	84.08	4.15
21.5	41.3	10.18	89.82	86.18	3.63
22	48.02	22.83	77.17	73.92	3.25
22.5	40.8	11.14	88.86	85.12	3.75
23	38.04	9.30	90.70	86.34	4.36
23.5	35.95	9.30	90.70	86.83	3.87
24	38.32	10.46	89.54	85.66	3.88
24.5	33.38	8.59	91.41	87.27	4.14
25	39.59	12.02	87.98	83.97	4.01
25.5	41.68	11.97	88.03	84.24	3.78
26	41.2	12.40	87.60	84.00	3.60
26.5	40.35	11.63	88.37	84.61	3.77

27	40.42	11.35	88.65	84.67	3.98
27.5	41.02	11.95	88.05	84.28	3.77
28	39.39	11.61	88.39	84.95	3.44
28.5	40.22	11.37	88.63	85.00	3.64
29	38.97	12.02	87.98	84.36	3.62
29.5	39.14	10.88	89.12	85.41	3.71
30	39.52	11.95	88.05	84.59	3.46
30.5	40.69	12.00	88.00	84.28	3.72
31	40.24	12.83	87.17	83.44	3.73
31.5	38.6	11.61	88.39	84.46	3.93
32	39.3	11.72	88.28	84.42	3.87
32.5	39.11	12.58	87.42	84.08	3.34
33	39.32	11.64	88.36	84.64	3.72
33.5	66.63	13.78	86.22	82.41	3.81
34	39.65	12.66	87.34	83.83	3.51
34.5	40.98	12.52	87.48	83.68	3.79
35	41.67	12.98	87.02	83.40	3.62
35.5	41.69	12.84	87.16	83.23	3.93
36	42.93	13.21	86.79	83.26	3.53
36.5	41.58	14.10	85.90	82.30	3.60
37	39.29	13.19	86.81	83.15	3.66
37.5	40.81	13.40	86.60	82.86	3.74
38	41.89	13.38	86.62	83.04	3.58
38.5	43.83	13.62	86.38	83.15	3.24
39	43.97	13.91	86.09	82.60	3.49
39.5	41.1	13.14	86.86	83.10	3.76

Table B.11. Loss-on-sequential heating, and organic carbon and nitrogen elemental and isotopic data for PAD 81 which includes water content (%H_2O), organic matter content (%OM), mineral matter content with carbonates (%MM IC), mineral matter content excluding carbonates (%MM EC), calcium carbonate content (%$CaCO_3$), organic carbon (%C), nitrogen content (%N), carbon to nitrogen ratio (C/N), organic carbon isotope composition ($\delta^{13}C$), nitrogen isotope composition ($\delta^{15}N$) and the respective depth (in cm).

Depth (cm)	%H2O	%OM	%MM IC	%MM EC	%$CaCO_3$	%C	%N	C/N	$\delta^{13}C$	$\delta^{15}N$
0	89.78	20.23	79.77	74.33	5.44	10.43	1.12	9.33	-27.80	-0.45
0.5	73.5	19.60	80.40	76.01	4.38	9.90	1.06	9.36	-27.77	-0.49
1	82.04	21.40	78.60	72.64	5.96	9.77	1.01	9.64	-27.88	-0.38
1.5	80.96	18.73	81.27	74.74	6.53	10.05	1.04	9.68	-27.75	-0.12
2	81	18.47	81.53	74.09	7.44	10.36	1.07	9.71	-27.64	-0.23
2.5	75.47	17.62	82.38	75.29	7.09	9.56	0.95	10.09	-27.70	0.19
3	61.82	16.83	83.17	77.22	5.95	9.06	0.83	10.94	-27.45	-0.27
3.5	65.57	14.76	85.24	78.74	6.50	8.02	0.72	11.07	-27.43	0.13
4	62.22	14.98	85.02	78.23	6.79	7.50	0.65	11.47	-27.38	0.00
4.5	58.87	14.64	85.36	78.72	6.65	7.63	0.66	11.54	-27.40	0.17
5	63.08	15.04	84.96	78.10	6.86	8.20	0.69	11.95	-27.26	-0.13
5.5	57.45	14.49	85.51	78.55	6.95	7.40	0.63	11.69	-27.31	-0.16
6	55.16	15.12	84.88	78.13	6.75	8.68	0.73	11.87	-27.38	0.53
6.5	57.07	16.20	83.80	76.83	6.96	9.13	0.72	12.63	-27.22	0.63
7	54.46	17.13	82.87	76.76	6.11	8.66	0.71	12.22	-27.48	0.31
7.5	50.92	16.56	83.44	76.79	6.64	8.59	0.69	12.36	-27.51	0.45
8	53.72	16.92	83.08	76.93	6.15	8.84	0.72	12.20	-27.43	0.18
8.5	50.88	16.18	83.82	77.27	6.55	8.56	0.70	12.18	-27.63	0.02
9	50.99	16.50	83.50	76.85	6.65	8.15	0.67	12.12	-27.54	0.56
9.5	50.61	17.23	82.77	76.61	6.16	8.86	0.72	12.36	-27.46	0.31
10	50.7	16.62	83.38	77.10	6.28	8.49	0.69	12.24	-27.59	0.23
10.5	49.55	18.21	81.79	75.61	6.18	9.04	0.76	11.89	-27.55	0.61
11						8.84	0.71	12.49	-27.47	0.97
11.5	50.65	17.60	82.40	76.41	5.98	9.18	0.73	12.61	-27.62	0.31
12	52.81	18.95	81.05	75.29	5.77	9.48	0.75	12.60	-27.45	0.38

12.5	52.45	18.54	81.46	75.55	5.92	9.76	0.77	12.61	-27.53	0.61
13	51.57	18.71	81.29	75.56	5.73	9.27	0.75	12.33	-27.78	0.36
13.5	52.69	18.74	81.26	75.32	5.94	9.47	0.75	12.54	-27.68	0.06
14	50.12	17.87	82.13	76.66	5.47	9.23	0.73	12.60	-27.75	0.45
14.5	51.83	18.50	81.50	76.03	5.47	10.06	0.79	12.73	-27.68	0.58
15	52.45	18.73	81.27	75.80	5.47	10.10	0.79	12.71	-27.71	0.56
15.5	52.49	17.88	82.12	76.59	5.54	9.21	0.73	12.65	-27.77	0.58
16	50.72	18.44	81.56	75.99	5.57	9.64	0.78	12.34	-27.77	0.69
16.5	51.79	17.75	82.25	76.61	5.64	9.82	0.77	12.72	-27.76	0.50
17	51.73	17.85	82.15	76.79	5.35	9.20	0.73	12.67	-27.78	1.05
17.5	49.83	17.29	82.71	77.58	5.14	9.21	0.73	12.67	-27.86	0.67
18	50.22	17.59	82.41	77.45	4.96	9.73	0.75	13.00	-27.80	0.39
18.5	53.34	19.42	80.58	75.38	5.20	9.00	0.71	12.74	-27.96	0.49
19	51.33	18.27	81.73	76.83	4.90	9.80	0.76	12.86	-28.22	1.07
19.5	48.03	16.36	83.64	78.08	5.56	9.00	0.71	12.75	-28.03	0.60
20	49.64	18.23	81.77	76.59	5.19	8.63	0.68	12.74	-28.03	0.23
20.5	44.63	14.53	85.47	80.88	4.60	8.25	0.66	12.46	-28.08	0.82
21	46.22	15.89	84.11	79.17	4.95	7.41	0.59	12.50	-28.23	0.43
21.5	46.3	16.13	83.87	79.09	4.79	7.25	0.58	12.57	-28.15	1.30
22	40.34	12.88	87.12	82.91	4.21	6.95	0.56	12.40	-28.01	0.58
22.5	45.11	15.54	84.46	79.63	4.82	6.70	0.54	12.33	-28.22	0.42
23	41.62	13.35	86.65	82.19	4.46	5.89	0.49	12.09	-28.12	1.01
23.5	42.12	13.67	86.33	82.04	4.29	7.57	0.61	12.40	-28.12	1.31
24	44.7	14.95	85.05	78.87	6.18	7.14	0.55	13.08	-27.33	1.04
24.5	42.11	13.24	86.76	82.80	3.96	7.29	0.59	12.30	-28.16	1.02
25	39.11	11.70	88.30	84.29	4.00	6.56	0.54	12.24	-28.11	1.03
25.5	43.17	14.82	85.18	80.81	4.37	5.54	0.46	12.16	-28.09	1.14
26	32.63	9.28	90.72	87.34	3.38	5.76	0.47	12.25	-28.07	0.78
26.5	36.66	11.80	88.20	84.46	3.74	5.89	0.48	12.35	-28.11	0.67

27	25.01	6.71	93.29	90.46	2.83	3.49	0.29	11.93	-27.15	1.40
27.5	27.4	7.93	92.07	88.99	3.09	3.53	0.30	11.58	-27.44	1.21
28	24.96	6.57	93.43	90.43	3.00	2.25	0.19	11.57	-27.25	0.83
28.5	27.68	7.48	92.52	89.48	3.05	1.78	0.16	11.30	-26.87	0.76
29	28.81	8.57	91.43	88.28	3.14	1.80	0.16	11.58	-27.16	0.66
29.5	26.66	7.26	92.74	89.60	3.14	2.00	0.17	11.90	-27.16	0.43
30	29.74	9.35	90.65	87.69	2.96	1.70	0.14	12.18	-26.56	1.41
30.5	26.82	7.68	92.32	89.72	2.60	1.86	0.16	11.51	-26.96	1.30
31	25.74	6.86	93.14	90.57	2.57	2.02	0.17	11.63	-27.08	0.92

Table B.12. Loss-on-sequential heating, and organic carbon and nitrogen elemental and isotopic data for PAD 82 which includes water content (%H_2O), organic matter content (%OM), mineral matter content with carbonates (%MM IC), mineral matter content excluding carbonates (%MM EC), calcium carbonate content (%$CaCO_3$), organic carbon (%C), nitrogen content (%N), carbon to nitrogen ratio (C/N), organic carbon isotope composition ($\delta^{13}C$), nitrogen isotope composition ($\delta^{15}N$) and the respective depth (in cm).

Depth (cm)	%H2O	%OM	%MM IC	%MM EC	%$CaCO_3$	%C	%N	C/N	$\delta^{13}C$	$\delta^{15}N$
0	99.42	19.83	80.17	70.05	10.12					
0.5	91.11	15.33	84.67	77.34	7.32	5.58	0.79	7.06	-35.01	0.94
1	85.45	11.78	88.22	80.26	7.96	4.63	0.57	8.12	-33.85	0.56
1.5	79.06	10.43	89.57	83.56	6.01	3.66	0.42	8.71	-32.67	0.75
2	68.81	9.70	90.30	85.93	4.37	2.61	0.28	9.32	-30.71	1.08
2.5	73.36	10.55	89.45	82.23	7.22	3.67	0.42	8.74	-32.71	0.02
3	78.22	12.39	87.61	80.80	6.81	4.68	0.53	8.83	-33.65	0.68
3.5	77.68	11.62	88.38	82.10	6.28	4.18	0.49	8.53	-33.20	0.97
4	70.53	10.26	89.74	83.68	6.06	2.85	0.31	9.19	-31.11	0.50
4.5	69.19	8.40	91.60	86.16	5.45	2.82	0.31	9.10	-30.68	1.13
5	71.93	10.18	89.82	82.66	7.16	3.20	0.36	8.89	-31.10	0.47
5.5	71.9	9.73	90.27	85.92	4.35	2.90	0.34	8.53	-30.78	0.66
6	69.64	7.64	92.36	87.08	5.28	2.42	0.27	8.96	-29.46	1.41
6.5	65.07	8.59	91.41	86.12	5.29	1.98	0.21	9.43	-28.33	1.38
7	68.12	8.79	91.21	86.22	5.00	2.20	0.24	9.17	-28.62	1.56
7.5	75.37	11.00	89.00	82.72	6.27	3.46	0.41	8.44	-30.46	0.76
8	75.67	11.29	88.71	81.25	7.46	3.82	0.45	8.49	-30.83	0.89
8.5	72.85	10.24	89.76	82.05	7.71	3.46	0.41	8.44	-31.17	0.87
9	70.7	8.44	91.56	86.00	5.55	3.04	0.34	8.94	-30.60	1.28
9.5	56.84	7.81	92.19	87.69	4.50	1.97	0.19	10.37	-27.87	1.94
10	48.71	6.60	93.40	87.47	5.93	1.68	0.15	11.20	-26.86	1.99
10.5	53.55	6.75	93.25	87.97	5.28	1.76	0.17	10.35	-27.66	1.66
11	64.44	7.47	92.53	86.24	6.29	2.08	0.22	9.45	-28.36	1.34
11.5	53.18	6.77	93.23	87.96	5.27	1.64	0.16	10.25	-27.01	1.56
12	61.6	8.41	91.59	86.05	5.54	2.54	0.26	9.77	-29.44	1.24

12.5	64.13	6.91	93.09	88.20	4.89	2.67	0.29	9.21	-29.70	1.65
13	69.09	9.79	90.21	84.12	6.09	3.17	0.35	9.06	-30.94	1.37
13.5	70.16	11.24	88.76	84.41	4.34	3.54	0.40	8.85	-31.09	1.49
14	72.03	9.17	90.83	84.79	6.04	3.79	0.43	8.81	-30.95	1.85
14.5	74.14	10.66	89.34	83.45	5.89	4.36	0.51	8.55	-30.78	2.20
15	78.14	11.68	88.32	80.93	7.38	4.45	0.53	8.48	-30.82	2.31
15.5	76.09	10.76	89.24	81.75	7.49	4.15	0.49	8.47	-30.52	2.67
16	75.19	9.76	90.24	82.62	7.62	3.50	0.43	8.14	-30.10	2.42
16.5	76.14	10.14	89.86	84.43	5.43	3.71	0.44	8.43	-29.75	3.01
17	72.41	8.32	91.68	85.69	6.00	2.90	0.34	8.53	-29.26	2.49
17.5	69	9.35	90.65	84.69	5.96	2.74	0.31	8.84	-28.86	2.46
18	73.63	8.97	91.03	85.56	5.48	3.11	0.37	8.41	-29.79	2.52
18.5	69.16	8.49	91.51	84.90	6.61	2.48	0.29	8.55	-28.96	1.86
19	67.24	7.98	92.02	85.81	6.21	2.11	0.24	8.79	-28.13	2.38
19.5	58.21	7.31	92.69	87.78	4.91	1.83	0.19	9.63	-27.24	2.18
20	53.68	5.74	94.26	88.97	5.28	1.77	0.17	10.38	-27.06	2.33
20.5	57.89	6.63	93.37	88.05	5.32	2.00	0.20	10.00	-27.70	2.78
21	65.36	7.75	92.25	85.64	6.61	2.14	0.23	9.30	-28.00	2.62
21.5	68.18	7.68	92.32	86.16	6.16	2.05	0.23	8.91	-27.78	2.23
22	58.24	5.61	94.39	89.66	4.72	1.81	0.18	10.06	-26.77	2.52
22.5	42.35	6.11	93.89	89.48	4.41	1.78	0.15	11.87	-26.34	2.18
23	39.8	5.64	94.36	88.40	5.96	1.79	0.14	12.79	-26.25	1.92
23.5	43.34	5.53	94.47	88.29	6.18	1.80	0.14	12.86	-26.17	2.12
24	47.52	5.74	94.26	89.11	5.15	2.05	0.19	10.79	-26.84	2.67
24.5	63.98	7.27	92.73	88.20	4.53	2.09	0.19	11.00	-26.81	2.72
25	61.58	7.97	92.03	87.11	4.92	2.05	0.20	10.25	-27.02	2.78
25.5	53.72	7.59	92.42	86.84	5.57	2.04	0.19	10.74	-27.07	2.63
26	59.26	6.84	93.16	87.81	5.35	2.09	0.20	10.45	-27.10	2.73
26.5	55.83	7.07	92.93	87.45	5.48	1.87	0.18	10.39	-26.53	2.70

27	48.2	5.36	94.64	90.28	4.36	1.84	0.16	11.50	-26.16	2.72
27.5	40.67	5.65	94.35	88.50	5.85	1.84	0.15	12.27	-26.14	2.72
28	42.78	4.60	95.40	89.30	6.11	1.87	0.14	13.36	-26.05	2.98
28.5	45.45	5.27	94.73	88.51	6.22	1.87	0.15	12.47	-26.27	2.80
29	56.89	7.05	92.95	87.56	5.39	2.13	0.19	11.21	-26.88	3.14
29.5	57.83	6.82	93.18	88.25	4.93	2.12	0.19	11.16	-26.80	2.90
30	50.6	7.04	92.96	88.85	4.10	2.02	0.17	11.85	-26.32	2.57
30.5	41.98	6.18	93.82	88.38	5.43	1.86	0.14	13.29	-25.94	2.65
31	39.23	5.17	94.83	89.62	5.21	1.81	0.13	13.92	-25.87	2.50
31.5	46.5	6.17	93.83	87.64	6.19	1.98	0.16	12.38	-26.43	2.38
32	57.94	7.40	92.60	86.96	5.64	1.99	0.16	12.44	-26.48	2.06
32.5	60.06	7.72	92.28	86.67	5.62	1.78	0.20	8.90	-27.47	2.10
33	49.52	5.67	94.33	88.97	5.36	1.57	0.16	9.81	-26.66	1.71
33.5	47.03	6.25	93.75	87.71	6.04	1.80	0.16	11.25	-26.78	1.58
34	54.88	5.99	94.01	88.11	5.90	1.91	0.19	10.05	-27.61	1.05
34.5	60.34	7.70	92.30	86.13	6.16	2.23	0.24	9.29	-32.00	1.36
35	60.1	8.22	91.78	86.16	5.62	2.17	0.24	9.23	-28.40	1.79
35.5	60.03	8.35	91.65	85.83	5.82	2.30	0.24	9.58	-28.84	1.98
36	49.45	6.76	93.24	87.66	5.59	1.73	0.18	9.61	-27.19	2.15
36.5	47.81	7.27	92.73	88.15	4.58	1.56	0.15	10.40	-26.60	2.08
37	38.45	5.12	94.88	89.66	5.22	1.47	0.13	11.31	-26.37	1.70
37.5	48.94	6.43	93.57	88.18	5.39	1.72	0.17	10.12	-26.95	2.02
38	54.33	7.57	92.43	86.75	5.68	2.32	0.25	9.28	-28.10	2.26
38.5	59.67	8.72	91.28	86.46	4.81	2.45	0.28	8.75	-28.66	2.17
39	60.74	8.69	91.31	86.22	5.09	2.51	0.29	8.66	-28.60	2.38
39.5	62.12	9.13	90.87	86.28	4.59	2.62	0.30	8.73	-28.68	2.31
40	65.39	9.24	90.76	84.99	5.77	2.77	0.31	8.92	-28.83	2.29
40.5	65.42	9.92	90.08	85.89	4.18	2.65	0.30	8.83	-28.76	2.39
41	63.91	8.96	91.04	85.93	5.11	2.58	0.29	8.90	-28.45	2.28

41.5	61.93	8.81	91.19	86.10	5.09	2.44	0.28	8.71	-28.38	2.71
42	62.91	8.09	91.91	86.67	5.24	2.08	0.24	8.67	-28.31	2.53
42.5	63.28	8.33	91.67	87.38	4.30	2.47	0.28	8.71	-27.97	2.49
44	65.51	8.71	91.29	85.10	6.20	2.55	0.30	8.50	-27.32	1.93
44.5	60	8.15	91.85	86.96	4.89	2.02	0.23	8.96	-26.68	2.10
45	52.15	7.73	92.27	87.66	4.61	1.67	0.18	9.28	-30.11	2.03
45.5	51.77	6.85	93.15	88.32	4.83	1.83	0.19	9.63	-26.60	1.85
46	57.32	7.47	92.53	86.72	5.81	2.06	0.23	8.96	-27.11	2.21
46.5	57.91	7.90	92.10	86.21	5.89	2.05	0.22	9.32	-27.35	1.81
47	59.54	7.97	92.03	86.45	5.59	2.05	0.22	9.32	-27.60	1.83
47.5	56.6	6.91	93.09	88.16	4.92	1.78	0.19	9.37	-27.47	1.85
48	49.85	6.65	93.35	87.80	5.55	1.59	0.16	9.94	-26.86	1.63
48.5	50.11	5.78	94.22	89.02	5.20	1.61	0.16	10.06	-26.69	1.86
49	48.39	6.58	93.42	87.52	5.90	1.68	0.17	9.88	-26.82	2.38
49.5	58.79	7.13	92.87	88.45	4.42	1.72	0.18	9.56	-26.87	2.43
50	52.77	7.78	92.22	87.24	4.98	1.66	0.16	10.38	-26.63	2.46
50.5	45.45	6.78	93.22	87.53	5.70	1.67	0.15	11.13	-26.65	2.30
51	47.76	5.39	94.61	89.86	4.75	1.69	0.16	10.56	-26.60	1.66
51.5	49.25	6.78	93.22	87.78	5.44	1.65	0.16	10.31	-26.91	1.86
52	56.67	6.85	93.15	87.75	5.40	1.63	0.16	10.19	-26.81	1.82
52.5	49.22	6.61	93.39	87.84	5.54	1.64	0.15	10.93	-26.63	2.03
53	48.24	7.06	92.94	87.43	5.51	1.70	0.16	10.63	-26.86	1.99
53.5	52.22	7.69	92.31	88.06	4.25	1.80	0.17	10.59	-27.04	1.96
54	45.55	6.71	93.29	87.61	5.68	1.53	0.14	10.89	-26.74	2.11
54.5	42.86	6.14	93.86	88.95	4.91	1.68	0.15	11.20	-26.94	2.29
55	49.48	6.11	93.89	88.63	5.26	1.77	0.16	11.06	-27.13	2.47
55.5	57.43	7.06	92.94	85.69	7.25	1.96	0.20	9.80	-27.55	2.49
56	56.22	7.51	92.49	87.84	4.64	1.85	0.18	10.28	-27.31	2.28
56.5	55.03	7.11	92.89	87.66	5.23	1.83	0.18	10.17	-27.14	2.23

57	54.67	7.44	92.56	87.99	4.58	1.90	0.18	10.56	-27.17	2.61
57.5	57.68	7.77	92.23	87.17	5.06	1.96	0.19	10.32	-27.47	2.77

Appendix C - Breakpoint Results

Table C.1. Breakpoint results for % mineral matter content (%MM) of the dated lakes from the Moose Island (PAD 52, 79, 82) and the Rocky Point transect (PAD 65, 72, 73, 74), indicating the break point (BP; year), upper and lower 95% confidence interval (CI; year), the adjusted R^2 (R^2_{adj}) value of the segmented linear regression, and the results from the analysis of variance (ANOVA) test which includes the F ratio (F) and P-value.

Lake	BP	95% CI (year)		R^2_{adj}	ANOVA	
	(year)	Lower	Upper		F	P-value
Moose Island transect						
PAD 52	1976.99	1966.46	1987.52	0.7575	27.801	$7.3x10^{-7}$
PAD 79	2011.34	2007.94	2014.74	0.4177	32.114	$1.3x10^{-11}$
PAD 82	2013.55	2011.67	2015.44	0.4658	30.882	$2.3x10^{-11}$
Rocky Point transect						
PAD 72	1982.8	1978.94	1986.66	0.9008	117.63	$< 2.2x10^{-16}$
PAD 65	1986.44	1979.92	1992.96	0.7933	49.97	$1.0x10^{-10}$
PAD 73	2003.97	2001.33	2006.62	0.7829	80.865	$< 2.2x10^{-16}$
PAD 74	2006.16	2003.07	2009.24	0.7031	44.687	$8.4x10^{-14}$

Table C.2. Breakpoint results for carbon to nitrogen ratio (C/N) data of the dated lakes from the Moose Island (PAD 52, 79, 82) and the Rocky Point transect (PAD 65, 72, 73, 74), indicating the break point (BP; year), upper and lower 95% confidence interval (CI; year), the adjusted R^2 (R^2_{adj}) value of the segmented linear regression, and the results from the analysis of variance (ANOVA) test which includes the F ratio (F) and P-value. A BP estimation has been added for instances where the BP failed to capture a marked point of change.

Lake	BP	BP	95% CI (year)		R^2_{adj}	ANOVA	
	(year)	Estimate	Lower	Upper		F	P-value
Moose Island transect							
PAD 52	2001.44	-	1992.46	2010.43	0.8681	15.686	$5.0x10^{-5}$
PAD 79	1942.52	1914	1913.68	1971.36	0.3768	4.7404	$1.1x10^{-2}$
PAD 82	1983.78	-	1973.14	1994.42	0.2115	13.748	$4.7x10^{-6}$
Rocky Point transect							
PAD 72	1980.4	-	1973.28	1987.52	0.6199	29.506	$1.4x10^{-9}$
PAD 65	1939.74	1968	1922.96	1956.53	0.8421	17.355	$9.8x10^{-6}$
PAD 73	2005.57	-	2000.96	2010.18	0.4958	19.428	$1.8x10^{-7}$
PAD 74	2005.04	-	2002.54	2007.55	0.8188	108.72	$< 2.2x10^{-16}$

Table C.3. Breakpoint results for $\delta^{15}N$ data of the dated lakes from the Moose Island (PAD 52, 79, 82) and the Rocky Point transect (PAD 65, 72, 73, 74), indicating the break point (BP; year), upper and lower 95% confidence interval (CI; year), the adjusted R^2 (R^2_{adj}) value of the segmented linear regression, and the results from the analysis of variance (ANOVA) test which includes the F ratio (F) and P-value.

Lake	BP	95% CI (year)		R^2_{adj}	ANOVA	
	(year)	Lower	Upper		F	P-value
Moose Island transect						
PAD 52	1984.92	1975.76	1994.08	0.7374	30.255	$3.6x10^{-7}$
PAD 79	1972.1	1961.84	1982.36	0.4146	17.319	$5.6x10^{-7}$
PAD 82	1996.1	1992.27	1999.93	0.6627	88.042	$< 2.2x10^{-16}$
Rocky Point transect						
PAD 72	1981.3	1976.52	1986.08	0.8905	67.612	$7.0x10^{-16}$
PAD 65	1987.96	1974.94	2000.97	0.3320	6.0962	$6.0x10^{-3}$
PAD 73	2006.23	2003.15	2009.3	0.6866	33.406	$5.5x10^{-11}$
PAD 74	1976.54	1970.51	1982.58	0.6689	71.044	$< 2.2x10^{-16}$

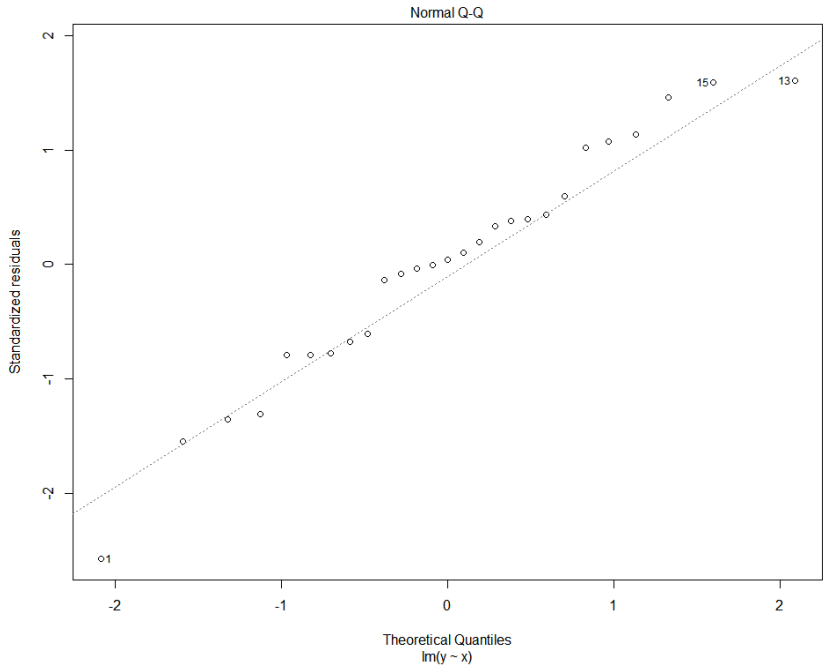

Figure C.1. Normal quantile (Q-Q) plot of the residuals for the piece-wise linear regression model completed on the mineral matter content by year for PAD 52.

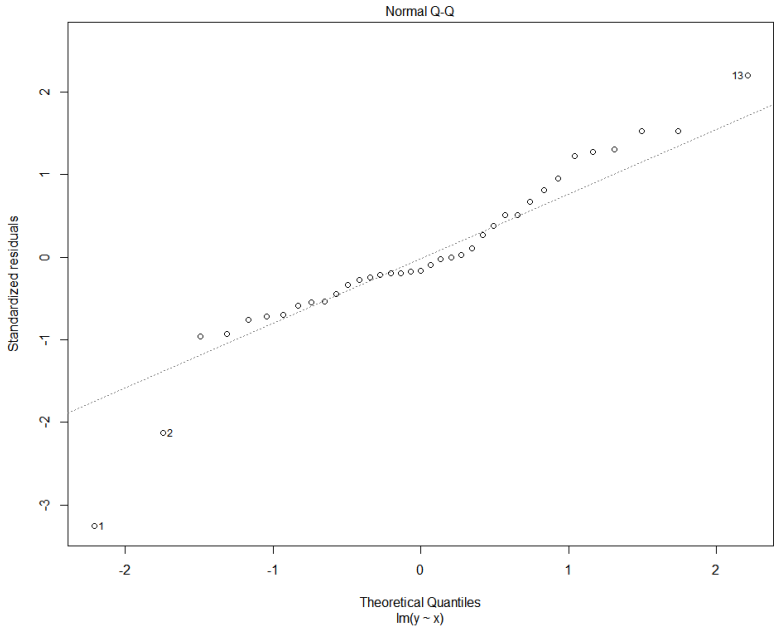

Figure C.2. Normal quantile (Q-Q) plot of the residuals for the piece-wise linear regression model completed on the mineral matter content by year for PAD 65.

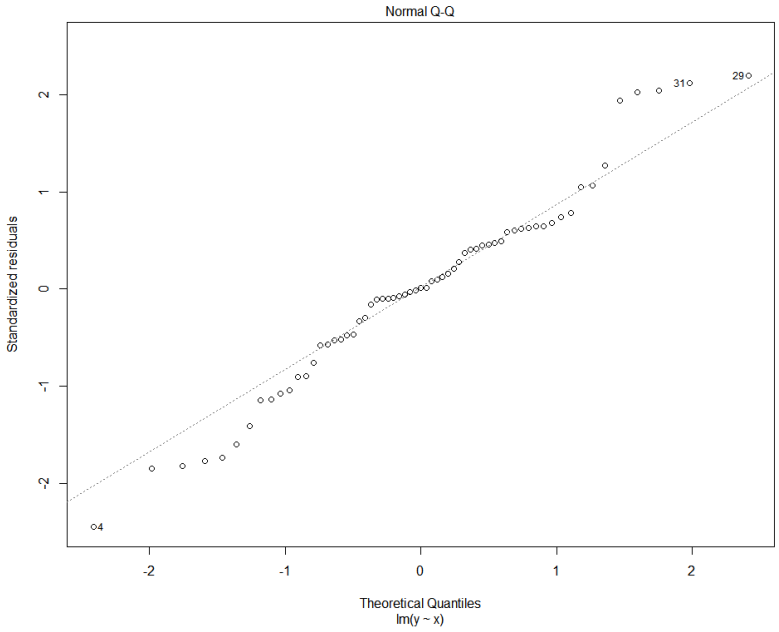

Figure C.3. Normal quantile (Q-Q) plot of the residuals for the piece-wise linear regression model completed on the mineral matter content by year for PAD 72.

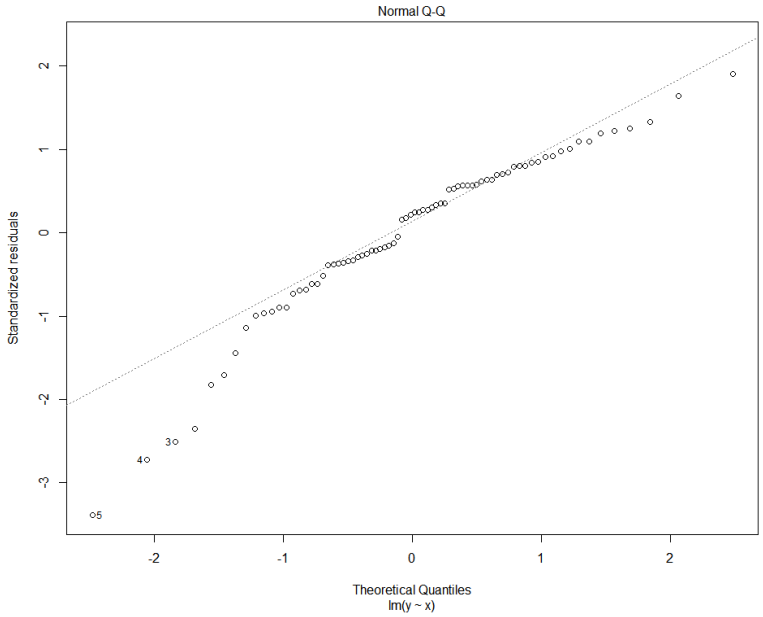

Figure C.4. Normal quantile (Q-Q) plot of the residuals for the piece-wise linear regression model completed on the mineral matter content by year for PAD 73.

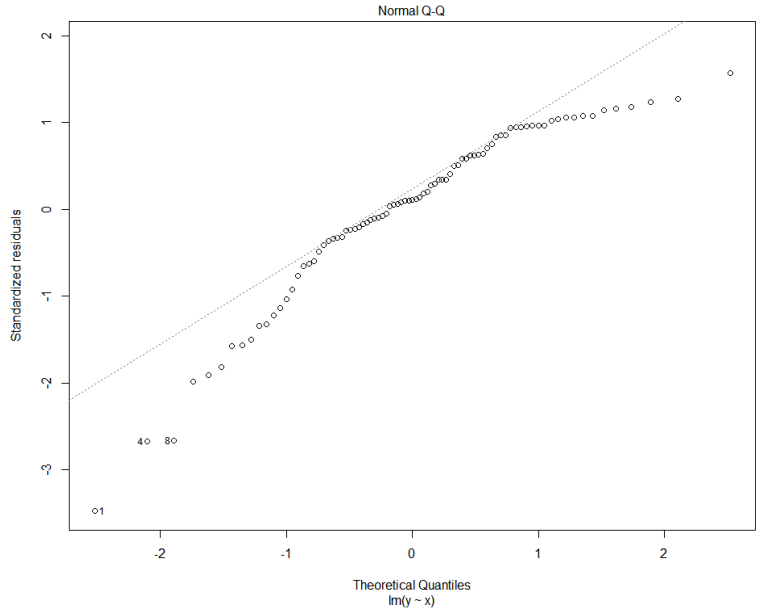

Figure C.5. Normal quantile (Q-Q) plot of the residuals for the piece-wise linear regression model completed on the mineral matter content by year for PAD 74.

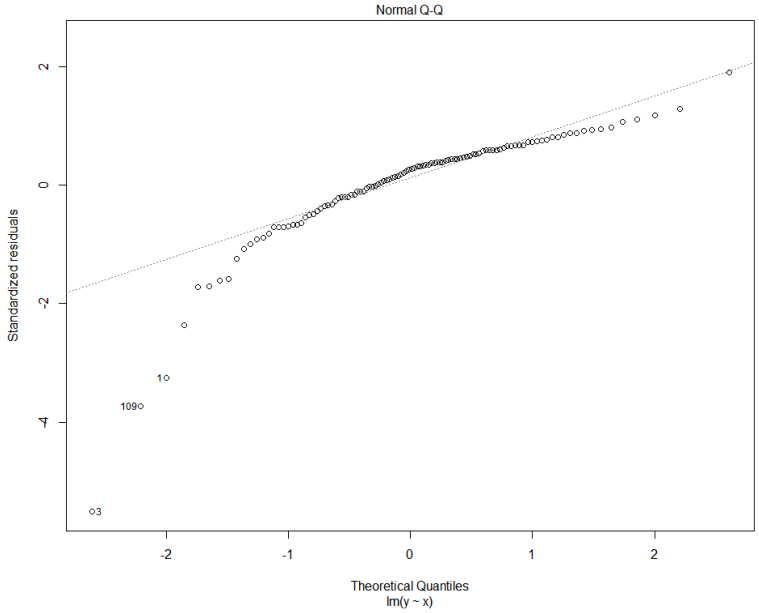

Figure C.6. Normal quantile (Q-Q) plot of the residuals for the piece-wise linear regression model completed on the mineral matter content by year for PAD 79.

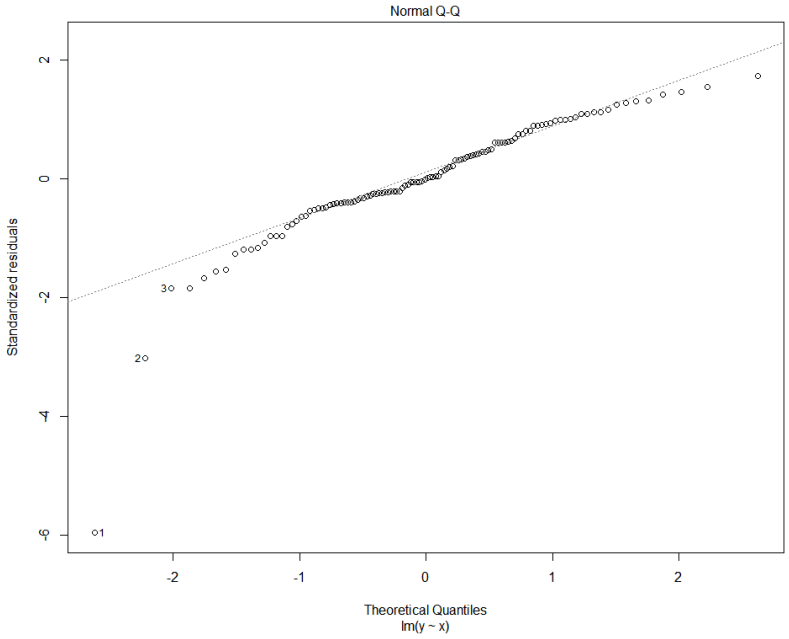

Figure C.7. Normal quantile (Q-Q) plot of the residuals for the piece-wise linear regression model completed on the mineral matter content by year for PAD 82.

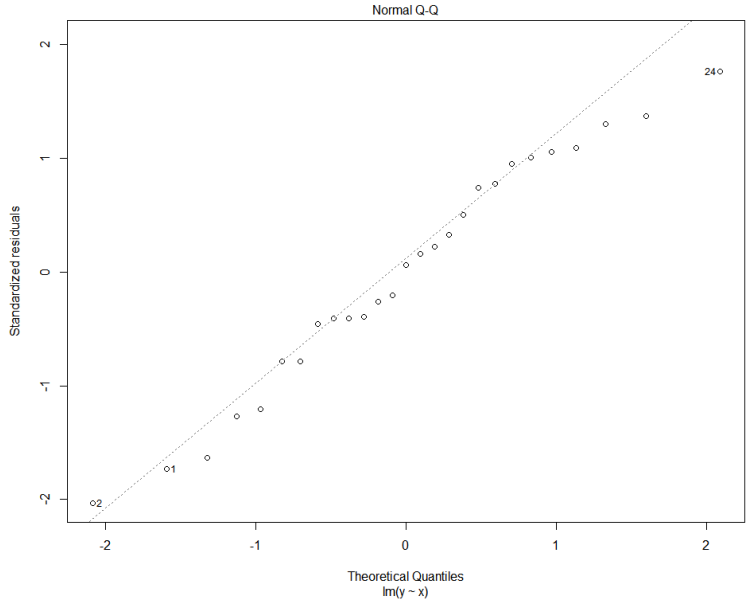

Figure C.8. Normal quantile (Q-Q) plot of the residuals for the piece-wise linear regression model completed on the elemental carbon to nitrogen ratio by year for PAD 52.

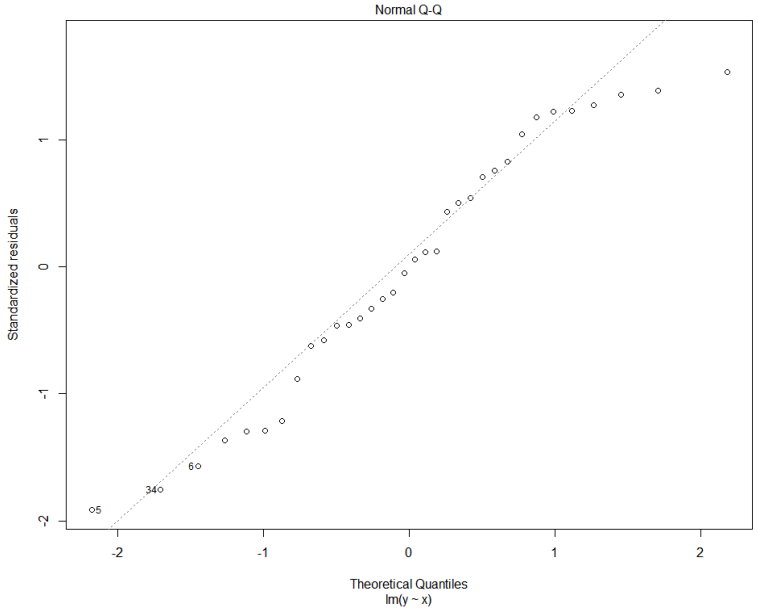

Figure C.9. Normal quantile (Q-Q) plot of the residuals for the piece-wise linear regression model completed on the elemental carbon to nitrogen ratio by year for PAD 65.

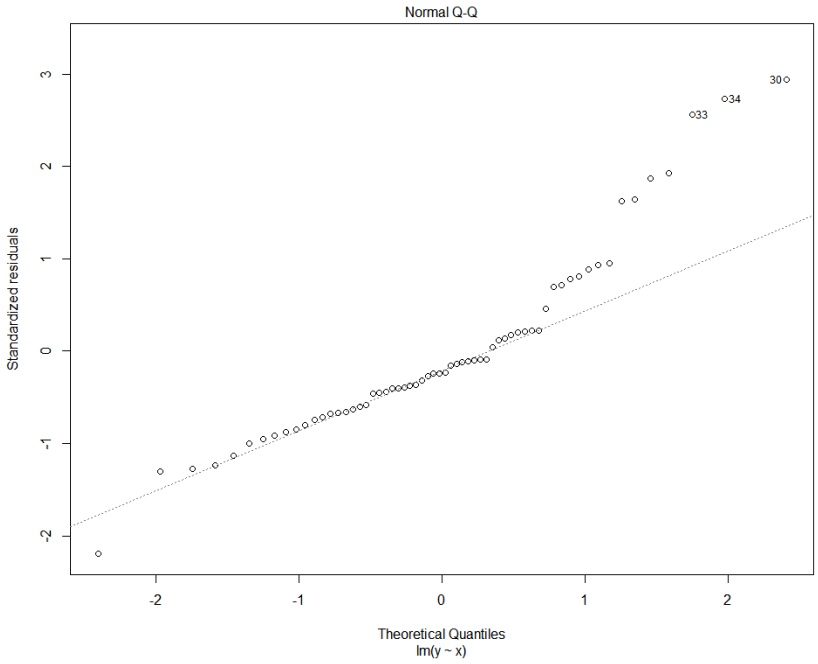

Figure C.10. Normal quantile (Q-Q) plot of the residuals for the piece-wise linear regression model completed on the elemental carbon to nitrogen ratio by year for PAD 72.

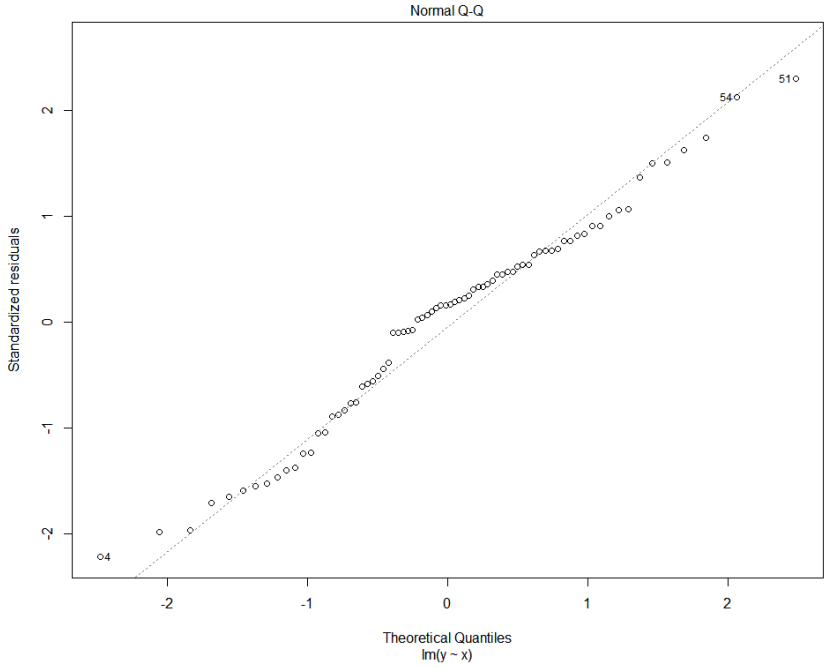

Figure C.11. Normal quantile (Q-Q) plot of the residuals for the piece-wise linear regression model completed on the elemental carbon to nitrogen ratio by year for PAD 73.

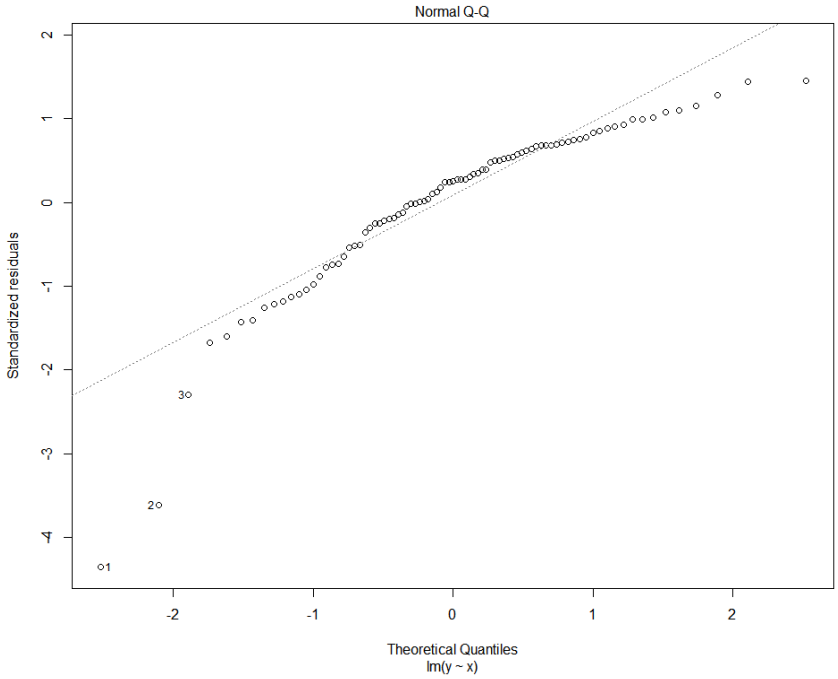

Figure C.12. Normal quantile (Q-Q) plot of the residuals for the piece-wise linear regression model completed on the elemental carbon to nitrogen ratio by year for PAD 74.

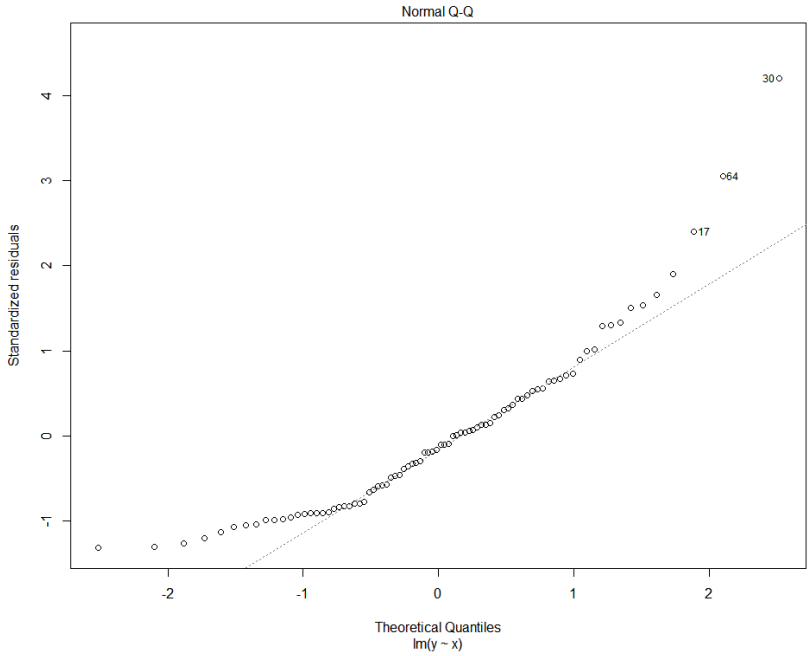

Figure C.13. Normal quantile (Q-Q) plot of the residuals for the piece-wise linear regression model completed on the elemental carbon to nitrogen ratio by year for PAD 79.

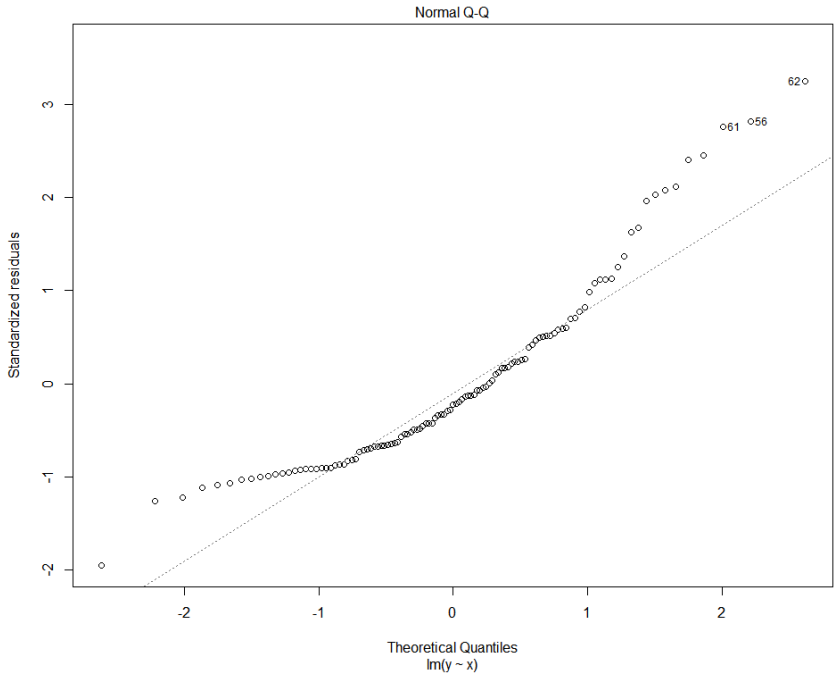

Figure C.14. Normal quantile (Q-Q) plot of the residuals for the piece-wise linear regression model completed on the elemental carbon to nitrogen ratio by year for PAD 82.

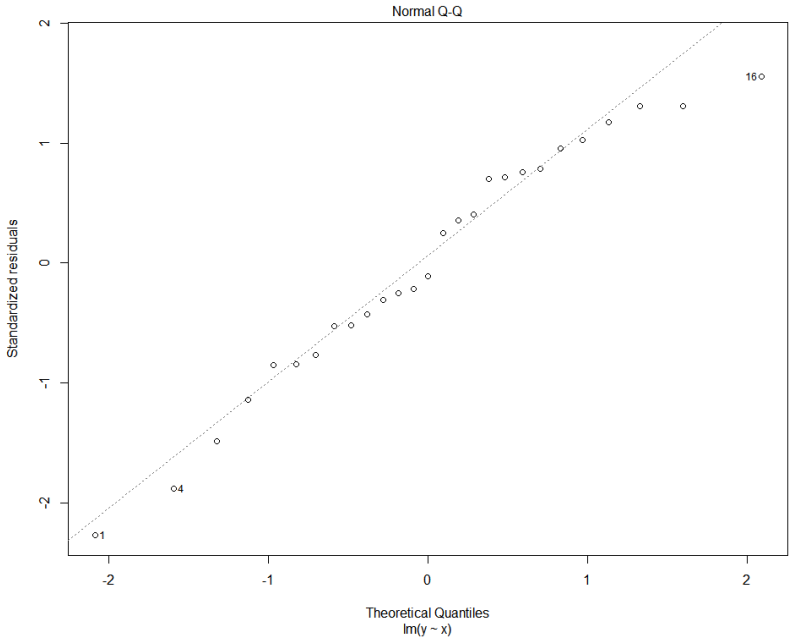

Figure C.15. Normal quantile (Q-Q) plot of the residuals for the piece-wise linear regression model completed on the $\delta^{15}N$ by year for PAD 52.

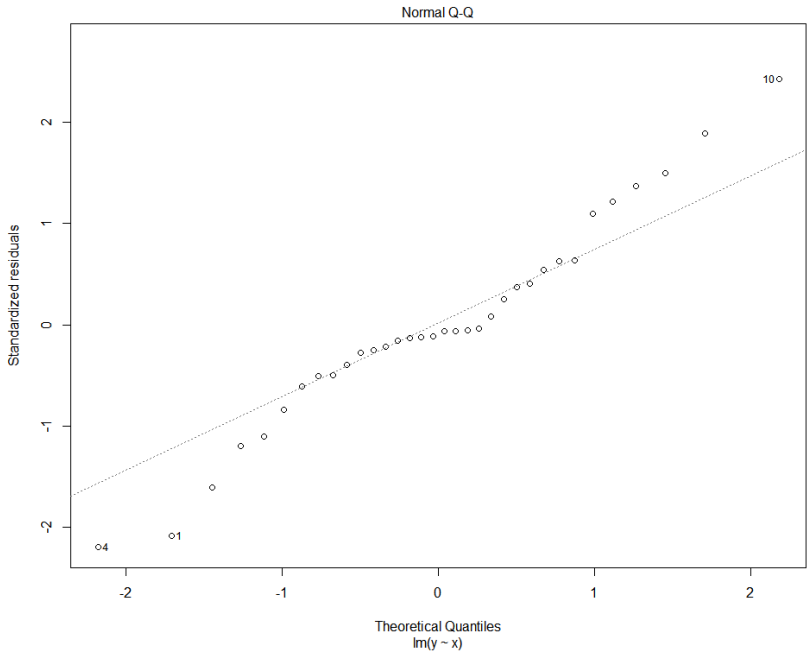

Figure C.16. Normal quantile (Q-Q) plot of the residuals for the piece-wise linear regression model completed on the $\delta^{15}N$ by year for PAD 65.

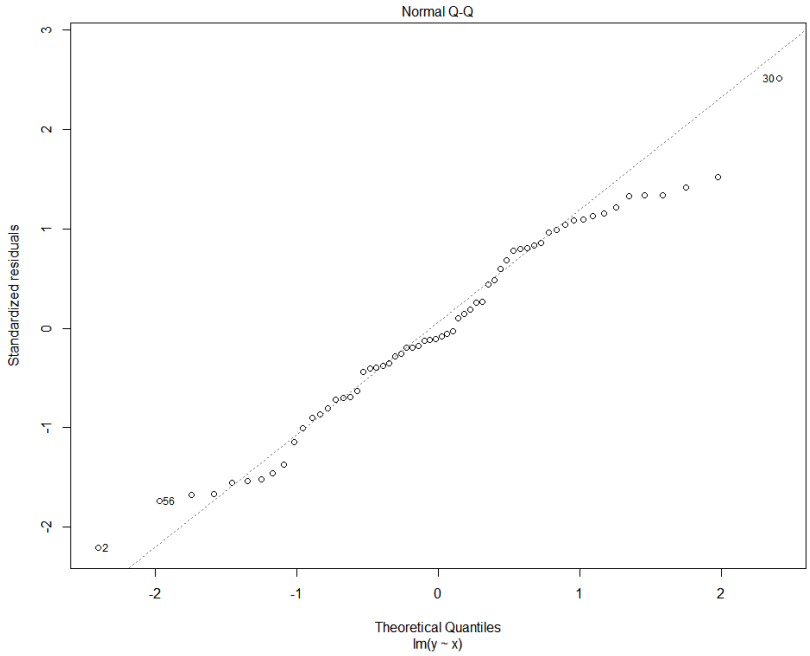

Figure C.17. Normal quantile (Q-Q) plot of the residuals for the piece-wise linear regression model completed on the $\delta^{15}N$ by year for PAD 72.

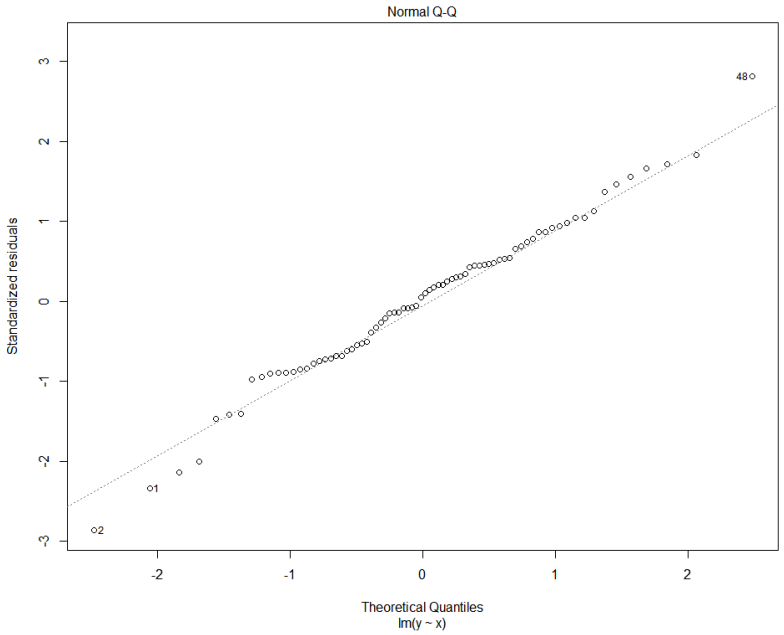

Figure C.18. Normal quantile (Q-Q) plot of the residuals for the piece-wise linear regression model completed on the $\delta^{15}N$ by year for PAD 73.

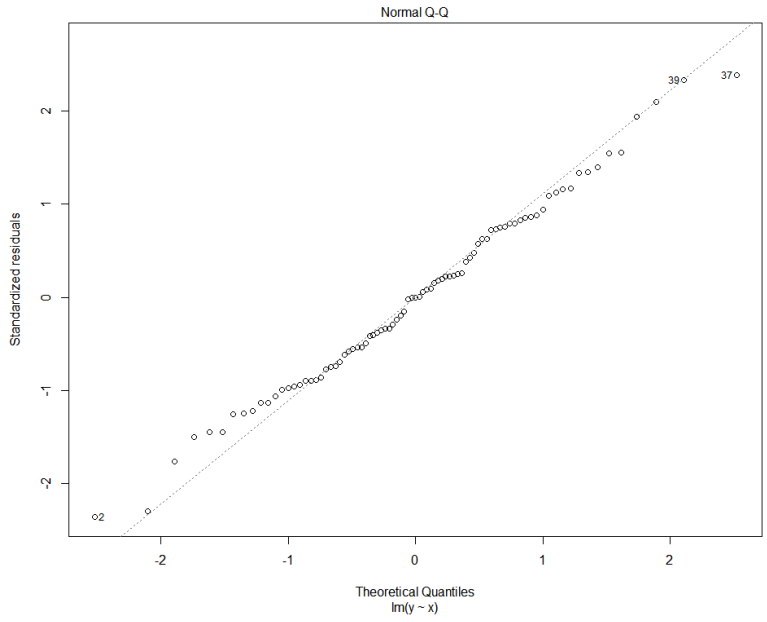

Figure C.19. Normal quantile (Q-Q) plot of the residuals for the piece-wise linear regression model completed on the $\delta^{15}N$ by year for PAD 74.

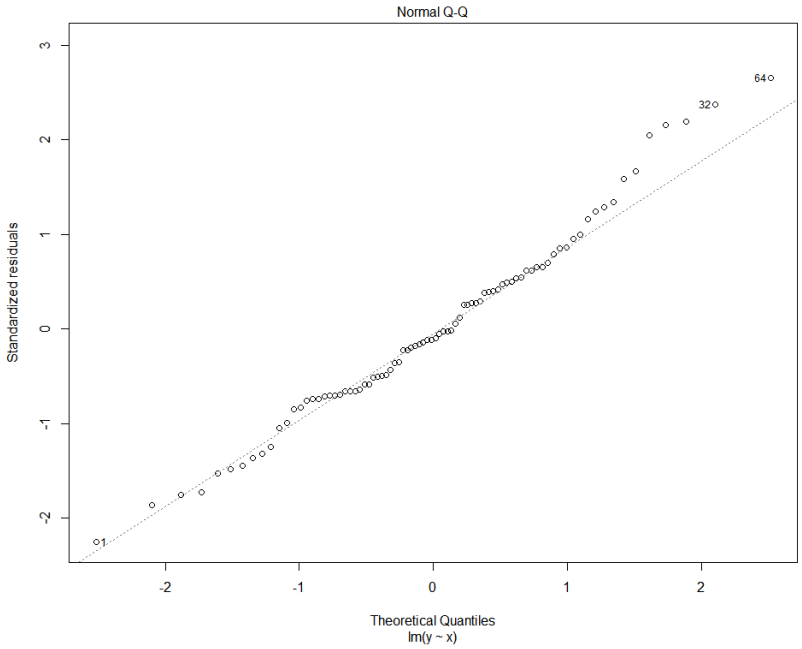

Figure C.20. Normal quantile (Q-Q) plot of the residuals for the piece-wise linear regression model completed on the $\delta^{15}N$ by year for PAD 79.

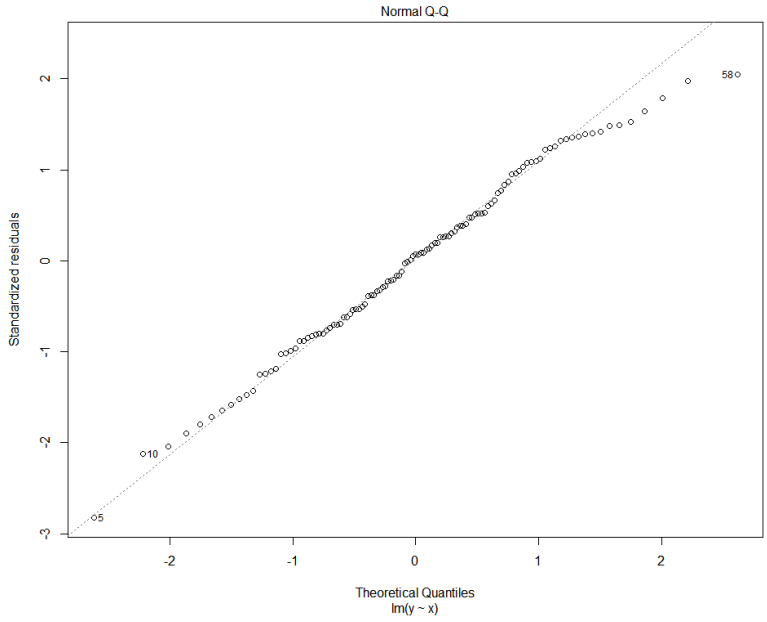

Figure C.21. Normal quantile (Q-Q) plot of the residuals for the piece-wise linear regression model completed on the $\delta^{15}N$ by year for PAD 82.